Application of Tight-Binding Method in Atomistic Simulation of Covalent Materials

by

Ahmet Isik

B.S., Hacettepe University
(1987)
S.M., Massachusetts Institute of Technology
(1992)

Submitted to the Department of Nuclear Engineering
in partial fulfillment of the requirements for the degree of

Doctor of Philosophy

at the

MASSACHUSETTS INSTITUTE OF TECHNOLOGY

May 1994

Author . . . . . .
Department of Nuclear Engineering
May 12, 1994

Certified by . . . . . .
Professor Sidney Yip
Professor
Thesis Supervisor

Accepted by . . . . . .
Allan F. Henry
Chairman, Departmental Committee on Graduate Students

Application of Tight-Binding Method in Atomistic Simulation of Covalent Materials

by

Ahmet Isik

Submitted to the Department of Nuclear Engineering
on May 12, 1994, in partial fulfillment of the
requirements for the degree of
Doctor of Philosophy

Abstract

The primary goal of this thesis is to develop and apply molecular dynamics simulation methods to elemental and binary covalent materials (Si, C, SiC) based on the tight-binding (TB) model of atomic cohesion in studies of bulk and deformation properties far from equilibrium. A second purpose is to compare results with those obtained using empirical interatomic potential functions in order to elucidate the applicability of models of interatomic interactions which do not take into account explicitly electronic structure effects.

Based on the assumption that the cohesive energy can be written as the sum of a band structure contribution and a repulsive short-range interaction contribution, we have calculated the former by using a basis set consisting of four atomic orbitals, one for the s state and three for the p states, constructing a TB Hamiltonian in the usual Slater-Koster parametrization, and diagonalizing the Hamiltonian matrix at the origin of the Brillouin zone. For the repulsive part of the energy we employ a function in the form of inverse power law with screening which is then fitted to the bulk modulus and lattice parameter of several stable polytypes, results calculated by ab initio methods in the literature.

Three types of applications have been investigated to demonstrate the utility of the present TB models and their advantages relative to empirical potentials. In the case of Si we show the calculated cohesive energy agrees to within a few persent with the ab initio local-density approximation (LDA) results. In addition, for clusters up to 10 atoms we find most of the energies and equilibrium structures to be in good agreement with LDA results (the failure of the empirical potential of Stillinger and Weber (SW) is well known). In the case of C clusters our TB model gives ring and chain structures which have been found both experimentally and by LDA calculations.

In the second application we have applied our TB model of Si to investigate the core structure and energetic of partial dislocations on the glide plane and reconstruction antiphase defect (APD). For the 90o partial we show that the TB description gives the correct assymetric reconstruction previously found by LDA (SW potential fails in this case). For the 30° partial, even though TB and SW potential both give

the correct reconstruction, TB gives better bond angles in the dislocation core. For the APD we have obtained a binding energy and activation for migration which are somewhat larger than the SW values, but the conclusion remains that APD is a low-energy defect which should quite mobile.

In the third application we formulate a simple TB model for SiC where the coefficients of the two-center integrals in Si-C interactions are taken to be simple averages of Si-Si and C-C intergrals (following the idea of universal TB for all covalent materials). Fitting is done on two polytypes, zincblende and rocksalt structures, and a simulated annealing procedure is used. The TB results are found in good agreement with LDA and experimental results in the cohesive energy, acoustic phonon modes, and elastic constants. In addition, we have investigated the elastic stability of beta-SiC under hydrostatic tension using the concept of elastic stiffness coefficients recently developed. We find that TB predicts a critcial pressure (0.38 Mbar) compared to 0.28 Mbar obtained by using an empirical potential proposed by Tersoff.

For conslusions we consider (1) applicability of TB to SiC, and (2) relative advantges over empirical. We believe, on the basis of the results presented, that TB(SiC) provides a reasonable (at least qualitatively correct) description of atomic cohesion and local bonding of SiC.Certain improvements, such as treating charge transfer, and computationally more efficient techniques, such as the recursion method (real space) should be considered in future studies. Relative to empirical potentials like SW and Tersoff, the present TB models are clearly more transferable. In all the properties we have examined in this work, we have not uncovered any property where TB is qualitatively deficient.

Thesis Supervisor: Professor Sidney Yip
Title: Professor

Acknowledgments

I would like to express my admiration and gratitude to Professor Sidney Yip. His efforts will not be forgotten.

I am grateful to Dr. Vasily Bulatov. He has been an exceptionally valuable source of information.

Thanks are due to Professors John J. Joannopoulos and Boris Altshuler who served as the members of the thesis committee.

Dr. Tuan Huu Cao kindly provided resources for parallel computing.

A special thanks goes to Dr. Arnaldo Dal'Pino for bringing some key papers to my attention.

I also thank Joao Justo, Randall Pfluger, and Meijie Tang for their friendship.

Athena workstations, MITSF and the Connection Machine were used to carry out calculations.

The financial support of the Ministry of Education of Turkey and the AFOSR is gratefully acknowledged.

Contents

List of Figures

List of Tables

Chapter 1

Introduction

1.1 Background and Motivation

In atomistic simulation of materials properties and behavior, significant advances are being made to develop methods of describing atomic cohesion in solids which can be combined with molecular dynamics for the purpose of studying technologically interesting solids. In the case of semiconductor and covalent materials such as Si, C, and SiC, it is well known that pair potential functions are unable to account for the strong electronic structure effects which give rise to the tetrahedral structure of these materials and the corresponding angle-dependent forces [1]. Empirical potential functions which attempt to take into account many-body interaction effects have been proposed for use in molecular dynamics (MD) simulations [2, 3]. Although there exists now a considerable body of literature on such studies of Si, no potential model can claim to be fully satisfactory in describing the physical properties of this material [4]. The basic concern is that all empirical potentials, by the nature of their construction and fitting to known properties, suffer from the lack of transferability. In other words, a potential which is constructed by fitting to only equilibrium properties may do very poorly in applications to highly nonequlibrium conditions. The best one can do is to include as many different properties as possible in the database when fitting the potential.

One can approach the problem of studying covalent materials by atomistic simu-

lation based on density functional theory [5, 6, 7, 8] which treats electronic structure effects quantum mechanically in a first principles or ab initio manner. In principle, this approach is the most fundamental and accurate; however, in practice simulation methods based on this formulation [9] require so much computational effort that, at the present time, the method is still restricted to a small number of atoms and quite short simulation times. For studies of mechanical and deformation properties, simulation cells containing at least several hundred atoms would be required and one cannot use the ab initio approach.

There exists an intermediate approach between the use of empirical potential functions and first principles total-energy calculation. This is known as the tight-binding (TB) method which is based on LCAO (linear combination of atomic orbitals) scheme in which electronic structure effects are treated through a basis set of atomic orbitals representing only the outer valence electrons. By approximate parametrization of the matrix elements of the Hamiltonian, [10] a description of the atomic cohesion can be developed and conveniently incorporated into MD simulation which the expectation is that the essential electronic structure effects can be taken into account, albeit in a quite simplified manner, without incurring the full computational burden of the ab initio method. Clearly, the TB approximation [1] will not be as accurate as first principles; the question which needs to be addressed is whether this approach provides a substantial improvement over the empirical potentials.

In a number of specific studies, TB models have been used to obtain results which compare well with first principles calculations which we will denote as local density approximation (LDA) to call attention to the treatment of electron exchange and correlation that is almost universally adopted [6]. For the covalent materials of interest in this thesis, one can point to existing models and results on properties which provide a basis for further investigation of the applicability of this method of describing atomic cohesion.

1.2 Problem Statement

The primary goal of this thesis is to develop and apply molecular dynamics simulation methods to elemental and binary covalent materials (Si, C, SiC) based on the TB model of atomic cohesion in studies of bulk and deformation properties far from equilibrium. A second purpose is to compare the TB results with those obtained using empirical interatomic potential functions in order to elucidate the applicability of models of interatomic interactions which do not take into account explicitly electronic structure effects.

Three types of studies have been carried out to demonstrate the utility of the present TB models and their advantages relative to empirical potentials. For clusters up to 10 atoms we find energies an equilibrium structures to be in good agreement with LDA results (the failure of the empirical potential of Stillinger and Weber (SW) in this case is well known). In the case of C clusters our TB model gives ring and chain structures which have been found both experimentally and by LDA calculations.

In the second study we have applied our TB model ot Si to investigate the core structure and energetics of partial dislocations on the glide plane and the reconstruction antiphase defect (APD). For the 90° partial we show that the TB description gives the correct asymmetric reconstruction previously found by LDA (SW potential fails in this case). For the 30° partial, even though both TB and SW potentials give the correct reconstruction, TB gives better bond angles in the dislocation core. For the APD we have obtained the binding energy and the activation energy for migration which are somewhat larger than the SW values, but the conclusion remains that APD is a low energy defect which should be quite mobile.

In the third study we formulate a simple TB model for SiC where the coefficients of the two-center integrals in Si-C interaction are taken to be simple averages of Si-Si and C-C integrals (following the idea of universal TB parameters for all covalent materials). The TB results are found to be in good agreement with LDA and experimental results in the cohesive energy, acoustic phonon modes, and elastic constants. In addition we have investigated the elasic stability of β SiC under hydrostatic tension

using the concept of elastic stiffness coefficients recently developed citej1.

Chapter 2

Development of Computational Methods

In this part of the thesis, we will derive the semiempirical TB method from the density functional theory by using the stationary property of the density functional theory. We need to solve the Schrödinger equation in order to find interatomic forces in a system which is composed of electrons and ions. But the exact solution of the Schrödinger equation is possible only for very simple systems, like the hydrogen atom [11]. Even for the He atom, we need to make approximations to solve the Schrödinger equation [12].

Ab-initio methods[8] solve the Schrödinger equation by making many significant approximations, but without resorting to the experimental data. Ab-initio methods, like Car-Parrinello method[9] permit simulation of only a few tens of atoms. But the simulation results are very important for comparision purposes.

Semiempirical methods are between empirical and ab-initio methods, most importantly the TB method [13, 14, 10]. The semiempirical methods enable us to incorporate the electronic effects on the one hand and simulate large number of (a few hundreds) atoms on the other hand. The orthogonal TB method [13, 15, 16] is a semiempirical method for calculating interatomic forces in semiconductors and transition metals. The results of the simulations are usually in good agreement with that of ab-initio simulations. Phonon frequencies[15], thermal expansion coefficients[17],

specific heats[18], and radial distribution functions[15] are in agreement within a few percent of the ab-initio results.

The basis of the method is to expand the total electronic wavefunction as a linear combination of atomic orbitals. The Hamiltonian is approximated as the sum of potential wells located on the nuclei. By using the expansion for the total electronic wavefunction, the Hamiltonian matrix elements are obtained. Then by using the analytical derivatives of Hamiltonian matrix elements, the interatomic forces are calculated. The interatomic forces are then used to carry out the MD simulation.

The TB method is transferable because the same formulation can be used to study bulk[15], liquid[18, 19] or cluster[20] properties of materials.

In its simplest form the atomic orbitals which constitute the basis set are assumed to be orthonormal to each other. Self consistency is ignored and the matrix elements between localized orbitals on a single atom are assumed to vanish.

2.1 The Adiabatic Approximation

The system we are dealing with is composed of electrons and nuclei which are moving in the potential field created by their own charges. Basically what we need is to solve the Schrödinger equation for the whole system and compute properties of the system by using the total wave function of the electron and nuclei. The solution of the Schrödinger equation for the system of electrons and nuclei is a hopeless task unless we make some approximations because of the enormous number of degrees of freedom of the system.

One of the first approximations we will make is called the adiabatic approximation[21] and enables us to solve the Schrödinger equation of electrons moving in the potential field created by the charge of the nuclei. The basis of this approximation is that electrons are so much lighter than the nuclei that the electrons adapt immediately to any change in the configuration of the nuclei. The electronic system is always very close to the ground state for a given nuclear configuration.

The total Hamiltonian of the electrons and nuclei can be written as

$$H = H_{el} + H_{ion} + H_{el-ion}. \tag{2.1}$$

For the electronic part of the Hamiltonian, we write

$$H_{el} = \sum_k \frac{P_k^2}{2m} + \frac{1}{8\pi\epsilon_0} \sum_{kk'}{}' \frac{e^2}{|\vec{r}_k - \vec{r}_{k'}|} \tag{2.2}$$

and similarly for the ion part we can write

$$H_{ion} = \sum_i \frac{P_i^2}{2M_i} + \frac{1}{4\pi\epsilon_0} \sum_{ii'} \frac{e^2 Z_i Z_{i'}}{|\vec{R}_i - \vec{R}_{i'}|} \tag{2.3}$$

and H_{el-ion} can be written as

$$H_{el-ion} = \frac{1}{4\pi\epsilon_0} \sum_{k,i} \frac{-e^2 Z_i}{|\vec{r}_k - \vec{R}_i|} \tag{2.4}$$

Let's suppose that we can write the Schrödinger equation for the electronic system as

$$(H_{el} + H_{el-ion})\psi = E_{el}\psi \tag{2.5}$$

where ψ is the total electronic wave function. Now we will assume that the total wave function of the system composed of the electrons and nuclei can be written as a product

$$\Psi = \psi(\vec{r}_1 ... \vec{r}_N; \vec{R}_1 ... \vec{R}_{N'})\varphi(\vec{R}_1 ... \vec{R}_{N'}) \tag{2.6}$$

where N, N' are the numbers of the electrons and the nuclei, respectively. Let us substitute this wave function into the Schrödinger equation as (2.1) is the Hamilto-

nian:

$$\begin{aligned} H\Psi &= (H_{el} + H_{ion} + H_{el-ion})\psi\varphi \\ &= \psi(H_{ion} + E_{el})\varphi - \sum_i \frac{\hbar^2}{2M_i}(\varphi\nabla_i^2\psi + 2\nabla_i\varphi.\nabla_i\psi) \end{aligned} \tag{2.7}$$

If the last term were absent, we would be able to separate ion and electron motion. If we neglect the last term we will have

$$(H_{ion} + E_{el})\varphi = E\varphi \tag{2.8}$$

The last term is shown to be small in [22], so we can neglect it. E_{el} depends on both ion and electron coordinates, so it brings a contribution from the ionic potential to the electronic problem. φ is a function of the only ionic coordinates so that it describes the motion of nuclei. So we developed a way to solve the Schrödinger equation by separating electronic and ionic motion by using the adiabatic approximation. Now we need to solve the electronic part of the Schrödinger equation first by using the potential due to ions as an external potential to the electronic system. Then we can solve the ionic problem by using the electronic energy as a potential function which has been calculated by solving the electronic Schrödinger equation. For more information about the adiabatic approximation, we refer the reader to the book by Haugh [23].

2.2 Density Functional Theory

In order to use the TB method efficiently, we need to derive it from a more basic theory like the density functional theory so that we will be able to appreciate limitations and capabilities of the TB method better. The density functional theory is the obvious choice for the more basic theory to derive the TB method from because there is a very close connection between the two theory on the intuitive level.

Hohenberg and Kohn[5] and Kohn and Sham[6] have proved that the ground state total energy of the electronic system under the external field created by the nuclei is

determined solely by the density distribution of electrons. We can write the energy functional for the electrons as

$$E[n] = T_s[n] + F[n] \tag{2.9}$$

where $T_s[n]$ is the kinetic energy of a noninteracting electron gas moving in the field created by the nuclei which creates the electronic density distribution n. Even though functional E is defined for all density distributions, only those densities which correspond to the ground state density of the noninteracting elctrons make sense. The total kinetic energy of the noninteracting electrons is not the same with the total kinetic energy of the interacting electron system, but they are of equal magnitude [24].

We can write the electrostatic potential energy functional $F[n]$ as

$$F[n] = \int V_{nucl}(r)n(r)d^3r + \frac{1}{2}\int\int \frac{n(r)n(r')}{|r-r'|}d^3r'd^3r + E_{xc}[n(r)] \tag{2.10}$$

where V_{nucl} is the potential energy created by the nuclear charges. (2.10) is the definition for the $E_{xc}[n(r)]$ which is the exchange and correlation energy. Now let's define the first two potential energies as

$$E_H = \frac{1}{2}\int\int \frac{n(r)n(r')}{|r-r'|}d^3rd^3r' \tag{2.11}$$

and

$$E_{el-nucl}[n(r)] = \int V_{nucl}(r)n(r)d^3r \tag{2.12}$$

then we can write (2.10) as

$$F[n(r)] = E_{el-nucl} + E_H[n(r)] + E_{xc}[n(r)] \tag{2.13}$$

Now we will make another approximation. The term $E_{xc}[n(r)]$ is not known exactly. We will make the local density approximation which says that the exchange-

correlation term can be calculated by integrating the exchange correlation energy per electron in a uniform noninteracting electron gas of the same density. So we can write the exchange-correlation energy as

$$E_{xc}[n(r)] = \int \epsilon_{xc}(n(r))n(r)d^3r. \tag{2.14}$$

ϵ_{xc} can be calculated by using Monte Carlo methods[25]. The ab-initio calculations using the LDA have been surprisingly accurate [9, 26].

Now let's try to evaluate the energy functional $E[n(r)]$. To do this, we need to find a potential $V(r)$ which produces the ground state density of noninteracting electron gas when plugged into the following equation:

$$[-\frac{1}{2}\nabla^2 + V(r)]\psi_i(r) = \epsilon_i\psi_i(r). \tag{2.15}$$

The density can be calculated by using the one-electron wave functions

$$n(r) = \sum_{i=1}^{N} \psi_i^*(r)\psi_i(r). \tag{2.16}$$

Then the kinetic energy functional can be calculated as

$$\begin{aligned} T_s[n(r)] &= \sum_{i=1}^{N} \int \psi_i^*(r)(-\frac{1}{2}\nabla^2)\psi_i(r)d^3r \\ &= \sum_{i=1}^{N} \epsilon_i - \int V(r)n(r)d^3r. \end{aligned} \tag{2.17}$$

The electrostatic potential energy $F[n(r)]$ is easy to calculate once we know the density. We can obtain $E[n(r)] = T_s[n(r)] + F[n(r)]$. However it is difficult to find the density which minimizes the energy functional which is what we want. The ground state density makes the energy functional stationary, so that we have

$$\begin{aligned} \delta E[n(r)] &= E[n(r) + \delta n(r)] - E[n(r)] \\ &= O([\delta n(r)]^2) \end{aligned} \tag{2.18}$$

For small fluctuations, $\delta n(r)$ obeys the following equation:

$$\int \delta n(r) d^3r = 0. \tag{2.19}$$

From (2.17) we can write that

$$\delta T_s[n(r)] = -\int V(r)\delta n(r) d^3r + O([\delta n(r)]^2) \tag{2.20}$$

so that we find that

$$\begin{aligned} \delta E[n(r)] &= \delta T_s[n(r)] + \delta F[n(r)] \\ &= \int [\frac{\delta F}{\delta n}|_{n(r)} - V(r)]\delta n(r) d^3r + O([\delta n(r)]^2). \end{aligned} \tag{2.21}$$

From this equation we see that $E[n(r)]$ is stationary whenever

$$\frac{\delta F}{\delta n}|_{n(r)} = V(r) + const. \tag{2.22}$$

The constant is arbitrary and can be set to zero. Then we have the following equation

$$\frac{\delta F}{\delta n} = V_{nucl}(r) + V_H[n(r)] + \mu_{xc}[n(r)], \tag{2.23}$$

where $V_H[n(r)]$ is the Hartree potential,

$$V_H[n(r)] = \frac{\delta E_H}{\delta n(r)} = \int \frac{n(r')}{|r - r'|} d^3r' \tag{2.24}$$

and $\mu_{xc}[n(r)]$ is the exchange and correlation potential

$$\mu_{xc}[n(r)] = \frac{\delta E_{xc}}{\delta n(r)}. \tag{2.25}$$

(2.22) is the self-consistency condition. it relates the one-electron potential in (2.15) to the potential obtained by using the density of the electrons obtained using this potential. (2.15) should be solved self-consistently. When we obtain the ground state

electron density, we can calculate the ground state energy as

$$\begin{aligned} E_0 &= T_s[n_0] + F[n_0] \qquad (2.26) \\ &= \sum_{i=1}^{N} \int \psi_i^*(r)(-\frac{1}{2}\nabla^2)\psi_i(r)d^3r + F[n_0(r)] \\ &= \sum_{i=1}^{N} \epsilon_i + F[n_0(r)] - \int \frac{\delta F}{\delta n}|_{n_0(r)} n_0(r) d^3r \\ &= \sum_{i=1}^{N} \epsilon_i - E_H[n_0(r)] + E_{xc}[n_0(r)] - \int \mu_{xc}[n_0(r)] n_0(r) d^3r. \qquad (2.27) \end{aligned}$$

where

$$F[n_0(r)] - \int \frac{\partial F}{\partial n}|_{n_0(r)} n_0(r) d^3r \qquad (2.28)$$

is the double counting energy.

2.3 Semiempirical TB Models

In the semiempirical TB models, the basic assumption is that we can write the total energy as a sum of the occupied one electron eigenvalues and a short range pair potential. We start with the expression for the semiempirical TB methods

$$E = \sum_{i=1}^{N} \epsilon_i + \frac{1}{2} \sum_{\alpha} \sum_{\beta} U(|R_\alpha - R_\beta|) \qquad (2.29)$$

where ϵ_i are eigenvalues of some non-self-consistent Schrödinger equation,

$$H\psi_i = [-\frac{1}{2}\nabla^2 + V(r)]\psi_i(r) = \epsilon_i \psi_i(r) \qquad (2.30)$$

where $V(r)$ is the one-electron potential energy whose form we want to determine and $U(|R_\alpha - R_\beta|)$ is a short range pair potential between atoms α and β. $\psi_i(r)$ are one-electron eigenfunctions.

There are similarities and differences between the DFT and the TB methods. In the TB method, the eigenvalues ϵ_i are calculated from a non-self-consistent Schrödinger

equation. The double counting energy which arise as a result of summing pairwise Coulomb interactions twice in the one-electron eigenvalues and the ion-ion interaction are represented by a short range pair potential. We need to prove that starting from the DFT we can develop a non-self-consistent Schrödinger equation for the one-electron eigenvalues and also represent the double counting term and the ion-ion interaction as a pair potential.

Now let us prove the stationary and variational property of the DFT. The ground state density $n_0(r)$ minimizes the total energy of the electronic system. For an arbitrary density which differs from the ground state density by $\delta n(r)$ we can expand the energy functional around n_0:

$$\begin{aligned} E[n_0+\delta n] &= E[n_0]+\frac{1}{2}\int\int \frac{\delta^2 E}{\delta n(r)\delta n(r')}|_{n_0}\delta n(r)\delta n(r')d^3r d^3r' \\ &+ (terms\ of\ higher\ order). \end{aligned} \tag{2.31}$$

The first-order term is zero due to the stationary property of the DFT. The second order term $\frac{1}{2}\int\int \frac{\delta^2 E}{\delta n^2}|_{n_0}\delta n\delta n$ is always greater than or equal to zero [27]. This is the variational principle of the DFT and tells us that for any density different from the ground state density the total energy is always greater than the ground state energy. The total energy of the system is written as a functional of the density as

$$\begin{aligned} E[n_{out}] &= T_s[n_{out}]+F[n_{out}] \\ &= \sum_{i=1}^{N}\int \psi_i^*(r)(-\frac{1}{2}\nabla^2)\psi_i(r)d^3r + F[n_{out}] \\ &= \sum_{i=1}^{N}\epsilon_i - \int V_{in}(r)n_{out}(r)d^3r + F[n_{out}] \end{aligned} \tag{2.32}$$

where V_{in} is the potential which makes n_{out} the ground state density of the noninteracting electron gas. From (2.22) and (2.23) V_{in} can be written as

$$\begin{aligned} V_{in}(r) &= \frac{\delta F}{\delta n}|_{n_{in}} \\ &= V_{nucl}(r)+V_H[n_{in}(r)]+\mu_{xc}[n_{in}(r)] \end{aligned} \tag{2.33}$$

where n_{in} is a guessed density which should be as close to the ground state density as possible.

To find $E[n_{out}]$ we first guess an input density for the electrons. Then we calculate V_{in} and then we solve the one-electron problem (2.15) and find the new density and then calculate $E[n_{out}]$ from (2.32). When we do that we find that

$$\begin{aligned} E[n_{out}] &= \sum_{i=1}^{N} \epsilon_i - \int \frac{\delta F}{\delta n}|_{n_{in}} n_{out} + F[n_{out}] \\ &= \sum_{i=1}^{N} \epsilon_i - \int\int \frac{n_{in} n_{out}}{|r-r'|} - \int \mu_{xc}[n_{in}] n_{out} + \\ &\quad \frac{1}{2}\int\int \frac{n_{out} n_{out}}{|r-r'|} + E_{xc}[n_{out}]. \end{aligned} \tag{2.34}$$

It is not possible to establish a relationship between (2.34) and the semiempirical TB method because of the existence of n_{out} in the formulation [27]. We need another energy functional which is stationary around the ground state density and which contains only n_{in} but is not necessarily variational. What is important to us is the stationarity of this new energy functional around the ground state density which guarantees that the approximate energies are better than the approximate densities used to produce them. The variational principle is unimportant as far as obtaining energies close enough to the ground state energy is concerned.

To demonstrate stationarity, let us write

$$\Delta n(r) = n_{out}(r) - n_{in}(r) \tag{2.35}$$

and expand $F[n_{out}(r)]$ about n_{in}

$$\begin{aligned} E[n_{out}] &= \sum_{i=1}^{N} \epsilon_i + F[n_{in}] - \int \frac{\delta F}{\delta n}|_{n_{in}} n_{in} \\ &\quad + \frac{1}{2}\int\int \frac{\delta^2 F}{\delta n^2}|_{n_{in}} \Delta n \Delta n + \ldots \end{aligned} \tag{2.36}$$

Now we can define our new functional which is a functional of n_{in} only:

$$\begin{aligned} E'[n_{in}] &= \sum_{i=1}^{N} \epsilon_i + F[n_{in}] - \int \frac{\delta F}{\delta n}|_{n_{in}} n_{in} \\ &= \sum_{i=1}^{N} \epsilon_i - E_H[n_{in}] + E_{xc}[n_{in}] - \int \mu_{xc}[n_{in}] n_{in} \end{aligned} \tag{2.37}$$

so that we can write

$$E'[n_{in}] = E[n_{out}] - \frac{1}{2} \int \int \frac{\delta^2 F}{\delta n^2}|_{n_{in}} \Delta n \Delta n + (higher\ order\ terms) \tag{2.38}$$

So we have reached our goal of obtaining the second functional which depends only on n_{in} and stationary about the ground state electron density.

We can calculate the electronic energy eigenvalues by solving a non-self-consistent Schrödinger equation:

$$\{-\frac{1}{2}\nabla^2 + V_{nucl}(r) + V_H[n_{in}(r)] + \mu_{xc}[n_{in}(r)]\}\psi_i(r) = \epsilon_i \psi_i(r) \tag{2.39}$$

and we can write the double counting energy as a functional of n_{in} only:

$$F[n_{in}] - \int \frac{\delta F}{\delta n}|_{n_{in}} n_{in} = -E_H[n_{in}] + E_{xc}[n_{in}] - \int \mu_{xc}[n_{in}] n_{in}. \tag{2.40}$$

Now we can derive the semiempirical TB method by using the functional $E'[n_{in}]$. From now on all the densities $n(r)$ are understood to denote $n_{in}(r)$ and we suppress the subscript.

$$\begin{aligned} E'[n] &= \sum_{i=1}^{N} \epsilon_i + F[n(r)] - \int \frac{\delta F}{\delta n}|_{n(r)} n(r) d^3r \\ &= \sum_{i=1}^{N} \epsilon_i - E_H[n(r)] - \int \mu_{xc}[n(r)] n(r) d^3r + E_{xc}[n(r)]. \end{aligned} \tag{2.41}$$

We can find the eigenvalues ϵ_i from a non-self-consistent Schrödinger equation

$$[-\frac{1}{2}\nabla^2 + V(r)]\psi_i = \epsilon_i \psi_i(r) \tag{2.42}$$

where the input potential is

$$V(r) = \frac{\delta F}{\delta n}|_{n(r)} = V_{nucl}(r) + V_H[n(r)] + \mu_{xc}[n(r)]. \tag{2.43}$$

We need to introduce another approximations which will enable us to neglect the core electrons. This approximation is called the *frozen core approximation*[28]. The basic idea behind this approximation is that the core electrons are localized around the nuclei and they are only slightly perturbed by the presence of other atoms. So we can take the core orbitals as a linear combination of slightly perturbed atomic orbitals. If the difference between core orbitals and atomic orbitals is on the order of λ, then we will write that [27]

$$\begin{aligned} \sum_{i,c} \epsilon_{ic} &= \sum_{i,c} < \psi_{ic}|[-\frac{1}{2}\nabla^2 + V(r)]|\psi_{ic} > \\ &= \sum_{a,c} < \phi_{ac}|[-\frac{1}{2}\nabla^2 + V(r)]\phi_{ac} > + O(\lambda^2) \\ &= T_c + \int n_c V + O(\lambda^2) \end{aligned} \tag{2.44}$$

where ψ_{ic} are core states and ϕ_{ac} are unperturbed atomic core orbitals and T_c is the total kinetic energy of the unperturbed cores. Then we can write (2.41) as

$$E'[n] = \sum_{i,v} \epsilon_{iv} + T_c + \int n_c V - E_H[n] - \int \mu_{xc}[n]n + E_{xc}[n]. \tag{2.45}$$

This equation can be written as

$$\begin{aligned} E'[n] &= \sum_{i,v} \epsilon_{iv} - E_H[n_v] - \int \mu_{xc}[n]n_v + E_{xc}[n] \\ &+ \frac{1}{2}\sum_{a}\sum_{\beta} \frac{Z_{va}Z_{v\beta}}{|\vec{R}_a - \vec{R}_\beta|} + C \end{aligned} \tag{2.46}$$

where C is the sum of free atomic core energies and Z_{av} are the number of valence electrons of atom at $\vec{R}_a$. The valence eigenvalues can be found by solving a Schrödinger

equation of the following form:

$$\begin{aligned} &\{-\frac{1}{2}\nabla^2 + V_{nucl} + V_H[n_c(r)] + V_H[n_v(r)] + \mu_{xc}[n_c(r) + n_v(r)]\}\psi_{iv}(r) \\ = \;& \epsilon_{iv}\psi_{iv}(r). \end{aligned} \tag{2.47}$$

At this point, we use a norm conserving pseudopotential[29] for the frozen cores. For the norm conserving pseudopotentials the real and pseudo wave functions are identical outside of the core. Then we can write the Schrödinger equation as

$$[-\frac{1}{2}\nabla^2 + \sum_a V_{ps,a} + V_H[n_v] + \mu_{xc}[n_v]]\psi_{ps,iv} = \epsilon_{iv}\psi_{ps,iv} \tag{2.48}$$

and the energy expression as

$$E'[n] = \sum_{i,v} \epsilon_{iv} - E_H[n_v] - \int \mu_{xc}[n_v]n_v + E_{xc}[n_v] + \frac{1}{2}\sum_a \sum_\beta \frac{Z_{va}Z_{v\beta}}{|\vec{R}_a - \vec{R}_\beta|}. \tag{2.49}$$

So by replacing the effect of the core electrons by a pseudopotential, we are able to neglect the core electrons. To solve the Schrödinger equation, we need to know the input density $n(r)$. Due to the stationary property even crude estimations of the density should give reasonable energies. The input valence electron density can be taken as a superposition of the atomic valence densities.

From (2.49) the electrostatic double counting energy can be written as

$$\begin{aligned} D_c[n_v] &= \frac{1}{2}\sum_a \sum_\beta \frac{Z_{va}Z_{v\beta}}{|\vec{R}_a - \vec{R}_\beta|} - \frac{1}{2}\int\int \frac{n_v(r)n_v(r')}{|r - r'|}d^3r d^3r' \\ &= A + \frac{1}{2}\sum_a \sum_\beta [\frac{Z_{va}Z_{v\beta}}{|\vec{R}_a - \vec{R}_\beta|} - \int\int \frac{n_{va}(r)n_{v\beta}(r')}{|r - r'|}d^3r d^3r'], \end{aligned} \tag{2.50}$$

where A is the minus intra-atomic Hartree energy. It is clear from (2.50) that the electrostatic part of the double counting term is pairwise. The double counting contribution of exchange and the correlation from (2.49) can be written as

$$D_{xc}[n_v] = \int [\epsilon_{xc}(n_v(r)) - \mu_{xc}(n_v(r))]n_v(r)d^3r. \tag{2.51}$$

We can approximate the exchange and correlation double counting term as [27]

$$D_{xc}[\sum_{a} n_{va}] = \sum_{a} D_{xc}[n_{va}] + \frac{1}{2}\sum_{a}\sum_{\beta}(D_{xc}[n_{va}+n_{v\beta}] - D_{xc}[n_{va}] - D_{xc}[n_{v\beta}]) + (\textit{three and higher - body interactions}) \quad (2.52)$$

The terms higher than pair interactions are very small [27], so that only pair interactions play a role. The exchange and correlation term can be approximately expressed as a pair potential. So we have reached our goal of showing that the double counting term can be expressed as a pair potential. We can write the double counting term as

$$\sum_{a} C_a + \frac{1}{2}\sum_{a}\sum_{\beta} U_{a\beta}(|R_a - R_\beta|) \quad (2.53)$$

where C_a is the double counting for an atom.

If we construct the input density as a superposition of atomic-like densities, we can write the one-electron potential as

$$V(r) = \sum_{a} V_a(r) + U(r) \quad (2.54)$$

where V_a can be written as

$$V_a(r) = V_{ps,a}(r) + V_H[n_{va}(r)] + \mu_{xc}[n_{va}(r)] \quad (2.55)$$

and $U(r)$ is

$$U(r) = \mu_{xc}[\sum_{a} n_{va}(r)] - \sum_{a} \mu_{xc}[n_{va}(r)]. \quad (2.56)$$

Now we have proved that the double counting term is pairwise and we also found the one-electron potential. The short range potential energy can be found from dimer calculations. It is perfectly transferable.

So we were able to show that the total energy in the TB models can be approximated as a sum of a band structure energy which is obtained by solving a non-

self-consistent Schrödinger equation and a pair potential. We have also found the one-electron potential which should be used in the one-electron Schrödinger equation.

2.4 Ab-Initio TB Method Applied to Crystalline Substances

The TB theory is based on the one-electron approximation. In the one-electron approximation, the energy levels of a given electron are determined in a crystal potential field. The TB method is based on the linear variation of parameters using the Block sum as basis. We can write

$$b_\alpha^i(\vec{k},\vec{r}) = (N)^{-1/2} \sum_\nu e^{i\vec{k}.\vec{R}_\nu} \phi_\alpha[\vec{r} - (\vec{R}_\nu + \vec{t}_i)] \tag{2.57}$$

where N is the total number of the unit cells in the crystal, $\vec{k}$ defines the region of the Brillouin zone under consideration, and where vectors $\vec{R}_\nu$ and $\vec{t}_i$ label the positions of the unit cells and of various atoms contained within each unit cell respectively. The expression $\phi_\alpha[\vec{r} - (\vec{R}_\nu + \vec{t}_i)]$ represents some "atomic-like" function $\phi_\alpha(\vec{r})$ centered about i-th atom of the ν-th unit cell. Traditionaly, these $\phi_\alpha(\vec{r})$ are chosen to be the Hartree-Fock orbitals of the free atom of which the crystal is composed. When this is done, and when care is taken to include those orbitals of the valence shell necessary to assure that the resultant trial function will possess the proper transformation properties under the operations of the group of the wavevector, we then call this a minimum basis set. Usually the atomic orbitals are used as the basis functions but Gaussian-type (GTO)[30] and Slater-type[31] (STO) orbitals can be used and the results can be significantly improved. Gaussian orbitals are constructed by using $\exp(-\alpha r^2)$ whereas the STO orbitals are constructed by using exponentials $\exp(-\alpha r)$. Atomic orbitals are similar to STO orbitals so STO orbitals give more accurate results but GTO orbitals are easier to deal with.

From the Block functions (2.57) we construct the trial wavefunction

$$\psi_n(\vec{k},\vec{r}) = \sum_a \sum_i a^i_{n,a}(\vec{k}) b^i_a(\vec{k},\vec{r}). \tag{2.58}$$

The variation of the linear parameters $a^i_{n\alpha}(\vec{k})$ yields an energy minimum when

$$det|H(\vec{k}) - ES(\vec{k})| = 0, \tag{2.59}$$

where

$$H^{ij}_{\alpha\beta}(\vec{k}) = \int b^{i*}_\alpha(\vec{k},\vec{r}) H b^j_\beta(\vec{k},\vec{r}), \tag{2.60}$$

and

$$\begin{aligned} &S^{ij}_{\alpha\beta}(\vec{k}) \int b^{i*}_\alpha(\vec{k},\vec{r}) d\tau \\ &\sum_\nu e^{i\vec{k}.\vec{R}_\nu} \int \phi^*_\alpha(\vec{r} - \vec{t}_i)\phi_\beta[\vec{r} - (\vec{R}_\nu + \vec{t}_i)] d\tau \end{aligned} \tag{2.61}$$

respectively, and where H is the one-electron Hamiltonian (in atomic units)

$$H = -\frac{1}{2}\nabla^2 + V_{cry}(\vec{r}). \tag{2.62}$$

so that we need to calculate several multicenter integrals of the form

$$\int \phi^*_\alpha(\vec{r}_A)\phi_\beta(\vec{r}_B) d\tau \tag{2.63}$$

$$\int \phi^*_\alpha(\vec{r}_A)(-\frac{1}{2}\nabla^2)\phi_\beta(\vec{r}_B) t\tau \tag{2.64}$$

$$\int \phi^*_\alpha(\vec{r}_A V_{cry}(\vec{r})\phi_\beta(\vec{r}_\beta) d\tau \tag{2.65}$$

The first two integrals in (2.63) can be calculated easily. The last integral is difficult to evaluate. One way of calculating those integrals is to write them as a

linear combination of STO

$$\phi_\alpha(\vec{r}) = \sum_i c_{\alpha,i} x_i^S(\vec{r}), \tag{2.66}$$

or GTO

$$\phi_\alpha(\vec{r}) = \sum_i c_{\alpha,i} x_i^G(\vec{r}), \tag{2.67}$$

and by expanding the periodic crystalline potential $V_{cry}(\vec{r})$ in a Fourier series

$$V_{cry}(\vec{r}) = \sum_\nu V_1(\vec{K}_\nu)\cos(\vec{K}_\nu.\vec{r}_c) + \sum_\nu V_2 \sin(\vec{K}_\nu.\vec{r}_c), \tag{2.68}$$

where $\vec{c}$ denotes the origin about which the potential is expanded. The required integrals can thus be decomposed into a sum of integrals of the form

$$\begin{aligned}\int x^{G*}(\vec{r}_A)V_{cry}(\vec{r})x^G(\vec{r}_B)d\tau \;=\; & \sum_\nu V_1(\vec{K}_\nu)\int x^{G*}(\vec{r}_A)cos(\vec{K}_\nu.\vec{r}_c)x^G(\vec{r}_B)d\tau + \\ & \sum_\nu V_2(\vec{K}_\nu)\int x^{G*}(\vec{r}_A)sin(\vec{K}_\nu.\vec{r}_c)x^G(\vec{r}_B)d\tau \end{aligned} \tag{2.69}$$

for expansion in GTO and an analogous expression for expansion in STO. The resultant integrals can be evaluated analytically for GTO but should be numerically evaluated for STO.

The basic integral to evaluate is

$$C^G_{1s,1s} = \int \exp(-\alpha_1 r_A^2)\cos(\vec{K}_\nu.\vec{r}_c)d\tau. \tag{2.70}$$

Using the following identity

$$\exp(-\alpha_1 r_A^2)\exp(-\alpha_2 r_B^2) = \exp(-\alpha_1\alpha_2 r_{AB}^2/(\alpha_1+\alpha_2))\exp[-(\alpha_1+\alpha_2)r_d^2] \tag{2.71}$$

where $\vec{r}_A$ and $\vec{r}_B$ are origins of the two basis functions. Those integrals are independent of $\vec{k}$ and need to be calculated only once for a crystalline material.

2.5 Orthogonal TB Method

In the previous sections we proved that the total energy of the system of electrons and cores can be written as a sum of a band structure energy and a short range pair potential. In this section we will discuss how to construct the secular equation and how to solve it. The secular equation is given as

$$det|H - \epsilon S| = 0 \tag{2.72}$$

where E are the eigenvalues of the Hamiltonian matrix H and the overlap matrix S is a unitary matrix.

There are only a few parameters to be fitted. If these parameters are fitted to the results of ab initio calculations accurate quantitative results can be obtained [32]. Unlike the free electron model which assumes that the electrons are free to move, the TB approximation starts from the free atoms and looks at how the bonds are formed when they are brought close to each other. This point of view permits obtaining of cohesive energies and bonds much more easily.

2.5.1 Band Structure Energy for the Simple Cubic System

The basic assumption of the TB method is that the total wavefunction of the system can be written as a linear combination of atomic-like orbitals, provided overlaps are not too strong. If $\varphi_\lambda(r-n)$ is the wave function corresponding to an orbital type λ on site n, we can write a wavefunction $\psi(r)$ as

$$\psi(r) = \sum_{n\lambda} a_n^\lambda \varphi_\lambda(r-n). \tag{2.73}$$

By this equation we mean that the density of electrons in the solid is a superposition of free atomic densities. A useful approximation we can make is to assume that the atomic orbitals are orthogonal. We can write that

$$S_{nm}^{\lambda\mu} = \int dr \varphi_l(r-n)\varphi_\mu(r-m) \tag{2.74}$$

We will neglect $S_{nm}^{\lambda\mu}$ if $n \neq m$. This approximation is not very accurate in practice but in general we can include the effects of nonorthogonality by renormalizing the TB parameters[33]. If we define the state $|n,\lambda>$ by the wavefunction $< r|n,\lambda >= \varphi_\lambda(r-n)$, then we can write that

$$< n,\lambda|m,\mu >= \delta_{mn}\delta_{\lambda\mu}. \tag{2.75}$$

Let's write the total TB Hamiltonian as a sum of the kinetic energy plus the sum of the atomic potential energy functions

$$H = T + \sum_n V_n^{at'} \tag{2.76}$$

where T is the kinetic energy operator. We can write this Hamiltonian as

$$H|m,\mu >= \epsilon^{at,\mu}|m,\mu > + \sum_{p\neq m} V_p^{at}|m,\mu >, \tag{2.77}$$

where $\epsilon^{at,\mu}$ is the atomic energy level for the orbital μ. We reach the conclusion that

$$\begin{aligned} < m,\lambda|H|m,\mu > &= \delta_{\lambda\mu}\epsilon^{at,\lambda} + < m,\lambda| \sum_{p\neq m} V_p^{at}|m,\mu > \\ &= \delta_{\lambda\mu}\epsilon^{at,\lambda} + a_m^{\lambda,\mu} \\ < n,\lambda|H|m,\mu > &= < n,\lambda|V_p^{at}|m,\mu >= \beta_{nm}^{\lambda\mu}; n \neq m \end{aligned} \tag{2.78}$$

In the previous calculation only the most important term was retained. When n,m,p are all different, we have small three center integrals which we will neglect:

$$< n,\lambda|V_p^{at}|m,\mu >= \int dr \varphi_\lambda(r-n)V^{at}(r-p)\varphi_\mu(r-m). \tag{2.79}$$

Let us assume that all atoms in the crystal are equivalent. In this case $a_m^{\lambda\mu} = a^\lambda\delta_{\lambda\mu}$ are independent of m and diagonal. a^λ is called crystal field integral, and $\beta_{nm}^{\lambda\mu}$ are called hopping integrals or transfer integrals. Hopping integrals decrease rapidly with the interatomic distance so that usually only taking into account nearest neighbors

is enough. The transfer integrals measure the ability of electrons to jump from one site to another.

Let us look at a simple example. Suppose there are only s states, so we will have only one transfer integral β and only one crystal field integral α. The Hamiltonian can be written as

$$H = \sum_n |n> (\epsilon^{at} + \alpha) < n| + \sum_{nm}{}' |n> \beta < m|, \tag{2.80}$$

where n and m are nearest neighbors. H can be diagonalized by using Block states

$$|k> = \frac{1}{\sqrt{N_a}} \sum_n e^{ik.n} |n> . \tag{2.81}$$

Then we have

$$H|k> = \epsilon_k |k> \tag{2.82}$$

where

$$\epsilon_k = \epsilon^{at} + \alpha + \beta \sum_R{}' e^{ik.R} \tag{2.83}$$

For simple cubic structure we have the following expression

$$\epsilon_k = \epsilon^{at} + \alpha + 2\beta(cosk_x a + cosk_y a + cosk_z a), -\pi <= k_x a, k_y a, k_z a <= \pi \tag{2.84}$$

2.5.2 The TB Hamiltonian and the Hamiltonian Matrix Elements

The TB Hamiltonian consists of two parts[34]

$$H = \sum_{i\mu} |i\mu > E_{i\mu} < i\mu| + \sum_{i\mu} \sum_{j\nu} |i\mu > t_{i\mu j\nu} < j\nu| \tag{2.85}$$

where $E_{i\mu}$ are the on site energies which are orbital energies of atoms. They are calculated by using the Hartree-Fock theory and tabulated [35]. $t_{i\mu j\nu}$ are the hopping integrals. They are the two center integrals and calculated by locating the two atomic orbitals on the two atoms and taking into account as Hamiltonian only the potential wells of the two atoms. We do not explicitly calculate the two-center integrals. They are approximated by empirical functions.

The symmetry properties and the transformations of the two-center integrals under arbitrary rotation are given by Slater and Koster[10]. They give transformation rules for s,p,d and f orbitals. Some of the rules they derived for the s and p orbitals are given below:

$$\begin{aligned} H_{ss} &= V_{ss\sigma}(r) \\ H_{sx} &= V_{sp\sigma}(r)cos(\theta_x) \\ H_{xy} &= (V_{sp\sigma}(r) - V_{pp\pi}(r)) * cos(\theta_x)cos(\theta_y) \end{aligned}$$

2.5.3 Interatomic Forces

We need to know the radial dependence of the hopping integrals in order to calculate interatomic forces. This radial dependence was given by Harrison as $1/r^2$ where r is the interatomic distance[36].

We calculate the interatomic forces by using the Hellmann-Feynman[37, 38] theorem. The theorem states that if ϕ is a normalizable eigenfunction of H with eigenvalue E, thus

$$H\phi = E\phi \tag{2.86}$$

and if σ is a real parameter in H, then according to the theorem

$$\frac{\partial E}{\partial \sigma} = \frac{<\phi|\frac{\partial H}{\partial \sigma}|\phi>}{<\phi|\phi>}. \tag{2.87}$$

Let us differentiate the identity

$$< \varphi | H - E | \phi >= 0 \tag{2.88}$$

with respect to σ to find

$$< \frac{\partial \phi}{\partial \sigma} | H - E | \phi > + < \phi | \frac{\partial H}{\partial \sigma} - \frac{\partial E}{\partial \sigma} | \phi > + < \phi | H - E | \frac{\partial \phi}{\partial \sigma} >= 0, \tag{2.89}$$

but because of

$$(H - E)|\phi >= 0 \; and \; < \phi | (H - E) = 0, \tag{2.90}$$

we reach this conclusion that

$$< \phi | \frac{\partial H}{\partial \sigma} - \frac{\partial E}{\partial \sigma} | \phi >= 0 \tag{2.91}$$

which of course is just (2.87). We know that the total energy of our system can be written as

$$E = \sum_{j} \sum_{m} \sum_{n} \sum_{m'} \sum_{n'} \lambda_{jmn} \lambda_{jm'n'} H_{mnm'n'} \tag{2.92}$$

Now we know everything to calculate the interatomic forces by using the TB method. The many-body force acting on atom n can be given as

$$\vec{F}_n = -\frac{\partial E}{\partial \vec{\tau}_n} = -\sum_{j} < \psi_j | \partial \hat{H} / \partial \vec{\tau}_n | \psi_j > \tag{2.93}$$

or

$$\vec{F}_n = -\sum_{j} \sum_{m} \sum_{m'} \sum_{n'} \lambda^{*}_{jmn} \lambda_{jm'n'} \partial H_{m'n'mn} / \partial \vec{\tau}_n \tag{2.94}$$

where λ_{jmn} are the components of the eigenvectors of the Hamiltonian and $H_{mnm'n'}$ are the Hamiltonian matrix elements

$$H_{mnm'n'} = < \phi_m(\vec{r} - \vec{\tau}_n)|H|\phi_{m'}(\vec{r} - \vec{\tau}_{n'}) > \tag{2.95}$$

where ϕ are atomic orbitals and $\vec{\tau}_n$ is the position vector of atom n. The force $\vec{F}_{nn'}$ is usually noncentral. The direction cosines used in the construction of the Hamiltonian matrix elements introduce a directional dependence to interatomic forces.

We have calculated the eigenvalues and eigenvectors of the Hamiltonian matrix by diagonalizing the Hamiltonian matrix. The computer time needed for the diagonalization of the Hamiltonian matrix grows as N^3, where N is the dimension of the Hermitian Hamiltonian matrix.

The two-body repulsive part of the potential can be calculated by subtracting the band-structure energy from the total energy and fitting a curve to the resulting graph [15]. We need to know the total energy curve of SiC from the ab-initio calculations in order to find the pair potential.

The two body part of the potential is used to calculate the total forces. The two-body forces are simply the minus gradient of the two-body potential energy function. We have fitted a fifth order polynomial to the pair potential.

After calculating the interatomic forces, the equations of the motion for the particles can be solved by using one of the standard integrators, for example the predictor-corrector method and the phase trajectory of the system is found.

2.5.4 The Basis Functions

The s-p bonded semiconductors can be treated by choosing a minimum basis set of sp^3. The electronic wavefunction is written as a linear combination of the atomic orbitals.

$$l = 0, m_l = 0, s = 1/2\sqrt{\pi}$$

$$l = 1, m_l = 1, p_{+1} = [\sqrt{3}/2/\sqrt{2\pi} sin\theta e^{i\phi}$$

$$l = 1, m_l = 0, p_0 = [\sqrt{3}/2\sqrt{2\pi}]cos\theta$$
$$l = 1, m_l = -1, p_{-1} = [\sqrt{3}/2\sqrt{2\pi}]sin\theta e^{-i\phi}.$$

We can use linear combinations of these orbitals as basis functions instead. The symmetries of the basis functions are more clear and the transformations are easier in the new forms:

$$\begin{aligned} s &= 1/2/\sqrt{\pi} \\ p_x &= \frac{1}{2}[p_{+1} + p_{-1}] = \sqrt{3}/2\sqrt{\pi}sin\theta\cos\phi \\ p_y &= \frac{1}{2}[-i(p_{+1} - p_{-1})] = \sqrt{3}/2\sqrt{\pi}sin\theta sin\phi \\ p_z &= \sqrt{3}/2\sqrt{\pi}\cos\theta. \end{aligned} \tag{2.96}$$

Those basis functions are shown if Figure 2-1.

The electronic wave function is expanded as a linear combination of atomic orbitals:

$$\psi = \sum_{m,n} \lambda_{m,n} f_{m,n}(\vec{r} - \vec{\tau}_n) \tag{2.97}$$

where $\lambda_{m,n}$ are the expansion coefficients, $f_{m,n}$ are the atomic orbital type m located on atom n and $\vec{\tau}_n$ are the position vector of atom n.

For transition metals which have d bands in the conduction bands range, use of the d bands are required. There are total 5 d basis functions and their transformation rules are given again by Slater and Koster[10]. But unlike the s-p Hamiltonian matrix elements, the d matrix elements have a $1/r^5$ dependence on interatomic distance r.

2.6 The Method of Slater and Koster

The TB method has important similarities with the H_2^+ problem shown in Figure 2-2. Two protons are located on the z axis with a distance R between them. An electron is moving around those two protons. To solve the Schrödinger equation we need to

use confocal elliptic coordinates μ, ν, and ϕ where

$$\begin{aligned} \mu &= (r_a + r_b)/R \\ \nu &= (r_a - r_b)/R \end{aligned} \tag{2.98}$$

and ϕ is the azimuthal angle about the z-axis with respect to XOY plane. The Laplacian in this coordinate system is then can be written as

$$\begin{aligned} \nabla^2 &= \frac{4}{R^2(\mu^2-\nu^2)}[\frac{\partial}{\partial\mu}\{(\mu^2-1)\frac{\partial}{\partial\nu}\}] + \frac{\partial}{\partial\nu}\{(1-\nu^2)\frac{\partial}{\partial\nu}\} \\ &+ \frac{\mu^2-\nu^2}{(\mu^2-1)(1-\nu^2)}\frac{\partial^2}{\partial\phi^2}]. \end{aligned} \tag{2.99}$$

If we use the seperation of variables method, we can write the solution as

$$\psi(\mu,\nu,\phi) = M(\mu)N(\nu)\Phi(\phi) \tag{2.100}$$

and we can write that

$$\frac{d^2\Phi}{d\phi^2} = -\lambda^2\Phi \tag{2.101}$$

where $-\lambda^2$ is the seperation constant. The values $|\lambda| = 0, 1, 2, ...$ are designated $\sigma, \pi, \delta...$ and the possible molecular orbitals (2.100) are then $1s\sigma, 2s\sigma, 2p\sigma, 2p\pi....$

We choose some atom on the center of the coordinate system and consider the vector $\vec{r}$ determined by any one of its neighbors located at point P. The direction cosines of $\vec{r}$ can be written as

$$l = x/r = \cos\phi\sin\theta, \quad m = y/r = \sin\phi\sin\theta \quad n = z/r = \cos\theta. \tag{2.102}$$

We want to set up another coordinate system OX'Y'Z' with the same origin as OXYZ

and with the OZ' axis lying along OP. The transformation can be written as

$$\begin{Bmatrix} x' \\ y' \\ z' \end{Bmatrix} = \begin{bmatrix} a_{11} & a_{12} & a_{13} \\ a_{21} & a_{22} & a_{23} \\ a_{31} & a_{32} & a_{33} \end{bmatrix} \begin{Bmatrix} x \\ y \\ z \end{Bmatrix} \tag{2.103}$$

where $a_{13} = l$, $a_{23} = m$ and, $a_{33} = n$. We can write that

$$x' = a_{11}x + a_{12}y + a_{13}z. \tag{2.104}$$

We can rewrite x' as

$$\begin{aligned} x' &= \frac{1}{2}[(a_{11} + ia_{12})(x - iy)] + \frac{1}{2}[(a_{11} - ia_{12})(x + iy)] + a_{13}z \\ y' &= \frac{1}{2}[(a_{21} + ia_{22})(x - iy)] + \frac{1}{2}[(a_{21} - ia_{22})(x + iy)] + a_{23}z \\ z' &= \frac{1}{2}[(a_{31} + ia_{32})(x - iy)] + \frac{1}{2}[(a_{31} - ia_{32})(x + iy)] + a_{33}z \end{aligned} \tag{2.105}$$

We note that

$$\begin{aligned} x + iy &= \sqrt{2}p_{+1} \propto \sin\theta e^{i\phi} \\ x - iy &= \sqrt{2}p_{-1} \propto \sin\theta e^{-i\phi} \\ z &= p_0 \propto \cos\theta \end{aligned} \tag{2.106}$$

We want to calculate the following integral

$$\begin{aligned} (x'^*|V'|x') &= (\{\frac{1}{2}[(a_{11} - ia_{12})(x + iy)] + \frac{1}{2}[(a_{11} + 1a_{12})(x - iy)] \\ &+ a_{13}z\}|V'|\{\frac{1}{2}[(a_{11} + ia_{12})(x - iy)] \\ &+ \frac{1}{2}[(a_{11} - ia_{12})(x + iy)] + a_{13}z\}). \end{aligned} \tag{2.107}$$

In (2.107) there are total nine integrals. Some of these integrals will vanish because

they contain terms like

$$\int_0^{2\pi} \exp(im_l\phi)d\phi = 0 \tag{2.108}$$

when $m_l = \pm 1, \pm 2, ...$ Two types of integrals won't vanish. We will use special symbols for them.

$$\begin{aligned}(p_0^*|V'|p_0) &= (3/4\pi)(\cos\theta|V'|\cos\theta) = V_{pp\sigma} \\ (p_{+1}^*|V'|p_{+1}) &= (3/8\pi)(\sin\theta e^{\mp i\phi}|V'|\sin\theta e^{\pm i\phi}) \\ &= (3/8\pi)(\sin\theta|V'|\sin\theta) = V_{pp\pi}\end{aligned} \tag{2.109}$$

where σ and π refer to $m_l = 0$ and $m_l = \pm 1$, respectively. Then we can write that

$$\begin{aligned}(x'^*|V'|x) &= \frac{1}{2}[(a_{11}^2 + a_{12}^2)](\sqrt{2}p_{+1}|V'|\sqrt{2}p_{-1}) + a_{13}^2(p_0|V'|p_0) \\ &= (1-l^2)V_{pp\pi} + l^2V_{pp\sigma}\end{aligned} \tag{2.110}$$

where we have used the well-known property of an orthogonal matrix:

$$a_{11}^2 + a_{12}^2 + a_{13}^2 = 1. \tag{2.111}$$

The rest of the terms can be found similarly.

The TB parameters for Si, C and SiC are given in Table 2.6[18].

	ϵ_s	ϵ_p	$V_{ss\sigma}$	$V_{sp\sigma}$	$V_{pp\sigma}$	$V_{pp\pi}$
Si	-5.25	1.2	-1.938	1.745	3.05	-1.075
C	-2.99	3.71	-5.550	5.910	7.78	-2.50
SiC	—	—	-3.744	3.827	5.42	-1.785

Table 2.1: TB parameters for Si, C, and SiC. All units are in eV.

2.7 Non-orthogonal TB Method

If the overlaps of the atomic orbitals are strong, we need to take into account explicitly the non-orthogonality of the atomic orbitals. In this case the secular equation includes the overlap matrix explicitly. Then the eigenvalue equation becomes

$$(H - E_n S)\psi_n = 0. \tag{2.112}$$

The eigenstates of this system can be written as a linear combination of ϕ_a

$$\psi_n = \sum_a c_a^n \phi_a \tag{2.113}$$

where ϕ_a are basis functions and c_a^n are the expansion coefficients. Then the eigenvalue problem (2.112) becomes

$$\sum_j (H_{ij} - E_n S_{ij}) c_a^n = 0 \tag{2.114}$$

where

$$H_{ij} = \int \phi_i^* H \phi_j dr \tag{2.115}$$

and

$$S_{ij} = \int \phi_i^* \phi_j dr. \tag{2.116}$$

Then in the matrix form (2.114) becomes

$$(H - E_n S)C^n = 0. \tag{2.117}$$

In order to find the eigenvalues and eigenvectors of Hamiltonian matrix H and the overlap matrix S we need to diagonalize them both simultaneously. But first we need to calculate the Hamiltonian and the overlap matrix elements.

The overlap elements are calculated by using the "Extended Huckel Approximation" [39]. Let us look at the matrix elements of the Hamiltonian between atomic orbitals on adjacent atoms, $< \beta|H|\alpha >$. If $|\alpha >$ were an eigenstate of the Hamiltonian, we could write

$$H|\alpha >= \epsilon_a|\alpha > . \tag{2.118}$$

Then if the overlap $< \beta|\alpha >$ is written as $S_{\beta a}$, the matrix element becomes $\epsilon_a S_{\beta a}$. This, however treats the two orbitals differently, so we might use the average instead of ϵ_a. However, experimental results show that we need to have a proportionality constant to obtain reasonable results,

$$< \beta|H|\alpha >= K S_{\beta a}(\epsilon_\beta + \epsilon_a)/2, \tag{2.119}$$

so that we can write

$$S_{\beta a} = \frac{2V_{\beta a}}{K(\epsilon_\beta + \epsilon_a)} \tag{2.120}$$

where $V_{\beta a}$ is $< \beta|H|\alpha >$. Now let us calculate the overlap between two hybrids which have opposite directions. The two hybrids can be written as

$$\begin{aligned} |h1 >&= cos\beta|s > + sin\beta|p > \\ |h2 >&= cos\beta|s > - sin\beta|p > \end{aligned} \tag{2.121}$$

where $|h1 >$ and $|h2 >$ are two hybrid orbitals and $cos^2\beta = \frac{1}{4}$ and $sin^2\beta = \frac{3}{4}$ for the sp^3 hybrid.

$$\begin{aligned} S_2 &= < h1|h2 >= cos^2\beta S_{ss\sigma} - 2sin\beta cos\beta S_{sp\sigma} - sin^2\beta S_{pp\sigma} \\ &= \frac{(S_{ss\sigma} - 2\sqrt{3}S_{sp\sigma} - 3S_{pp\sigma})}{4} \end{aligned} \tag{2.122}$$

where $S_{ss\sigma} =< s|s >$,$S_{sp\sigma} =< s|p >$ and $S_{pp\sigma} =< p|p >$. Similarly for H_2 we obtain

$$\begin{aligned} H_2 &= < h1|H|h2 >= cos^2\beta H_{ss\sigma} - 2sin\beta cos\beta H_{sp\sigma} - sin^2\beta H_{pp\sigma} \\ &= \frac{H_{ss\sigma} - 2\sqrt{3}H_{sp\sigma} - 3H_{pp\sigma}}{4} \end{aligned} \tag{2.123}$$

where $H_{ss\sigma} =< s|H|s >$, $H_{sp\sigma} =< s|H|p >$, and $H_{pp\sigma} =< p|H|p >$. Harrison et al. [40] approximated $H_{ll'm}$ as

$$H_{ll'm} = V_{ll',m}(1 - S_2^2) + \frac{1}{2}(\epsilon_l + \epsilon_{l'})S_{ll'm}. \tag{2.124}$$

By using (2.120) and (2.122) we obtain the following equation

$$H_{ll'm} = V_{ll',m}[1 + \frac{1}{K} - S_2^2]. \tag{2.125}$$

So now we are able to calculate the Hamiltonian matrix elements and the overlap elements, so that we can construct the secular equation and solve it by matrix diagonalization.

To calculate interatomic forces, let us take the derivative of (2.117) with repect to x and then multiply it on the left with C^{n+}. Then we obtain

$$C^{n+}(\frac{\partial H}{\partial x} - \frac{\partial E_n}{\partial x}S - E_n\frac{\partial S}{\partial x})C^n + C^{n+}(H - E_nS)\frac{\partial C^n}{\partial x} \tag{2.126}$$

Clearly the second term is zero. From the first term we obtain that

$$\frac{\partial E_n}{\partial x} = \frac{C^{n+}(\partial H/\partial x - E_n\partial S/\partial x)C^n}{C^{n+}SC^n} \tag{2.127}$$

This is the electronic part of the total force. The forces due to the pair potential can be calculated by taking the gradient of the pair potential.

2.8 Self-Consistent TB Method

When there is a charge transfer between atoms it is necessary to apply some sort of self-consistency to the solution of the TB method. One of the methods which is used is the local charge neutrality approximation [41, 42]. In this approximation, the diagonal elements of the Hamiltonian matrix are modified until there is no net charge transfer between atoms. This means that each atom will have four electrons at the end. The perturbation of the site energies $\epsilon_s - \epsilon_p$ due to charge transfer between two or more atoms can be given as

$$d\epsilon = (1 - Cx)^{-1} C dq \tag{2.128}$$

where $d\epsilon$ is the change in the site energy, C is the Coulomb matrix and x is the linear response matrix and dq is the charge transferred. For charge neutral condition (2.128) is reduced to $x^{-1}dq$. The calculation of the linear response matrix x is computationally demanding. Instead of calculating this matrix, the charge transfer is assumed to be proportional to the site energy shift, the proportionality constant is approximately 1 eV which was found by trial and error. Usually one or two iterations are enough to eliminate the charge transfer.

The self-consistency arises as a result of the fact that all one-electron energy levels depend on the electron population which is determined in turn by the one-electron energies.

If we do not enforce charge neutrality, we need to carry out fully self-consistent calculations. The TB Hamiltonian is expressed using the local orthogonal basis as

$$H = \sum_{i\mu} |i\mu > E_{i\mu} < i\mu| + \sum_{i\mu} \sum_{j\nu} |i\mu > t_{i\mu j\nu} < j\nu| \tag{2.129}$$

where $|i\mu >$ is the ket for atom i orbital μ, and $E_{i\mu}$ and $t_{i\mu j\nu}$ are the on-site and hopping energies. Effective Coulomb potential arising due to charge transfer is included

in $E_{i\mu}$ self-consistently

$$E_{i\mu} = E^0_{i\mu} + U_i(Q_i - Z_i)V(\vec{R}_j, \vec{R}_i) + f_{i\mu}, \tag{2.130}$$

where $E^0_{i\mu}$ is the orbital energy of the neutral free atom i, U_i is an average of the interatomic Coulomb integrals of the valence electrons of the atom i, Z_i and Q_i are the charge of the ion core and total valence occupancy of this atom. Q_i is given as

$$Q_i = \sum_{\mu} \sum_{n} | < n|i\mu > |^2. \tag{2.131}$$

All these occupancies should be calculated self-consistently. The third term in (2.130) is the electrostatic interatomic potential at site i due to cores and electrons in the system. The fourth term $f_{i\mu}$ is the non-orthogonality correction and given by the overlap matrix elements between atomic orbitals. The total energy of the system of electrons and ion cores is given as

$$E_{tot} = E_{bs} - E_{e-e} + E_{i-i} \tag{2.132}$$

where

$$E_{bs} = \sum_{n}^{occ} E_n = \sum_{n}^{occ} < n|H|n > . \tag{2.133}$$

E_{e-e} and E_{i-i} are the electron-electron and ion-ion interaction energies. E_n is the eigenenergy and E_{bs} is the band structure energy, where the electron-electron interaction is double counted. By using (2.129), (2.130), and (2.133) we obtain that

$$\begin{aligned} E_{bs} &= \sum_{i\mu} Q_{i\mu} E_{i\mu} + \sum_{i\mu} \sum_{j\nu} P_{i\mu j\nu} t_{i\mu j\nu} = \\ &= \sum_{i\mu} Q_{i\mu} E^0_{i\mu} + \sum U_i Q_i (Q_i - Z_i) + \sum_{i} \sum_{j \neq i} Q_i (Q_j - Z_j) V(\vec{R}_j, \vec{R}_i) + \\ &\quad \sum_{i\mu} Q_{i\mu} f_{i\mu} + \sum_{i\mu} \sum_{j\nu} P_{i\mu j\nu} t_{i\mu j\nu} \end{aligned} \tag{2.134}$$

where $P_{i\mu j\nu}$ is the bond order and given as

$$P_{i\mu j\nu} = \sum_{n}^{occ} < n|i\mu >< j\nu|n > . \tag{2.135}$$

A more explicit total energy expression can be given as

$$\begin{aligned} E_{tot} &= E_{atom} + E_{overlap} + E_{Mad} + E_{cov} \\ E_{atom} &= \sum_i \{\sum_\mu Q_{i\mu}(E^0_{i\mu} - U_i Z_i) + \frac{1}{2} U_i Q_i^2\} \\ E_{overlap} &= \sum_{i\mu} Q_{i\mu} f_{i\mu}, \\ E_{Mad} &= \frac{1}{2} \sum_i \sum_{j \neq i} (Q_i - Z_i)(Q_j - Z_j) V(\vec{R}_j, \vec{R}_i) \\ E_{cov} &= \sum_{i\mu} \sum_{j\nu} P_{i\mu j\nu} t_{i\mu j\nu} \end{aligned} \tag{2.136}$$

The total energy should be computed self-consistently. The meaning of the various terms are clear. E_{atom} is the total energy of the isolated atoms whose occupancies are Q_i. $E_{overlap}$ is the overlap interaction energy which is the increase in the kinetic energy of the electrons upon compression. E_{Mad} is the Madelung energy, which is a sum of Coulomb interactions between atoms with effective charges, $Q_i - Z_i$. E_{cov} is the covalent energy. For ionic systems E_{Mad} and $E_{overlap}$ are dominant terms. In the covalent systems E_{cov} and $E_{overlap}$ are dominant.

2.8.1 Hamiltonian Matrix in the SCTB Model

In order to find the eigenvalues and eigenvectors of the Hamiltonian, we need to construct the Hamiltonian matrix first. The Hamiltonian matrix elements are constructed by assuming the r^{-2} dependence on the interatomic distance r as

$$H_{ll'm} = \eta_{ll'm} \hbar^2 / m r^2 \tag{2.137}$$

where $\eta_{ll'm}$ are universal TB parameters and m is the electron mass.

The overlap matrix elements are calculated by using extended Huckel theory. The

determination of $S_{ll'm}$ is important because the interatomic repulsion is determined by those terms. Kohyama et al. [34] adopted a $1/r^3$ form

$$S_{ll'm} = \eta_{ll'm}[2/(E^0_{il} + E^0_{jl'})](\hbar^2/m)(d_0/Kr^3) \tag{2.138}$$

where $d_0 = e^2(1/U_i + 1/U_j)/2$. Majewski and Vogl [32] determined the values of K and U_i for each row of the periodic table to obtain agreement with the bond length and bulk modulus of various sp bonded semiconductors and insulators. The non-orthogonality correction to the Hamiltonian matrix elements is given as

$$f_{i\alpha} = -\sum_{j\beta} S_{i\alpha j\beta} H_{j\beta i\alpha}. \tag{2.139}$$

In this sum only the nearest neighbors are taken into account. Now we know everything to find the Hamiltonian matrix. After finding the Hamiltonian matrix, we need to diagonalize it to find eigenvalues and eigenvectors.

2.8.2 Atomic Forces in the SCTB Model

In the SCTB model diagonal terms of the Hamiltonian also depend on the ionic coordinates, so calculation of the interatomic forces is a little bit tricky. We express the eigenvector $|n>$ as $\sum_{i\mu} C^n_{i\mu}|i\mu>$ so that we can write (2.131) and (2.135) as

$$Q_{i\mu} = \sum_n^{occ} C^{n*}_{i\mu} C^n_{i\mu} \tag{2.140}$$

and

$$P_{i\mu j\nu} = \sum_n^{occ} C^{n*}_{i\mu} C^n_{j\nu}. \tag{2.141}$$

The normality condition of the eigenvectors are given as

$$\sum_{i\mu} C^{n*}_{i\mu} C^n_{i\mu} = 1. \tag{2.142}$$

The derivative of the total energy is given as [43]

$$\frac{\partial E_{tot}}{\partial \vec{R}} = \sum_{i\mu} Q_{i\mu} \frac{\partial f_{i\mu}}{\partial \vec{R}_l} + \frac{1}{2} \sum_i \sum_j (Q_i - Z_i)(Q_j - Z_j) \frac{\partial V(\vec{R}_j, \vec{R}_i)}{\partial \vec{R}_l} + \sum_{i\mu} \sum_{j\nu} P_{i\mu j\nu} \frac{\partial t_{i\mu j\nu}}{\partial \vec{R}_l}. \tag{2.143}$$

There are three terms in the derivative of the total energy. Those terms are explicit functions of the interatomic distances. All of the three terms can be differentiated analytically and the bond order $P_{i\mu j\nu}$ can be calculated by diagonalizing the Hamiltonian matrix.

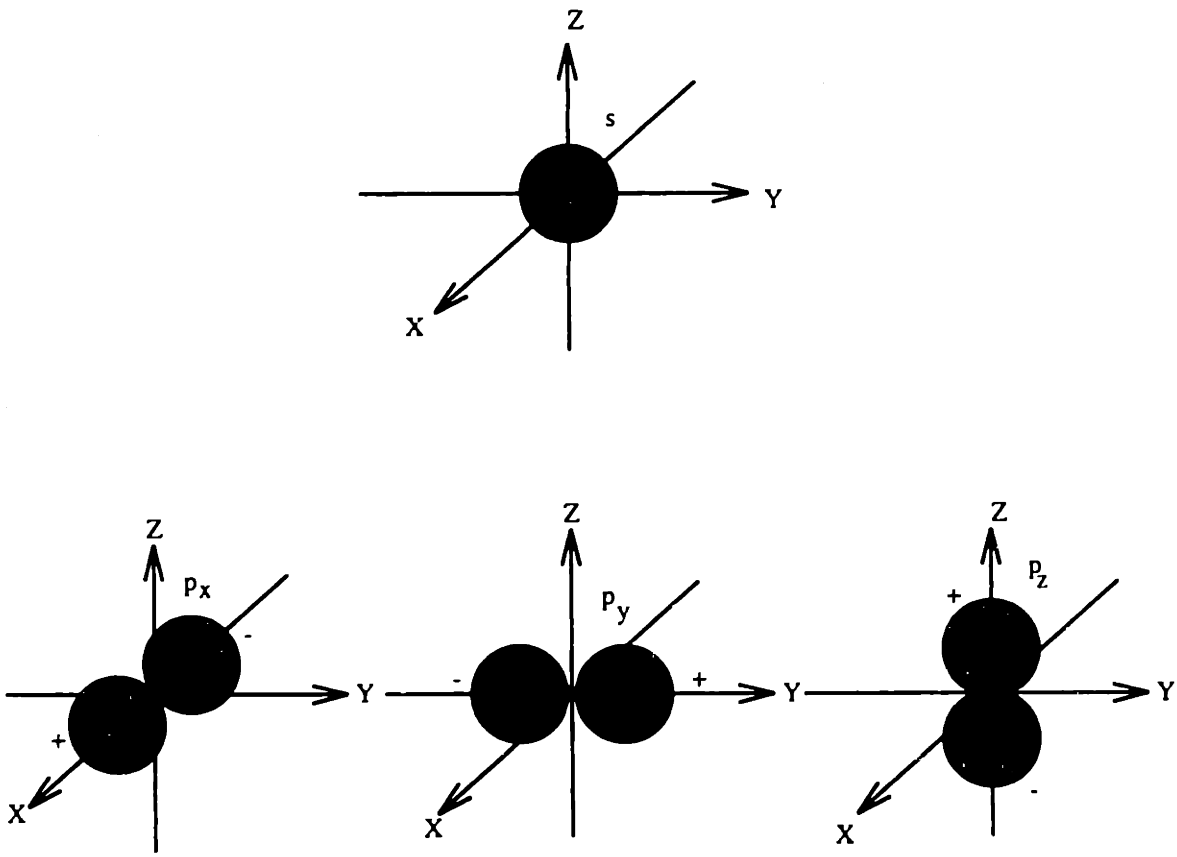

Figure 2-1: The atomic orbitals for l=0 and l=1.

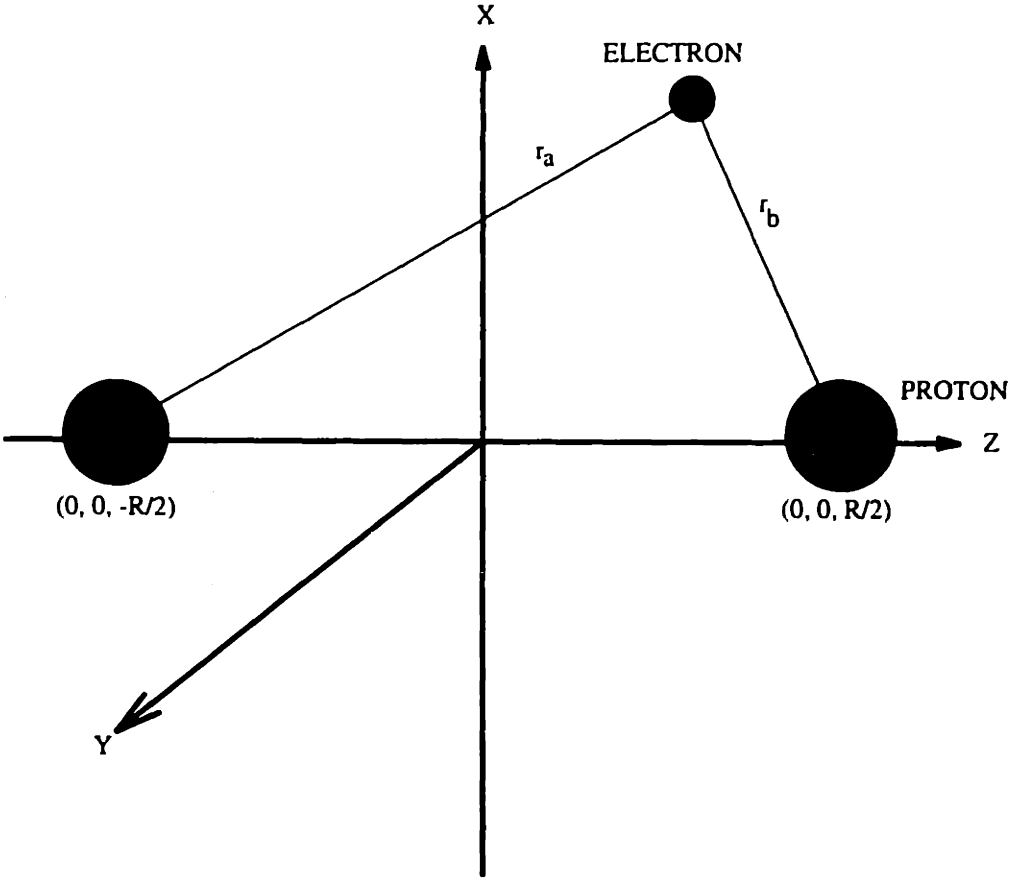

Figure 2-2: The geometry used for H_2^+.

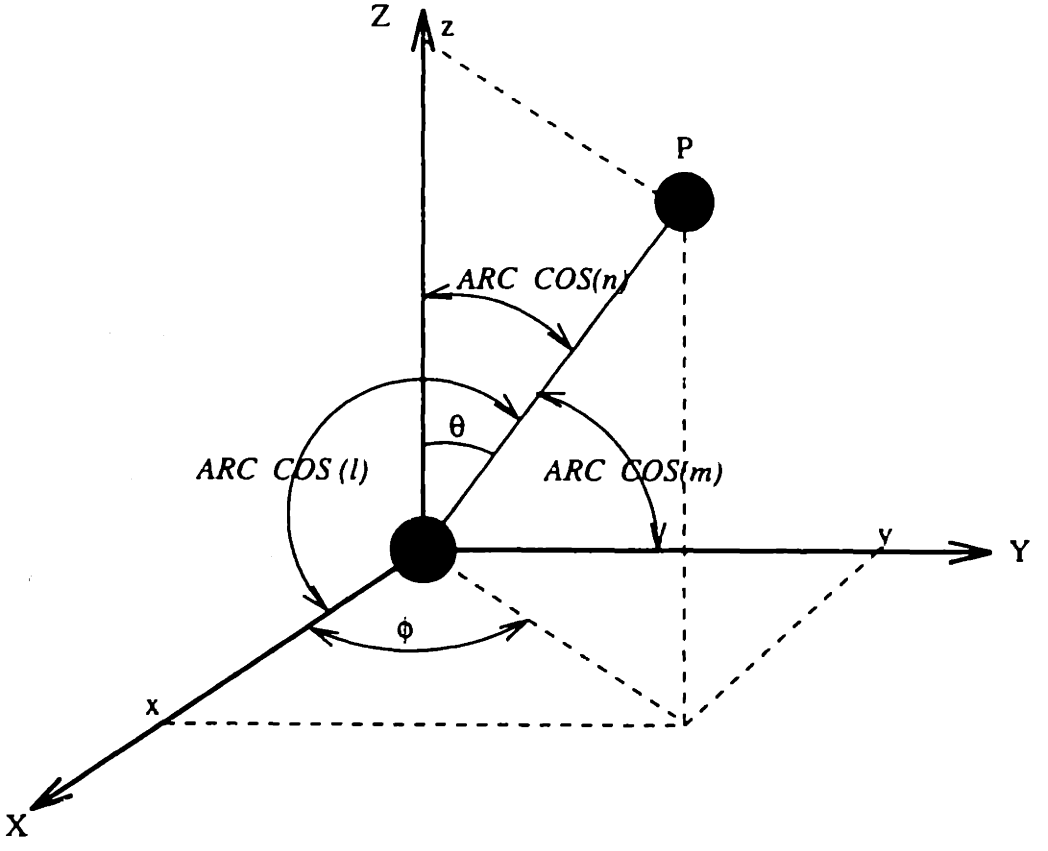

Figure 2-3: Coordinates used for two-center integrals.

Chapter 3

Bulk and Cluster Properties of Silicon and Carbon

In this chapter, we will investigate bulk properties of carbon and silicon and also calculate cluster energies and structures. Calculating properties of silicon and carbon provides an important check for the TB method because there are extensive experimental and theoretical data to compare our results with. Correct prediction of cluster structure and energies shows that the TB method is transferable.

3.1 Total Energy and Band-Structure Energy

The total energy is one of the most important quantities which determine properties of materials. Materials want to minimize their free energy which is a function of the total energy. Most of the phenomena observed in materials, like phase transitions can be explained as the material trying to reduce its free energy to reach a more stable state. At zero temperature it consists of the potential energy of all the particles.

Total energy is in general a very complicated function of the particle coordinates. Usually we are interested in the total energy of a given crystal structure. Then the number of variables is reduced greatly. For example, if we assume that the crystal is diamond-cubic, then the only variable on which the total energy depends is the bond length. One of the most reliable ways of calculating the total energy is the density

functional approach [7]. To find the equilibrium bond length, the total energy is calculated for various bond lengths for a given structure and a curve is fitted to the data. The bond length at the minimum of the curve is the zero temperature equilibrium bond length.

The TB total energy consists of two parts. One part is the band-structure energy which is the sum of the twice electron-electron interaction energy plus the electron-ion interaction energy. The other part is a pair potential which is the ion-ion interaction energy minus the electron-electron interaction energy. The sum of the pair potential and the band-structure energy gives the total energy. Calculation of the band structure energy is computationally most expensive part of the TB method. We will give an example for how to calculate the band-structure energy. Suppose that there are only two atoms and only one orbital located on these atoms. Suppose that the TB matrix element V changes exponentially with the interatomic distance. Then the Hamiltonian matrix can be written as

$$H = \begin{pmatrix} \epsilon_1 & V \\ V & \epsilon_2 \end{pmatrix} \tag{3.1}$$

where ϵ_1 and ϵ_2 are orbital energies of the two atoms. Then the eigenvalues of the Hamiltonian can be written as

$$\epsilon_{\pm} = \frac{1}{2}(\epsilon_1 + \epsilon_2) \pm \frac{1}{2}[(\epsilon_1 - \epsilon_2)^2 + 4V(r)^2]^{1/2}. \tag{3.2}$$

Since the bonding state (valence band) is doubly occupied and the antibonding state (conduction band) is unoccupied, the total energy of the system can be written as

$$U(r) = 2\epsilon_- + \phi(r) \tag{3.3}$$

where $\phi(r)$ is the corrective pair potential. As r decreases, $|V(r)|$ increases, so ϵ_- decreases and the electronic force is attractive. Suppose that the pair potential is

given as

$$\phi(r) = \phi_0 exp[-\beta(r-d)] \tag{3.4}$$

and the Hamiltonian matrix element is given as

$$V(r) = V(r_0) exp[-\alpha(r-r_0)]. \tag{3.5}$$

Then the total force can be written as

$$\begin{aligned} F(r) &= -\frac{dU(r)}{dr} \\ &= -2\alpha[1+[\frac{\epsilon_1-\epsilon_2}{2V(r)}]^2]^{-1/2}|V(r)| + \beta\phi(r). \end{aligned} \tag{3.6}$$

An important point to notice in (3.6) is that the force depends on the difference between orbital energies and not on their absolute values. It means that we can choose orbital energies arbitrarily provided their difference is constant.

We have discussed how to calculate the band-structure energy for arbitrary number of atoms in Chapter 2 in detail. The band-structure energy creates an attractive potential. One way of calculating the purely repulsive pair potential is to subtract the band-structure energy from the the total energy for the diamond-cubic structure and fit a function to it. Another method is to assume an exponentially decaying pair potential and fit the coefficient of the exponential to obtain the experimental lattice parameter. We will use both of these methods. For silicon, we will use the first method which is subtracting the band-structure energy from the total energy. For carbon, we will fit an exponentially decaying function to obtain the correct lattice parameter.

We took the total energy for silicon from [45]. We obtained the pair potential for diamond-cubic structure and used it in our MD simulation.

A good empirical potential function should give correct total energy for a given system. We calculated the total energy with respect to the lattice parameter for the empirical potentials constructed by Stillinger-Weber and Tersoff [3, 2] for silicon and

plotted (Figure 3-1). It is seen that the Tersoff potential gives unphysical results for large interatomic distances. The reason for this is the cutoff function used to bring the total energy smoothly to zero at large interatomic distances. For short interatomic distances, Tersoff potential function gives closer results to the ab-initio calculations than the Stillinger-Weber potential.

In the TB method for silicon, the ab-initio total energy is used for the calculation of the pair potential. The most important component of our total energy comes from the band-structure energy calculations. To find the total energy, we need to subtract the electron-electron energy and add the ion-ion interaction energy. In Chapter 2 we proved that this correction can be represented as a pair potential. This correction is obtained by subtracting the band-structure energy from the ab-initio total energy. The result is expressed as a fifth order polynomial of nearest neighbor distance.

Actually, we don't have to use ab-initio total energy results in our MD simulation program. We can choose an exponential pair potential and fit the coefficient and exponent of the exponential to obtain correct lattice parameter at zero temperature. This is the method used by Menon et al. [46]. The advantage of this method is that instead of fitting a curve, we only need to fit a number. For carbon, we developed a code which employs this method. We explicitly took into account the overlap interactions as well. The results for the carbon calculations will be given in the following Chapter.

3.1.1 Calculation of Pressure

Pressure can be calculated by taking the derivative of the total energy with respect to volume:

$$P = -\frac{dE}{dV}. \tag{3.7}$$

For the diamond-cubic structure, we have eight atoms in the unit cell. The volume change with lattice parameter is a known function of the structure. By using the

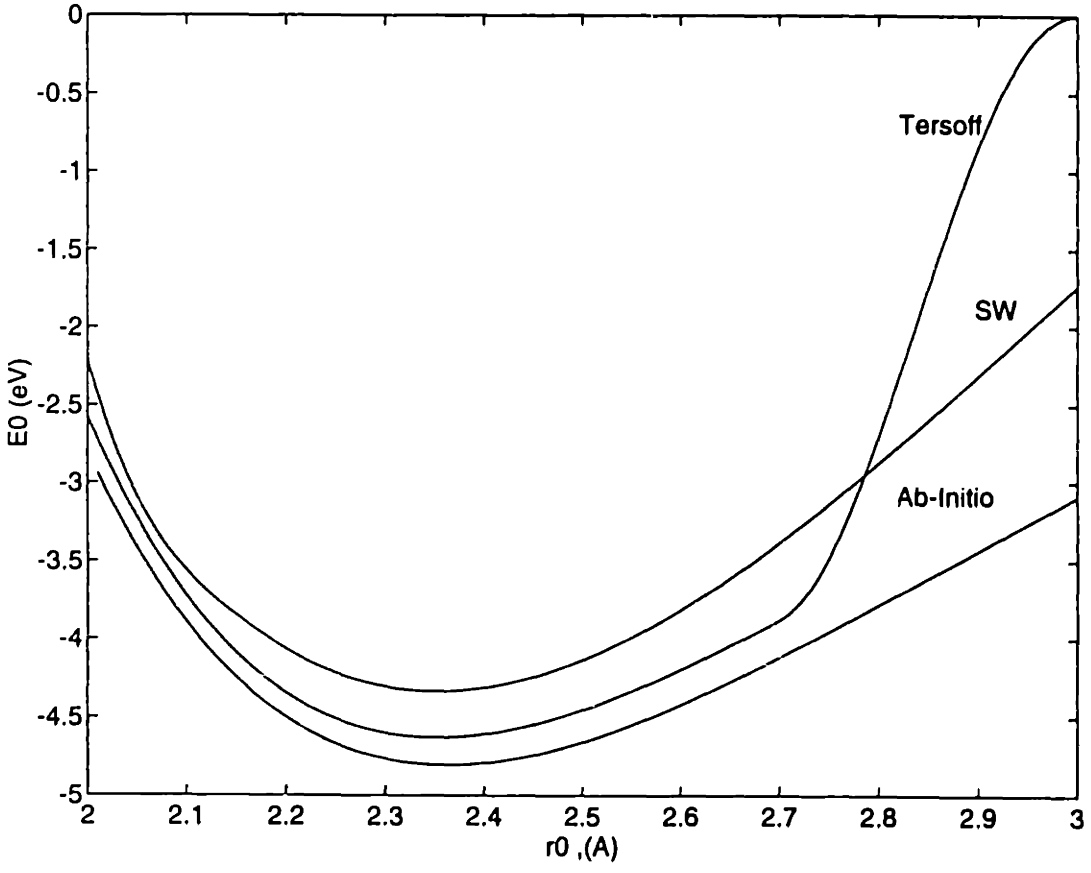

Figure 3-1: The total energy for silicon from ab-initio, Tersoff and Stillinger-Weber potentials.

chain rule we can calculate the pressure as

$$P = -8\frac{\partial E}{\partial d}\frac{\partial d}{\partial V}. \tag{3.8}$$

The second term can be easily found for any crystal structure. The bulk modulus can be calculated by taking the second derivative of the total energy with respect to volume

$$B = V\frac{\partial^2 E}{\partial V^2}. \tag{3.9}$$

Again, because we know the structure of the unit cell and the dependence of the total energy on interatomic distance, we can calculate the bulk modulus. The cohesive energies and the bulk moduli of Si and C are given in references [47, 48].

3.1.2 Phase Transitions at High Pressures

Many materials undergo a phase transition under sufficiently high pressures. Some of the materials undergo multiple phase transitions depending on pressure. Silicon is one of the materials which show many different phases under various pressures [49]. These phase transitions are actually observed by using the diamond anvil cell technique. In this technique, the material is put in a cylindirical hole in a flat metallic plate. The hole is filled with a liquid, usually a mixture of ethanol, methanol and water. Then the hole is crushed from the top and the bottom by flat surfaced diamond anvils and the substance is observed with a TV camera through the diamond anvils. Under these conditions it was observed that at about 100 kBar silicon becomes a yellow shiny metal [49].

The differece between metals and semiconductors is that semiconductors have a band-gap at the conduction level but metals do not. The metallization process can be described as a band-gap closure phenomenon. When silicon transforms to β Sn structure, the band-gap disappears and bands overlap. As a result there will be many electrons in the half-filled conduction bands which is a characteristics of

metallic structure [50]. Actually, insulator-conductor transition is a complicated phenomenon. When atoms are far apart, the system is an insulator because the electrons are strongly localized. When we bring atoms closer, electrons get delocalized and the system becomes conductor. There is a lattice parameter at which the insulator-conductor transition takes place. By using the TB method, we can determine this lattice parameter. As this phenomenon suggests, properties of materials are strongly dependent on their electronic structures and empirical potential functions can give only qualitative results because they do not take into account electronic structure effects.

Total energy can be used to predict phase transitions at high pressures. To predict a phase transition between two different crystal structures, we need to compute free energies at zero temperature. Phase transition takes place at a pressure which makes the free energies of the two structures equal. Free energy is the driving force of the phase transitions. Materials want to minimize their free energies so that when there is a structure with lower free energy, we expect a transition to this structure. Usually phase transitions do not take place exactly at the free energy which is the same for the both structure. The pressure at which the free energies are the same is the minimum pressure at which a phase transition may be obseved. But to start the actual transition, there should be defects in the material like surfaces or point defects. In a perfectly ordered material, we need to go to much higher pressures to observe the phase transition. The free energy is nothing but the sum of the total energy and PV because the entropy term is zero at zero temperature. To find the pressure at which a phase transition is expected, we need to find the common tangent to the two total energy curves. Then the phase transition pressure can be calculated as[32]

$$P_t = \frac{E(V_1) - E(V_2)}{V_1 - V_2} \tag{3.10}$$

where E is the total energy and V_1 and V_2 are volumes at which the tangent touches the total energy curves. I calculated the phase transition pressure for silicon as 95 kbar in close agreement with the result in [49](105 kbar).

Diamond may undergo a phase transition at extremely high pressures, even though such pressures have not been obtained experimentally yet. M. Cohen[51] calculated the transition pressure for diamond by using the density functional theory as 23 MBar. He calculated total energy curves for various crystal structures for carbon and found the pressure at which the free energies are the same for given two structures. The transition is to the simple cubic structure and carbon is still insulating at this phase. It should be noted that the transition takes place at an extremely high pressure. The reason for this is that diamond cubic crystal for carbon has smaller volume than all the other crystal structures of carbon, so in effect for carbon the diamond-cubic structure is close packed. Phase transition can take place only at extremely high pressures. This pressure is a theoretical limit for the pressures attainable with the diamond anvil cells.

3.2 Elastic Constants

Elastic constants yield valuable dynamical and mechanical information about materials. For example, through the Born relations they yield information about the stability and strength of solids. The comparision of the experimentally determined and theoretically calculated elastic constants is an important way of testing interatomic potentials. Because the origin of the elastic constants lies in the interatomic forces, elastic constants provide a powerful tool to investigate interatomic forces.

A solid body changes its shape when subjected to a stress. If the stress is kept below a certain limit, the strain is recoverable, that is to say, when the stress is removed, the body returns to its original shape. For higher stresses the body cannot recover its original shape and will eventually fail. For small enough stresses the amount of strain is proportional to the magnitude of the applied stress (Hooke's Law). Hooke's Law states that

$$\sigma = c\epsilon. \tag{3.11}$$

(3.11) can be generalized to obtain general stress-strain relationship in tensor form. A homogeneous stress and a homogeneous strain are each specified by second rank tensors[95]. If a general homogeneous stress σ_{ij} is applied to a crystal, the resulting homogeneous strain ϵ_{ij} is such that each component is linearly related to all components of the stress. The stresses may be expressed in terms of strains by the equations

$$\sigma_{ij} = c_{ijkl}\epsilon_{kl} \tag{3.12}$$

where c_{ijkl} are the 81 elastic constants of the crystal[95]. Those 81 components form a fourth rank tensor. Stress and strain tensors are symmetric, which requires that the elastic constant tensor is also symmetric. We may write that $c_{ijkl} = c_{ijlk}, c_{ijkl} = c_{jikl}$. Symmetry of the elastic constants tensor reduces the number of the independent elastic constants to 36. Crystal symmetry reduces the number of independent elastic constants further. Detailed information about elastic constants for various crystal groups is given in [95]. In cubic crystals there are only three independent elastic constants, namely c_{11}, c_{12}, and c_{44}. In a molecular dynamics simulation, all the elastic constants can be calculated. Some of the elastic constants will be required to be zero and some will be required to be equal to the others. By calculating these elastic constants which are supposed to be equal to each other as a result of crystal symmetry, we can check whether the MD results are converging or not.

We will use Voigt's notation for elastic constants. In this notation, four indices of the elastic constants are reduced to two according to the following convention:

$$11 \rightarrow 1,\ \ 22 \rightarrow 2,\ \ 33 \rightarrow 3,\ \ 23\ 32 \rightarrow 4,\ \ 31\ 13 \rightarrow 5,\ \ 12\ 21 \rightarrow 6 \tag{3.13}$$

According to this notation, c_{1112} is written as c_{16}.

Elastic constants are determined experimentally by using various techniques including Brillouin scattering, ultrasonic wave propogation, and neutron scattering [52, 53, 54, 55]. If the potential function is known for a material, elastic constants can be calculated by MD or Monte Carlo simulation and it is possible to peredict the behavior of the material under normal or extreme loading.

The theory of calculations of elastic constants using Monte Carlo simulation was first developed by Squire et al. [56]. In this method the elastic constants are calculated by using the fluctuation formulas. To use this method, we need to calculate the stress tensor fluctuations, a kinetic energy term and a Born term which requires second derivatives of the potential function and gives elastic constants at zero temperature.

The (E,h,N) ensemble is especially suitable for calculation of elastic constants where E is the system energy, h is a matrix constructed using the three vectors spanning the MD cell $(\vec{a}, \vec{b}, \vec{c})$, and N is the number of particles. The difference between (E,h,N) and (E,V,N) ensembles is important. In the (E,V,N) ensemble not only the volume but also the shape of the simulation cell is conserved. It is only by allowing the shape to change are we able to calculate elastic constants by MD simulation. The shape of the molecular dynamics cell is not arbitrary, but is always a parallelopiped.

To find the elastic constants, we need to define strain first. Strain is defined according to a reference state. The reference state of the system is defined by $\mathbf{h_0}$ and the volume $\Omega_0 = \det(\mathbf{h_0})$. Finding the reference state is an important step in calculating the elastic constants. The Parrinello-Rahman method[98] can be used to maintain the system at zero stress, and $\mathbf{h_0}$ can be obtained at the end of the simulation. Another method is to run a microcanonical ensemble MD simulation several times in order to find zero pressure configuration. Elastic constants are very sensitive functions of the reference state, so the components of the $\mathbf{h_0}$ must be calculated to high accuracy.

We may define a coordinate transformation by using $\mathbf{h_0}$

$$\vec{r_0} = \mathbf{h_0}\vec{s}. \tag{3.14}$$

A homogeneous deformation of the system changes $\mathbf{h_0}$ to $\mathbf{h}$ moving $\vec{r_0}$ to $\vec{r}$ where

$$\vec{r} = \mathbf{h}\vec{s} = \mathbf{h}\mathbf{h_0^{-1}}\vec{r_0}. \tag{3.15}$$

We obtain the displacement $\vec{u}$ due to distortion as

$$\vec{u} = \vec{r} - \vec{r}_0 = (\mathbf{h}\mathbf{h}_0^{-1} - 1)\vec{r}_0. \tag{3.16}$$

Now we may use the definition of Landau and Lifshitz[99] for strain

$$\epsilon_{\lambda\mu} = \frac{1}{2}(\frac{\partial u_\lambda}{\partial x_\mu} + \frac{\partial u_\mu}{\partial x_\lambda} + \sum \frac{\partial u_\nu}{\partial x_\mu}\frac{\partial u_\nu}{\partial x_\lambda}). \tag{3.17}$$

From (3.16) we find that

$$\frac{\partial u_\lambda}{\partial x_\mu} = a_{\lambda\mu} - \delta_{\lambda\mu} \tag{3.18}$$

where $a_{\lambda\mu}$ is an element of matrix $\mathbf{h}\mathbf{h}_0^{-1}$. By using (3.17) we find that

$$\begin{aligned} \epsilon_{\lambda\mu} &= \frac{1}{2}(a_{\lambda\mu} - \delta_{\lambda\mu} + c_{\mu\lambda} - \delta_{\mu\lambda} + \sum(a_{\nu\mu} - \delta_{\nu\mu})(a_{nu\lambda} - \delta_{\nu\lambda})) \\ &= \frac{1}{2}(\sum_\nu a_{\nu\mu}a_{\nu\lambda} - \delta_{\mu\lambda}). \end{aligned} \tag{3.19}$$

It follows from (3.19) that

$$\epsilon = \frac{1}{2}(\mathbf{h}_0'^{-1}\mathbf{G}\mathbf{h}_0^{-1} - I) \tag{3.20}$$

where $\mathbf{G} = \mathbf{h}'\mathbf{h}$.

It is known that[95] in the case of central force potentials like the Lennard-Jones potential, $c_{12} - c_{44} = 0$. This eqaution is known as Cauchy relation. In actual crystals, the Cauchy relation is always violated. For a potential function to represent a material realistically, it should violate the Cauchy relation.

First principles calculation of the elastic constants at 0 K is given in [100]. The second derivatives of the total energy of the system with respect to various strains need to be calculated. The weakness of this calculation is that at high temperatures $30 - 40\%$ of the magnitudes of the elastic constants is due to thermal fluctuations which are ignored in this calculation [57].

All elastic constant calculations by using fluctuation formulas require second derivatives of the potential energy. In the case of the TB method, we need to find the second derivative of the band structure energy. Calculation of the second derivative of the band-structure energy is not straightforward. We know from the Hellmann-Feynman theorem that[37]

$$\frac{\partial U}{\partial \lambda'} = \int \psi^*(\frac{\partial H}{\partial \lambda'})\psi d\tau \tag{3.21}$$

where H is the Hamiltonian and λ is a real variable. By taking the second derivative we find that [103]

$$\frac{\partial^2 U}{\partial \lambda' \partial \lambda''} = \int \psi^*(\frac{\partial^2 H}{\partial \lambda' \partial \lambda''})\psi d\tau + \int \psi^*(\frac{\partial H}{\partial \lambda'})(\frac{\partial \psi}{\partial \lambda''})d\tau - \int (\frac{\partial \psi^*}{\partial \lambda''})(\frac{\partial H}{\partial \lambda'})\psi d\tau. \tag{3.22}$$

The first term poses no problems, but the calculation of the second and third terms is difficult. A perturbation approach can be used to calculate the second derivative of the band-structure energy. The result is [104]

$$(\frac{\partial^2 E_{b\vec{k}}}{\partial \gamma_\lambda^2}) = H_{bb}^{(\lambda 2)}(\vec{k}) + 2\sum_{b'}{}' \frac{|H_{bb'}^{(\lambda 1)}(\vec{k})|^2}{E_{b\vec{k}} - E_{b'\vec{k}}} \tag{3.23}$$

where $H_{bb'}^{(\lambda 1)}$ is the matrix element of the first derivative of the Hamiltonian and $H_{bb'}^{(\lambda 2)}$ is the matrix element of the second derivative of the Hamiltonian.

Lee and Joannopoulos used Green's function approach to calculate the second derivative of the band-structure energy[105]. Their formula is applicable not only to periodic systems, but also to disordered systems. They obtained the following result

$$\frac{\partial^2 E_{BS}}{\partial x_\alpha^i \partial x_\beta^j} = -\frac{1}{\pi}\int_{-\infty}^{\epsilon_F} d\epsilon Im Tr\{G_B(\epsilon)\frac{\partial^2 H}{\partial x_\alpha^i \partial x_\beta^j} + G_B(\epsilon)\frac{\partial H}{\partial x_\alpha^i}G_B(\epsilon)\frac{\partial H}{\partial x_\beta^j}\} \tag{3.24}$$

where $\partial^2 H/\partial x_\alpha^i x_\beta^j$ and $\partial H/\partial x_\alpha^i$ are the derivatives of the Hamiltonian with respect to ionic coordinates and $G_B(\epsilon)$ is bulk Green function.

We calculated elastic constants by using stress-strain curves. We applied a strain to the system and calculated resulting stress. We used the following equations to

	C_{11}	C_{12}	C_{44}
SW	1.5	0.76	0.6
Tersoff	1.5	0.8	0.7
TB	1.54	0.87	0.82
Exp't	1.66	0.64	0.80

Table 3.1: Elastic constants of Si obtained by using SW potential, Tersoff potential, and the TB method compared with the experiment.

	C_{11}	C_{12}	C_{44}
TB	9.5	1.7	5.05
Exp't	10.8	1.25	5.77

Table 3.2: Elastic constants of C obtained by the TB method compared with experiment.

calculate the elastic constants:

$$\sigma_{11} = c_{11}\epsilon_{11} + c_{12}\epsilon_{22} + c_{12}\epsilon_{33} \tag{3.25}$$

$$\sigma_{22} = c_{12}\epsilon_{11} + c_{11}\epsilon_{22} + c_{12}\epsilon_{33} \tag{3.26}$$

$$\sigma_{33} = c_{12}\epsilon_{11} + c_{12}\epsilon_{22} + c_{11}\epsilon_{33} \tag{3.27}$$

$$\sigma_{23} = c_{44}\gamma_{23} \tag{3.28}$$

$$\sigma_{13} = c_{44}\gamma_{13} \tag{3.29}$$

$$\sigma_{12} = c_{44}\gamma_{12} \tag{3.30}$$

To calculate c_{11}, we changed h_{11} and for each value of h_{11} we calculated σ_{11}. Then we fitted a curve to the stress-strain graph and the slope of this curve gave us c_{11}. To obtain c_{12}, we calculated σ_{22} and plot the $\sigma_{22} - \epsilon_{11}$ graph. From the slope of this graph we ontained c_{12}. c_{44} is calculated by simultaneously changing ϵ_{12} and ϵ_{21} and calculating σ_{12}. Then the stress-strain curve is plotted and the slope of the curve is found. The elastic constants of Si and C calculated by using the TB method, Tersoff potential, SW potential compared with respect to experimental data are given in Tables 3.1 and 3.2.

3.3 Silicon Clusters

Empirical potential functions in general fail to produce correct energies and structures of clusters. Empirical potential functions are usually fitted to the bulk properties of materials and give poor results for structures radically different from crystal structure. The TB method is superior to the empirical potential functions and give good results for both bulk and cluster properties. A good prediction of the cluster properties means that the TB method is capable of treating short-range order as seen in liquids and amorphous materials. We investigated cluster properties by using the method developed by Goodwin et al. [41]. Our results are shown in Figure 3-2.

Silicon clusters were extensively investigated by using Stillinger-Weber potential [2] by Barojas and Levesque [58]. These authors have also looked at charged clusters. They carried out MD simulation of clusters up to 22 atoms. The cluster structures are not in agreement with ab-initio and TB results for small clusters. As the number of particles in clusters increase, the structure becomes diamond cubic. They observed liquid-solid like phase transitions in clusters. They concluded that a potential like SW potential which was fitted to the bulk properties of crystals cannot describe cluster properties adequately. Cluster properties should be used in the fitting process too. They showed that if atoms in the cluster are charged, the structure of the cluster is modified significantly.

There are extensive ab-initio results for silicon clusters[59, 60, 61], but not much experimental results. In the case of the ab-initio calculations, only a local minimization is applied, usually the bond lengths are optimized for a given geometrical structure.

Our results for Si cluster energies and structures are given below:

The binding energy for Si_2 is $E_2 = -3.04eV$ and the equilibrium distance between atoms is $d = 2.27A$. The experimental value for the binding energy of Si_2 is $3.24eV$[61].

The binding energy for Si_3 is $E_3 = -7.35eV$ and the cluster is an isosceles triangle with a side length of $2.15A$ and an opening angle of $\theta = 80°$. These results are very

close to those obtained in [62, 63] and the energy is in good agreement with the experimental value of $-7.4 \pm 0.5eV$.

For Si_4 the minimum structure is a flat rhombus with a side length of $2.35A$ and the diagonal lengths of $2.50A$ and $4.05A$. The binding energy of this structure is $E_4 = -12.60eV$

In the case of Si_5 the binding energy is $-15.6eV$. The structure is highly asymmetric.

For Si_6 the minimum energy structure is a tetracapped trigonal prism with minimum energy of $E_6 = -20.80eV$. The bond lengths are between 2.4 to $2.6A$.

The minimum energy configuration for Si_7 is the pentagonal bipyramid with side length $2.5A$ and cap-to-basis distance $2.6A$. The minimum energy for this structure is $E_7 = -26.5eV$ and very close to the result in [61].

The minimum energy for Si_8 is $E_8 = -29.6eV$. The structure is similar to that of Si_7.

The minimum energy configuration for Si_9 is the tricapped trigonal prism. The energy for this structure is $E_9 = -33.1eV$.

The minimum energy structure for Si_{10} is tetracapped trigonal prism structure with minimum energy of $E_{10} = -39.1eV$.

Chelikowsky and Glassford[64] investigated silicon clusters by developing their own potential function. This potential function is based on "covalent-metallic" phase transition. They found that Si_n clusters follow an icosahedral pentagonal growth sequence.

3.4 Carbon Clusters

Xu et. al. developed a transferable TB method for carbon[66] that is suitable for both bulk and cluster properties of carbon. Their approach is based on the method used by Goodwin et al.[41]. The total energy is represented as a sum of a band-structure

N	Bond	$d_{ab-initio}(\AA)$	$d_{TB}(\AA)$	N	Bond	$d_{ab-initio}(\AA)$	$d_{TB}(\AA)$
2	1-2	2.23	2.25		1-3	2.53	2.55
3	1-2	2.17	2.26		1-5	2.56	2.72
		$\theta = 77.2$	$\theta = 80$		1-2	3.26	3.24
4	1-2	2.30	2.36		2-3	2.57	2.68
	1-3	2.40	2.45		1-6	2.77	2.25
5	2-4		2.40		2-5	2.79	2.70
	2-5		2.45	8	2-6	2.49	2.56
	1-2		3.05		3-4	2.48	2.45
	2-3		2.62		4-5	2.32	2.33
	1-5		2.75		5-6	2.48	2.45
6	1-2	2.86	2.55		1-8	2.37	2.40
	1-3	2.49	2.67		3-8	2.42	2.39
	1-5	2.69	2.66		1-6	2.57	2.56
	3-5	2.93	2.66	9	1-2	2.50	2.52
	5-6	2.38	2.38		1-9	2.53	2.65
7	3-4	2.48	2.63		1-2	2.75	2.72
	1-3	2.47	2.74	10	1-9	2.56	2.54
	1-2	2.58	2.68		5-9	2.54	2.55

Table 3.3: Bond lengths for Si clusters calculated with TB method and ab initio method. N is the number of atoms in the cluster.

N	Bond	$d_{ab-initio}(\AA)$	$d_{TB}(\AA)$
2	1-2	1.245	1.4133
3	1-2	1.278	1.310
4	1-2	1.271	1.311
	2-3		1.326
6	1-2	1.316	1.331
10	1-2	1.290	1.312

Table 3.4: Same as Table 3.3 except for C clusters.

energy and a repulsive potential:

$$E_{tot} = E_{bs} + E_{rep}. \tag{3.31}$$

The band structure energy is calculated by solving the Schrödinger equation for a parametrized Hamiltonian. The short range repulsive potential energy is written as

$$E_{rep} = \sum_i f(\sum_j \phi(r_{ij})) \tag{3.32}$$

where $\phi(r_{ij})$ is a pair potential function and f is a fourth order polynomial with argument $\sum_j \phi(r_{ij})$. The scaling function for the Hamiltonian matrix elements is given as

$$s(r) = (r_0/r)^n exp\{n[-(r/r_c)^{n_c} + (r_0/r_c)^{n_c}]\} \tag{3.33}$$

and $\phi(r_{ij})$ for the repulsive potential function is given as

$$\phi(r) = \phi_0(d_0/r)^m exp\{m[-(r/d_c)^{m_c} + (d_0/d_c)^{m_c}]\}. \tag{3.34}$$

Various parameters in these equations are given in [66]. In this paper, the scaling functions are extrapolated by polynomials.

We worked on the properties of carbon clusters. Our results for C clusters compared with ab-initio calculations are given in Table 3.4.

3.5 Phonon Dispersion Relations

The phonon dispersion relation of the crystals is a very important property and the basis of the lattice dynamics theory. Phonon dispersion is usually based on the harmonics approximation. In this approximation, it is assumed that the atoms move from their equilibrium positions only a small amount. The lattice cell is described by three elementary vectors $\vec{a}_1, \vec{a}_2, \vec{a}_3$. Then the position vector of the particle at the vertex of any cell is

$$\vec{r}^{\,l} = l^1\vec{a}_1 + l^2\vec{a}_2 + l^3\vec{a}_3 \tag{3.35}$$

where l^1, l^2, l^3 are integers.

If there are s particles with masses $m_k (k = 1, 2, ..., s)$ and $\vec{r}_k$ is the position vector of the kth particle from the cell vertex, then

$$\vec{r}[lk] = \vec{r}^{\,l} + \vec{r}_k \tag{3.36}$$

defines the position of the particle $[lk]$ in equilibrium. The rectangular components of $\vec{r}[lk]$ are $x_\alpha[lk](\alpha = 1, 2, 3)$.

Now consider small arbitrary displacements $\vec{u}[lk]$ of the particles from equilibrium. The potential energy Φ of the deformed lattice can be expanded in powers of the rectangular components $u_\alpha[lk](\alpha = 1, 2, 3)$ of $\vec{u}[lk]$. The linear terms vanish in equilibrium and the second-order terms are

$$\Phi_2 = \frac{1}{2}\sum_{lk}\sum_{l'k'}\sum_{\alpha\beta}\Phi_{\alpha\beta}[ll'kk']u_\alpha[lk]u_\beta[l'k'](\alpha, \beta = 1, 2, 3), \tag{3.37}$$

$$\Phi_{\alpha\beta}[ll'kk'] = \frac{\partial^2\Phi}{\partial x_\alpha[lk]\partial x_\beta[l'k']}. \tag{3.38}$$

These second derivatives in equilibrium depend only on the difference of the cell

indices $(l - l')$ and satisfy the condition

$$\Phi_{\alpha\beta}[lkk'] = \Phi_{\beta\alpha}[-lk'k]. \tag{3.39}$$

The equation of motion of a particle of type k, mass m_k, is then

$$m_k u_\alpha[lk] + \sum_{l'k'} \sum_{\beta} \Phi_{\alpha\beta}[l - l'kk']u_\beta[l'k'] = 0. \tag{3.40}$$

Introduce a "reduced" displacement vector

$$\vec{v}[lk] = \sqrt{m_k}\vec{u}[lk], \tag{3.41}$$

and define the elements of the dynamical matrix of the lattice as

$$D_{\alpha\beta}[l - l'kk'] = \frac{1}{\sqrt{m_k m_{k'}}}\Phi_{\alpha\beta}[l - l'kk']. \tag{3.42}$$

Then (3.40) becomes

$$v_\alpha[lk] + \sum_{l'k'} \sum_{\beta} D_{\alpha\beta}[l - l'kk']v_\beta[l'k'] = 0. \tag{3.43}$$

A solution of this equation for an independent normal vibration of the lattice is a plane wave:

$$\vec{v}[lk] = \vec{V}(k)e^{-i\omega t}e^{i\vec{q}\vec{r}^l}. \tag{3.44}$$

Then (3.43) becomes

$$\omega^2 V_\alpha(k) - \sum_{k'} \sum_{\beta} D_{\alpha\beta}[l - l'kk']V_\beta(k') = 0 \tag{3.45}$$

and

$$D_{\alpha\beta}[qkk'] = \sum_{l'} D_{\alpha\beta}[l - l'kk']e^{-i(\vec{q}(\vec{r}^l - \vec{r}^{l'}))} = \sum_{l} D_{\alpha\beta}[lkk']e^{-i(\vec{q}.\vec{r}^l)}. \tag{3.46}$$

$D(\vec{q})$ is the dynamical matrix in the reciprocal space.

The equations of motion (3.45) for a wave-vector q in the reciprocal space of the lattice are a set of $3s$ homogeneous equations in the reduced amplitudes $V_\alpha(k)$. The necessary and sufficient condition that this set should have a nontrivial solution is that

$$|D(\vec{q}) - \omega^2 I| = 0, \tag{3.47}$$

where I is the unit matrix of the order $3sx3s$. For a particular wave-vector $\vec{q}$, the characteristic equation (3.47) has $3s$ roots ω_j. Three of these roots, the acoustic branches, as function of $\vec{q}$, tend to zero as $\vec{q} \rightarrow 0$. The remaining $3s - 3$ roots, the optical branches, tend to finite limits as $\vec{q} \rightarrow 0$.

The TB method can be used to calculate phonon dispertion relations. As discussed above, we need to find the dynamical matrix for the diamond-cubic structure. The total energy of the system consists of the pair potential and the band-structure energy. The dynamical matrix is easy to calculate for the pair potential part, so we will discuss the band-structure part.

3.5.1 Dynamical Matrix for Band-Structure Energy

Clearly, we need to find the second derivatives of the band structure energy. As discussed before, the band-structure energy consists of the sum of the occupied eigenvalues of the Hamiltonian matrix. The second derivatives of the eigenvalues of the Hamiltonian can be calculated from the second-order perturbation theory.

The second derivatives of an eigenvalue of the Hamiltonian matrix can be calculated by the following exact equation:

$$\frac{\partial^2 E_n}{\partial\lambda\partial\lambda'} = (\frac{\partial^2 H}{\partial\lambda\partial\lambda'})_{nn} + 2\sum_{m\neq n}\frac{(\partial H/\partial\lambda)_{nm}(\partial H/\partial\lambda')_{mn}}{E_n - E_m} \tag{3.48}$$

where λ and λ' are two parameters of the Hamiltonian matrix. In our case, λ and λ' are coordinates of particles. We can prove (3.48). The Schrödinger equation can be

written as

$$(H - E_n)\psi_n = 0, \tag{3.49}$$

where the eigenfunctions ψ_n can be taken to be orthonormal, and will be assumed non-degenerate, so that

$$\int \psi_n^* \psi_m d\tau = \delta_{nm}. \tag{3.50}$$

Differentiation of (3.49) with respect to a parameter λ gives

$$(\frac{\partial H}{\partial \lambda} - \frac{\partial E_n}{\partial \lambda})\psi_n + (H - E_n)\frac{\partial \psi_n}{\partial \lambda} = 0. \tag{3.51}$$

By multiplying this equation by ψ_m^*, integrating over all coordinates and making use of the Hermitian property of the H, one obtains

$$(\frac{\partial H}{\partial \lambda})_{mn} - \frac{\partial E_n}{\partial \lambda}\delta_{nm} + (E_m - E_n)\int \psi_m^* \frac{\partial \psi_n}{\partial \lambda} d\tau = 0. \tag{3.52}$$

When this equation is differentiated with respect to λ', the following equation is obtained

$$\frac{\partial^2 E_n}{\partial \lambda \partial \lambda'} = (\frac{\partial^2 H}{\partial \lambda \partial \lambda'})_{nn} + \int [\psi_n^* \frac{\partial H}{\partial \lambda'}\frac{\partial \psi_n}{\partial \lambda} + \frac{\partial \psi_n^*}{\partial \lambda}\frac{\partial H}{\partial \lambda'}\psi_n] d\tau \tag{3.53}$$

If it is assumed that the eigenfunctions ψ_n form complete sets for all values of λ, the derivative $\partial \psi_n / \partial \lambda$ occuring in this equation can be expressed in the form

$$\partial \psi_n / \partial \lambda = \sum_m c_{nm} \psi_m. \tag{3.54}$$

The coefficients c_{nm} can be found by substituting the series (3.54) into (3.51), which leads to the formula

$$c_{nm} = \frac{(\partial H / \partial \lambda)_{nm}}{E_n - E_m} (n \neq m). \tag{3.55}$$

The derivation of (3.48) can be completed by substituting (3.54) and (3.55) for $\partial \upsilon_n / \partial \lambda$ into (3.53).

We calculated the phonon dispersion relations for Si using the method described above. Our result is shown in Figure 3-4.

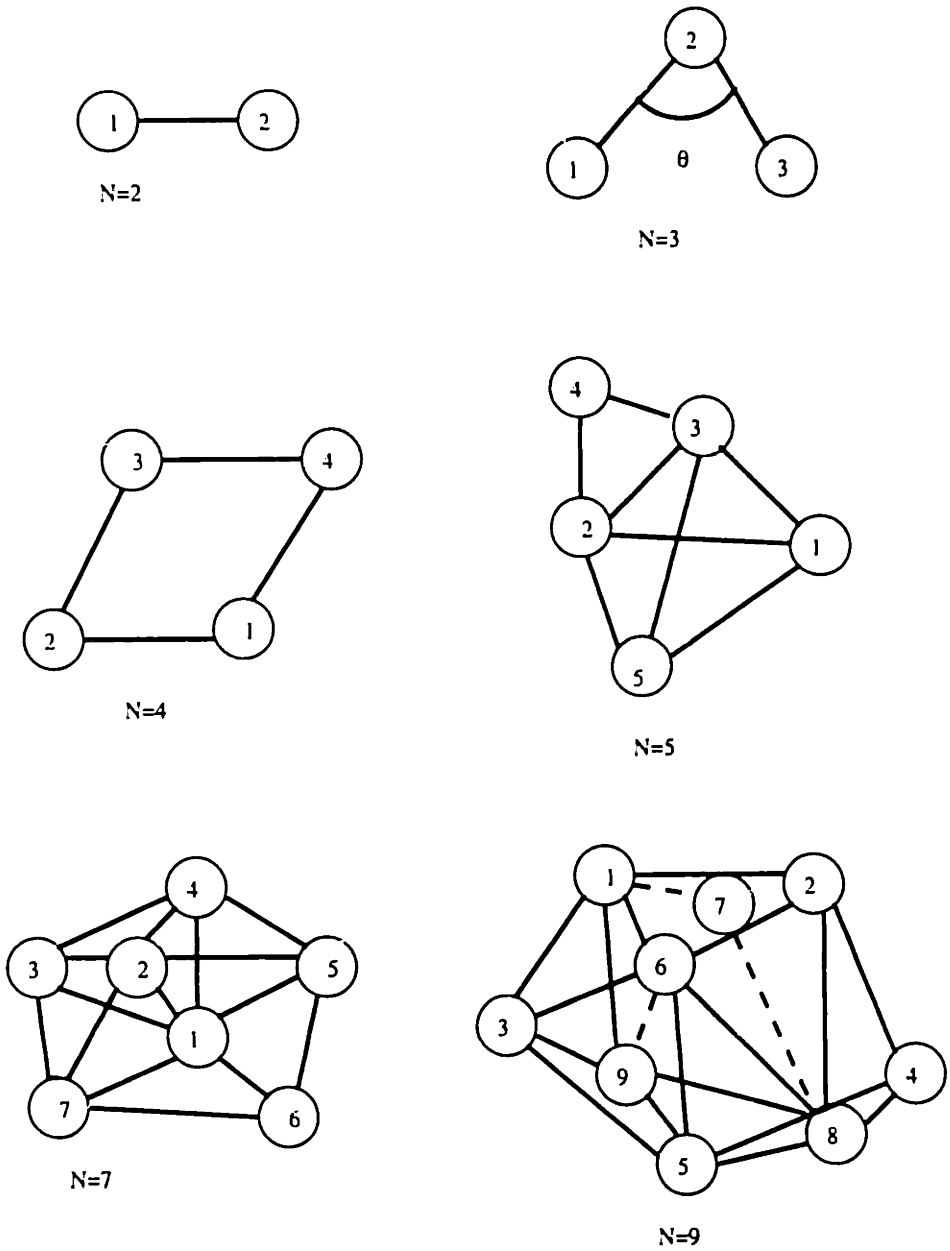

Figure 3-2: Structures of small silicon clusters.

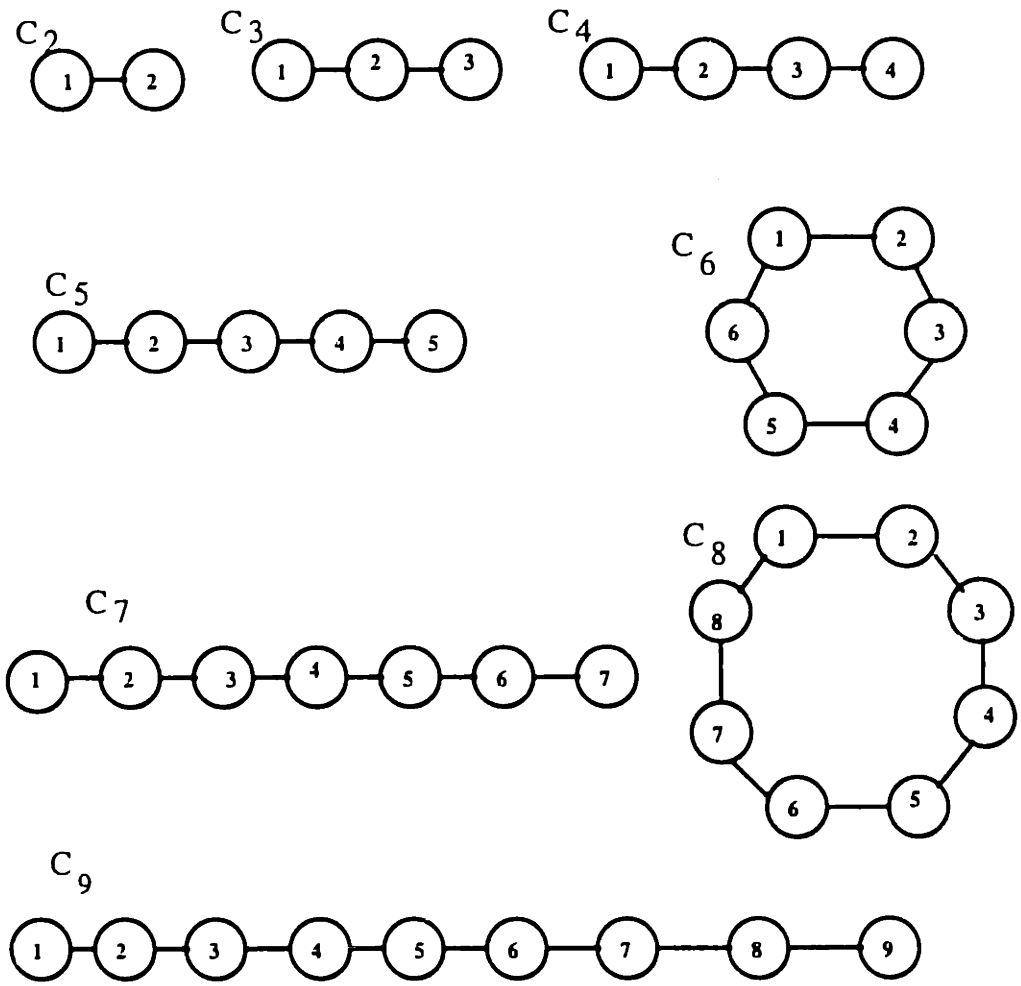

Figure 3-3: Structures of small carbon clusters.

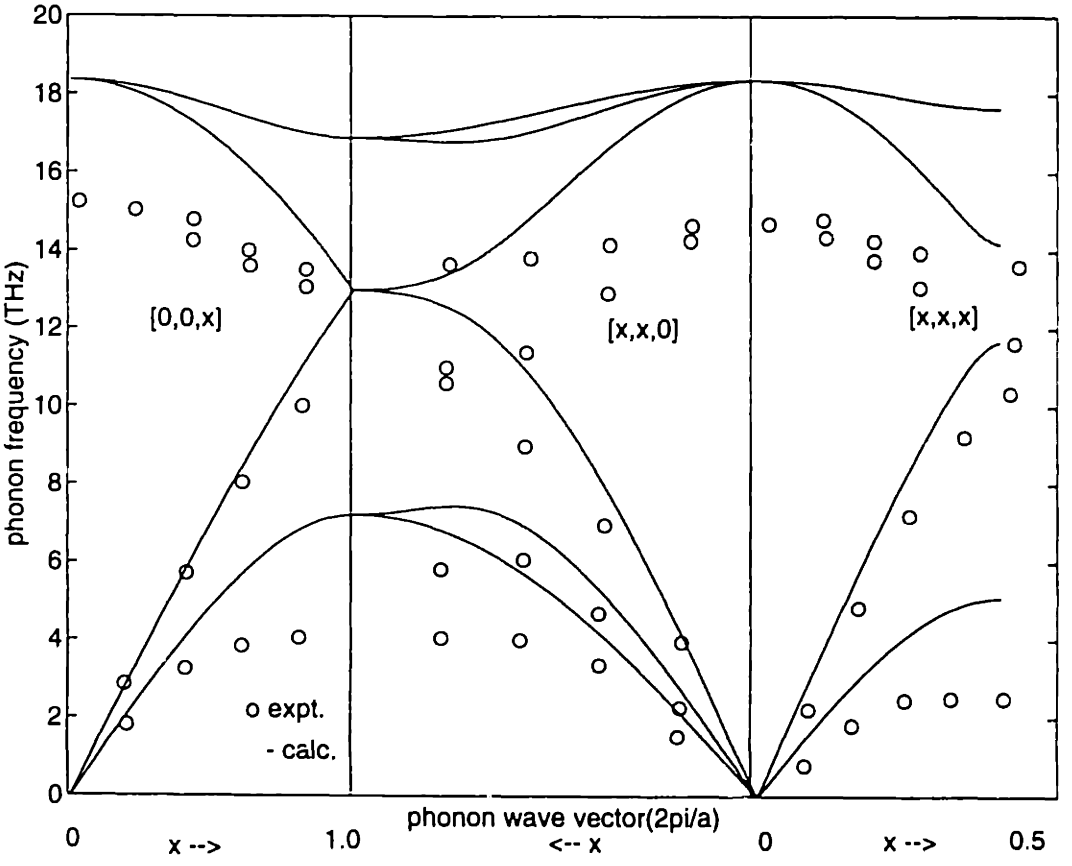

Figure 3-4: Phonon dispersion curves for Si by the TB method (solid lines) and from experiments (circles).

Chapter 4

Structure and Mobility of Dislocations in Si

Most physical properties characteristic of the crystalline state are affected to a greater or lesser extend by the presence of dislocations, simply because of the consequent degradation in geometric perfection. In the majority of cases the extend of this influence is determined by the long range, elastic strain field of the dislocation which, for distances more than a few atomic spacings from the center, is described well by continuum elasticity. The dislocation center is surrounded by a region, known as the core, within which linear continuum elasticity ceases to be a good approximation. The dislocation core region is responsible for structural differentiation in physical properties. The most pronounced examples of structure-dependent dislocation influence are to be found in the mechanical properties, specifically the plasticity of crystalline materials. The mechanism of plastic flow was established to be the sliding of close-packed crystal planes across one another, always in the direction of densest atomic packing. Plastic flow begins when the resolved shear stress on a possible slip system reaches a constant, critical value, known as the critical resolved shear stress (crss). The slip process in a perfect crystal requires the simultaneous breaking and rejoining of all bonds acting across the slip plane. Optimistic estimates indicate that the required stress for this transition is at least 0.04μ, where μ is the shear modulus; the observed values are several orders of magnitude lower. This problem was not resolved until

1934, when Taylor [67] proposed that dislocations might be the agents responsible. Peierls showed theoretically that this model could lead to a suitable small cssr.

In the previous chapters we have tested the limits of transferability of the TB method. These are definitely wider than those of the empirical potentials. Most important is that the TB method seems to describe reasonably well local bonding arrangements that are distinctly different from the ideal tetrahedral bonding in diamond cubic lattice of silicon. This is a very inviting property when it comes to simulating defect and interface properties. In particular, we intend here to apply the same methods discussed in the previous chapters to simulations of dislocations in Si. In what follows we emphasize that the TB method is not just a feasible framework for theoretical studies of dislocations in semiconductors, but it seems to be the only reasonable way to address the very challenging issues associated with dislocation mobilty.

The challenge is two-fold. First is that in the presence of the band gap various electro-mechanical effects may occur. Indeed, earlier studies[68] showed that it was absolutely necessary to account for electronic degrees of freedom to predict dislocation properties of silicon. In particular, it was established that by changing electronic properties, e.g. by doping, the barriers for kink motions are effectively reduced[69]. This was related to the existance of in-gap levels corresponding to electronic states possibly localized on dislocations. Such states may serve as traps for the carriers and become charged. Accordingly, moving dislocations can provide undesirable conducting paths or otherwise substantially affect the electronic properties[68].

It was realized that theoretical understanding of dislocation mobility in silicon will require to fully account for re-distribution of the electron density in the course of dislocation motions. In principle, this can be done in the framework of the Density Functional Theory. However, computational effort involved in any kind of realistic simulations of dislocation motions from the first priciples is immense. Accordingly, no attampt has been ever made to model dislocation motions with full account of electronic degrees of freedom. To our knowledge there exist only two results reported in the literature on dislocations using the DFT/LDA approach: these are both con-

cerned with in-core reconstruction of 90° partial dislocation in {111} glide subsystem of silicon [70]. Although important, the issue was relatively well adressed in the earlier work [71] so that the recent DFT/LDA results simply confirmed the expectations that the 90° partial dislocation reconstructs in the asymmetric sense.

The existing computational limits fall far below levels required to perform any reliable calculation of dislocation structures and motions, since, because of the long range elastic fields associated with dislocations, these must include many atoms. For that purpose DFT calculations are just not there yet to address the issues.

On the other hand, as was clearly shown lately [72], the known empirical potentials generally fail to describe quantitatively highly distorted atomic environments characteristic of dislocations and kinks in semiconductors. It is quite clear that by using the TB approach instead we may be able to do a relatively good job in describing structural aspects and energetics of dislocation motions in Si and at a reasonable computational cost. Important to note that due to the complex nature of the problem the theory of dislocations in semiconductors is yet to be developed. Therefore, even small increments of knowledge in this area are very important. In this chapter we present the first results of numerical simulations related to dislocation mobility in silicon using a semi-empirical TB method.

The chapter is made up of a few sections. In section 4.1 the practical importance of understanding of dislocations in Si is discussed where the role of dislocations in the Brittle-to-Ductile (BDT) transition in Si is introduced. The relevant previous theoretical work is discussed. The following section 4.2 contains results of our TB simulations related to 90° partial dislocation. In this section comparison is given with the published results obtained by DFT/LDA and empirical potentials. A better transferability of the TB potential compared to the empirical potentials is tested again for the specific case of dislocations in Si. Section 4.3 discusses our original results obtained for 30° partial dislocation in Si, where no previous work which accounts for electronic effects has been done. However, comparison is given with the empirical potentials: SW, Tersoff, and KP. In section 4.4 results of TB calculations for structure and energy of the reconstruction (APD) defect are presented. And lastly, APD motion

barrier is computed along the appropriate motion coordinate and the implications of the obtained results are discussed.

4.1 Brittle-to-Ductile Transition and Dislocations in Si

Phenomenologically BDT manifests itself as a notable increase of the fracture energy with increasing temperature. Consequently, material that shows brittle fracture behavior at low temperatures may become ductile at a higher temperature. The transition temperature for silicon is in the range of $0.75T_m$ and it is very sensitive to doping and the applied strain rates [73].

For the following reasons silicon is a very interesting object for studying the fundamental questions about BDT in crystals in general:

1. its BDT is rather dramatic in that the fracture energy increases 20-30 times in a very narrow temperature interval, $3-4^oK$. This is very helpful for experimental studies of BDT.

2. it is possible to obtain Si single crystals with almost zero dislocation density and to directly monitor motions of individual dislocations.

3. a very substantial theoretical and experimental effort was dedicated to Si, so much about dislocations in Si is relatively well understood. On the other hand, more very serious questions have arisen that await their answers.

In short, silicon represents an ideal testing ground for development of theory of dislocations and of the BDT in semiconductors.

Currenlty, understanding is there that BDT in Si is controlled by dislocation emission and transport away from the crack tip. Unlike close packed metals, where a dislocation, once generated, moves very easily, silicon is a material with characteristically high Peierls barrier (or stress), meaning that lattice resistance to dislocation motion is high. Therefore, even when stress concentration near the crack tip is high

enough to make dislocation nucleation an easy process, dislocations may not be able to move away fast enough compared to the crack propagation velocity. Accordingly, this channel for energy dissipation may be ineffective. This is certainly true at room temperature, while at higher temperatures the crack drags along a dense cloud of dislocations as it advances through the crystal[74]. Hence, is crucial for understanding of BDT in Si to examine temperature and stress dependences of dislocation mobility. This adds yet another dimension to the importance of theory of dislocations in semiconductors, while earlier efforts were focused on understanding of mechanisms by which dislocations affect properties of electronic devices.

It is a distinctive characteristic of silicon that its BDT is mostly dislocation mobility controlled, as opposed to the close packed materials where BDT is mostly controlled by nucleation of dislocations from the crack tip[75]. We consider this as a simplifying aspect because dislocation nucleation process by itself is not well understood, but in Si it is a less important factor than dislocation mobility.

Since to a large extent the onset of BDT in Si is controlled by dislocation mobility it is very important to establish the easiest modes of dislocation motions by which energy can be effectively channelled away from the growing crack. As was shown earlier, even motion of a single dislocation is in fact a very complex process involving many different atomic mechanisms. Earlier calculations performed by Hirsch and others in early 80s were successful in giving qualitative understanding of electronic effects involved in dislocation transport. On the other hand, atomic mechanisms considered were based on intuition developed on ball-and-spoke models at best. The situation remained unchanged until recently when the first direct study of dislocation mobilty is Si was performed[76].

It has become clear from those latest results that the atomic mechanisms important for dislocation mobility in silicon are multiple and that due to the particular geometry of diamond cubic lattice and the ability of diisocation cores to reconstruct there exists a large set of interrelated processes simultaneously contributing to dislocation transport.

In particular, it was established that the in-core reconstruction has a profound

effect on the way dislocations move[76]. The meaning of that previous work in the context of our study is that it isolated a few most important atomic mechanisms that contribute the most into dislocation motions. It will be the focus of our work here to obtain more reliable data that shall allow to further distinguish the easiest mechanisms of dislocation transport using the transferable TB method.

4.2 Structure and Energetics of 90^o Partial Dislocation

Si has diamond cubic structure consisting of two inter-penetrating fcc sub-lattices displaced relative to each other by the vector $< 111 >$. The smallest repeat vector in dc lattice is $a/2 < 110 >$ and the most close packed planes are $\{111\}$. Accordingly, just like in fcc materials $\{111\}$ planes play a dominant role in crystallographic plasticity while $a/2 < 110 >$ is the Burgers vector of dislocations gliding on $\{111\}$ planes. However, due to non-primitive structure of the dc lattice two distinct sub-sets of 111 slip systems are present: shuffle and glide sets. These are shown on Figure 4-1.

The widely spaced set of atomic planes, the shuffle set, has a spacing of $\sqrt{3}a/4$, while the closely spaced set is separated by only $\sqrt{3}/12$. Of the two, only the glide set dislocations may dissociate into Shockley partials. At the same time, it is very well established experimentally that both static and mobile dislocations in $\{111\}$ planes of Si are dissociated[77]. For that reason only the glide plane dislocations are regarded as active in the crystallographic slip.

At moderate strains there are two full dislocations present on $\{111\}$ systems of Si: screw and 60^o (mixed) dislocations. They dissociate into two 30^o partials (screw) or one 30^o and one 90^o partial (60^o mixed) according to the following equation:

$$a/2[\bar{1}01] = a/6[\bar{1}11] + a/6[\bar{1}\bar{1}2]. \tag{4.1}$$

Shown on Figure 4-2 is a triangular dislocation loop consisting of segments of dissociated screw and mixed 60^o dislocations. Of the two Shockley partials, 30^o partial

dislocation has received much less attention than 90° partial, even though it is involved in both dissociations, while 90° partial is only involved in dissociation of the mixed 60° dislocations.

Since full dislocations in the glide set dissociate, the resulting partials are thought to be the major plasticity carriers. In this section we focus on the core structure of 90° partial dislocation. 30° partial will be discussed in the following sections 4.3 and 4.4.

In order to obtain fully relaxed core structures of the partial dislocations we performed appropriate calculations based on the TB method using the periodic boundary conditions. In such geometry, dislocations can be introduced by two (or more) at a time. Consequently, we always had a dipole of dislocations in the periodic supercell. Two dislocations were obtained starting from the perfect dc structure by cutting between two atomic planes of the glide set and displacing atoms above the cut by half of an appropriate Burgers vector, while displacing the atoms below the cut by the same amount but in the opposite direction. In order to actually have dislocations, the cut should be terminated somewhere in the bulk of the crystal.

Because each one of the Burgers vectors of the partial dislocations does not give a full lattice period, between the two partials lies an area of stacking fault. Associated with the stacking fault is certain excess energy proportional to the stacking fault area. Specific (per unit area) energy of the stacking fault is an important materials property related to the relative stability of fcc (or dc) lattice to hcp packing. In silicon this parameter is relatively small which means that dislocations must dissociate and be well separated, as is known from the results of electron microscopy[77].

By making an appropriate Burgers displacement, the core structure of a straight 90° partial dislocations is obtained shown in Figure 4-3a.

Here atoms above the glide cut plane are shown as open circles, and those below are shaded. Each atom has 4 bonded neighbors, except the in-core atoms that have 3. The energy of such a core is apparently rather high, but this energy can be reduced substantially by virtue of the reconstruction shown in Figure 4-3b where a moderate distortion in the core allows the dangling bonds to pair. Clearly, the

reconstruction is associated with certain atomic displacements in the direction parallel to the dislocation line, and there is additional energy of the corresponding elastic distortion. On the other hand reconstructed bonds are formed bridging the atoms across the dislocation line, which lowers down the overall energy. As a result all the atoms are again four-fold coordinated.

Alternative to such, asymmetric reconstruction is another type of in-core structure suggested in [72], which is shown in Figure 4-3c. Here atoms on the opposite sides of the dislocation line simply move closer to each other so that quasi-fivefold coordination is established. The latter, symmetric reconstruction was shown to give a very different band structure with rather deep in-gap states. Alternatively, the asymmmetric reconstruction results in only very shallow levels hardly split from the major bands.

Both experiments[78] and DFT[70] calculations seem to favor the asymmetric reconstruction of the 90° partial. For that reason, the ability to predict this asymmetric structure was used as a test ground for various models of Si. In [79] it was shown that SW and KP empirical potentials clearly fail to reproduce the asymmetric structure shown in Figure 4-1b. Among the potentials tested in [79], only Tersoff's [3] potential gave the correct reconstruction. Subsequently, applicability of the empirical potentials to model dislocations in Si was questioned. Jumping ahead, Tersoff's potential, heralded in [70] as the most transferable, failed miserably to desribe energetics of 30° partial dislocation in Si, as discussed in the following sections. Hence, the general trend observed in the earlier simulations was that empirical potentials fail to reproduce structures that were not explicitly or implicitly included in the databases used for fitting.

To obtain the low energy core structure of 90° partial dislocation we used a constant volume periodic supercell with 96 atoms. Since, it is only possible to intruduce dislocations in pair in a periodic supercell, we used a recipe suggested in [70] to reduce distortion stresses due to dislocation walls appearing when small supercells are used. That recipe includes using a tilted periodic box that generates a quadrupolar arrangement of dislocations.

Dislocation dipoles were introduced by making an appropriate cut in the glide {111} subsystem and displacing atoms on both sides of the cut in the following way: atoms just above were shifted halfway along the Burgers vector of 90° (edge) partial and atoms below were shifted halfway in the opposite direction. After that the conjugate gradient method was used to minimize the energy of the system. This procedure resulted in in an asymmetrically reconstructed core shown in Figure 4-3b. Atoms just above the {111} glide plane are shown as open circles, while atoms just below are shown as filled circles. Dots in the centers of open circles indicate the bonds pointing up perpendicular to {111} plane. Atoms below the glide plane also have bonds pointing down from the plane (not shown). The excess energy of this configuration is 2.22 eV per repeat distance along the dislocation core. This energy actually includes, in addition to the core energy, interaction energy of the partial dislocations within the dipole as well as with other images, and the stacking fault energy. This energy compares better with the corresponding values calculated using SW potential (1.79 eV/b), than with Tersoff (3.96 eV/b) or KP (3.93 eV/b) empirical potentials, even though SW potential does not predict an asymmetric reconstruction.

By comparing our results with the results obtained using empirical potentials we conclude that the TB method gives both the correct, i.e. asymmetric reconstruction (unlike the SW potential) and a more reasonable, lower value for the dislocation excess energy (unlike the Tersoff and the KP potential).

4.3 Core Structure and Energy of 30° Partial Dislocations in Si

The same procedure as above was used to obtain the relaxed structure of 30° partial dislocation, except that the direction of atomic displacements was changed appropriately, i.e. along the Burgers vector of the 30° dislocation. Immediately after the displacement but before relaxation atoms in the dislocation core have only 3 bonded neighbors, i.e. each one of them has a dangling bond (Figure 4-4a). After relaxation was completed the reconstructed structure was obtained shown in Figure 4-4b.

The core energy is reduced substantially by in-core atoms moving to each other close enough for the dangling bonds to form bonding orbitals. This, so called "symmetry-breaking" reconstruction doubles the repeat distance along the dislocation line and results in the core energy of 2.69 eV/b.

This energy falls between the energiess obtained using SW potential (1.91 eV/b) and higher values of 3.12 eV/b for Tersoff and 3.10 eV/b for KP empirical potentials. Having in mind that the TB method is more transferable than either one of the empirical potentials we expect that structure and energetics of the 30^0 reconstructed core is better reproduced by the TB method.

Worth mentioning, however, that 30^o partial (2x1) reconstruction is a more robust effect than 90^o partial asymmetric reconstruction and is reproduced one way or another by all of the tested empirical potentials. However, as discussed in the following section, the situation is different when it comes to in-core defects.

4.4 Structure, Energy and Motion of Reconstruction Defects in 30^o Partial Dislocation

It was conjectured earlier[68] and confirmed recently by the direct atomistic simulations[76] that in-core reconstructions have profound effects on the ways dislocations in Si move. The key issue here turned out to be the presence of the so called "reconstruction defect" or "antiphase defect" (APD). The last term originates from the fact that APDs divide two perfectly reconstructed domains out of phase with each other. Another common name for that defect is soliton[80], similar to the domain wall soliton introduced in the theory of ferromagnetics[81].

It was demonstrated that the ease with which partial dislocations move in Si is determined to a great extent by the motion barrier of APD[76]. Therefore, it was the focus of our work to calculate this energy barrier.

Earlier calculations based on empirical potentials failed to adress this issue, as no appreciable motion of dislocations was detected. Only recently the APD motion barrier was obtained for SW model of Si, and it was found to be very low (0.17 eV).

Although, it took substantial computational effort to obtain that energy, it may not be considered very reliable until compared against more transferable methods. On the other hand, that recent study gives us an apportunity to save immense computational effort by specifying the most important collective atomic modes for APD motions.

We intend to explore this opportunity and apply the more transferable TB method to compute APD motion barrier. But first we obtain the structure and the energy of APD reconstruction defect in the core of 30° partial dislocation. For that we used the same kind of procedure as in the previous section, however the system size was increased to 144 atoms. This was necessary to have at least 3 repeat distances along the dislocation line, so that, when the reconstruction occurs, one of the in-core atoms is necessarily left over making thus an APD.

The resulting fully equilibrated structure is shown in Figure 4-4 where only one of such defects is shown, and it has the excess energy of 0.93 eV.

This energy compares reasonably well with the SW value of 0.81 eV, while KP energy is way too high (2.55 eV). However, Tersoff potential gives even worse result [72]: the APD energy is negative (-0.13)! This should indicate instability of the core towards the alternating reconstructed pairs and APDs, which corresponds to a very high concentration of APDs (33%). Experimentally it was found that concentration of APDs in the core is of the order of a few percent (in no case higher than 5%), which is in disagreement with the Tersoff potential results. On the other hand, KP potential predicts too low concentration of APDs. Clearly, only SW and the TB models give reasonable (and comparable) energies.

It should be noted, however, that there are certain differences between SW and TB results other than that in the APD energies. The APD atom shown in Figure 4-4b is somewhat tilted from the center-symmetric position taken by the same atom in Figure 4-4. This tilt is a spurious feature of the SW empirical potential resulting from the specific angular-dependent three-body term chosen to enforce the tetrahedral arrangement of the bonded neighbors. Accordingly, even when one of the four bonded neighbors is not present, the tetrahedral angle is still enforced, thus producing the tilt. As is well known, however, bonding angles must become closer to 120° when

Si atoms have only three bonded neighbors. Clearly, this situation is much better reproduced by the TB method, compared to SW potential. If such relatively minor effects are ignored, the SW potential provides a reasonable description of APD defect in a 30° partial. As was noted in the previous section, and was just discussed, the TB method is clearly superior when it comes to reproducing highly distorted atomic arrangements in the dislocation cores compared to all of the so far tested empirical potentials.

Having studied energetics of the static APDs we proceed by computing the APD motion barrier. It was established that the lowest energy atomic mechanism for APD motion is triggered by the APD attacking a neighboring reconstructed pair, with the subsequent bond switching. Therefore, the distance between the APD atom and its reconstructed neighbor in the core is a proper motion coordinate. With this we can use efficient methods of minimization for computing the energy profile along the motion coordinate.

The calculations were performed using MD simulated annealing method where the system was constrained in such a way that the two atoms were kept at a fixed distance from each other. By making such constrained relaxations at a few points along the motion coordinates the maximum (minimax) was found corresponding to an energy barrier of 0.31 eV as shown in Figure 4-5.

Although, we did not impose any kind of symmetry apriori, the saddle-point structure is obviously center-symmetric around the atom flanked by the two in-core neighbors.

The energies computed along the motion coordinate are scattered somewhat erratically, because we stopped minimizations at all points when the maximum force on atoms became $10^{-2}eV/A$. This tolerance was not sufficient to obtain accurate energies for the intermediate constrained configurations along the path. However, it was just enough to see whether the barrier state was reached. At one point, after one more increment was made for the motion coordinate, the system's energy went down compared to the previous point. This indicated that the system was driven past the saddle. Then, the previous configuration, relaxed to the high tolerance of $10^{-2}eV/A$,

was subjected to still further relaxation until the maximum force became as low as $10^{-4}eV/A$. This was identified as the saddle-point state.

The above procedure allowed us to save substantial computational effort involved in finding the eigenstates of the TB Hamiltonian. Typically, it was possible to reach the high tolerance of $10^{-2}eV/A$ for the maximum force in 30-60 mins of CPU time of CRAY XMP. However, it required more than 3 hours of the CPU time to reach the low tolerance of $10^{-4}eV/A$. For that reason, more accurate relaxations were performed only for the stable configuration and the saddle-point state. All the other, intermediate states along the path were not fully relaxed, hence the scatter. Having in mind the cost, and the relative unimportance of the intermediate points we decided not to relax them any further. For that reason, the energies shown in Figure 4-5 for the intermediate points on the motion coordinate must be regarded as upper estimates for the real energy profile.

Although the TB energy barrier is notably higher (0.31 eV) that the SW barrier of 0.17 eV (also shown on Figure 4-5), these two results are still surprisingly similar in that they are much lower than the corresponding energies of the static APD defect (0.93 for TB, and 0.81 for SW). Indeed, as discussed in [76], this APD energy conveniently defines an energy scale on which various atomic mechanisms can be compared. With respect to the APD energy of 0.93 the APD motion barrier is very low, in full agreement with the earlier result obtained with SW potential.

Physically, the low barrier energy of 0.31 eV implies that once there is an atom with a dangling bond, such as APD or, alternatively a left kink bound to an APD [76], the motion barrier for such a defect is low. Although, we have not yet computed the motion barrier for other defects of this type, we expect these to be low as well.

We intend to apply the TB method to compute the other barriers important for the dislocation motions, as identified in [76]. However, our first result obtained for the APD motion barrier strongly suggests that the in-core reconstruction, and specifically APD defect, greatly affect the operative atomic mechanisms of motion of 30° partial dislocation in Si. This influence must be through possible low barrier mechanisms of dislocation transport "lubricated" by the presence of an APD.

The above results are very important, because they relate directly to the fastest, hence dominant, mechanisms of dislocation transport. Consequently, since 30° partial dislocation is one of the major plasticity carriers in Si, these mechanisms determine eventually the onset of the Brittle-to-Ductile transition in Si.

On the other hand, the very same mechanisms must contribute prominently in various dislocation-related effects in electronic properties in Si and, possibly, other semiconductors. In order to actually evaluate the importance of APD-mediated dislocation motion, we must eventually perform total energy calculations within the framework of DFT/LDA approach. For that, the present results provide a very valuable input, as they specify semi-quantitatively the most important targets: stable in-core defects, atomic mechanisms of their motions and nucleations, etc.

Future work will demonstrate whether the TB approach is fully adequate for quantitative assessment of operative mechanisms of dislocation glide in semiconductors, or it can be used only as a method of preliminary targeting. We consider the present work as a first, but very promising step in that direction.

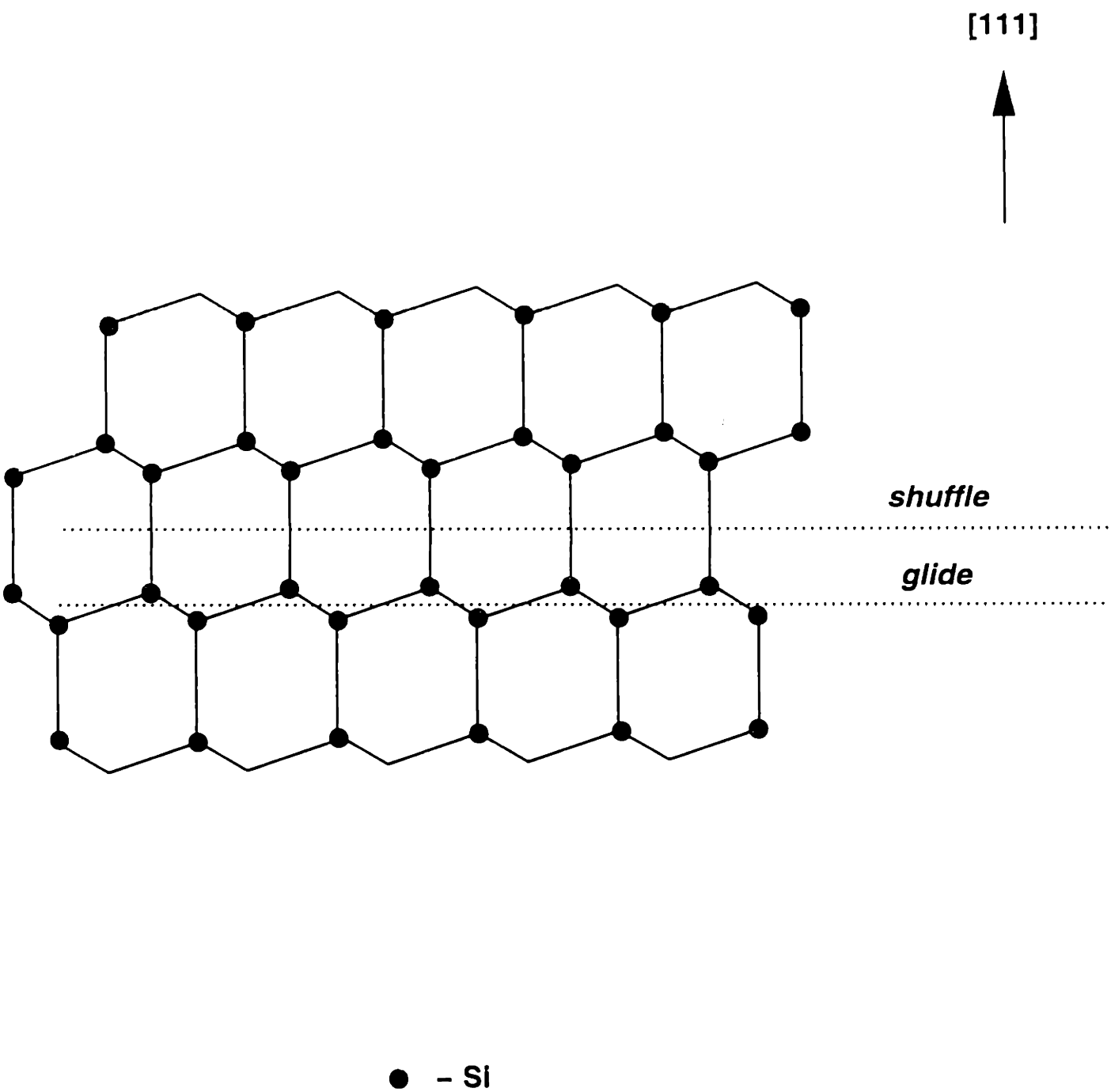

Figure 4-1: A $[\bar{1}01]$ projection of the diamond cubic lattice. Dashed lines show examples of *glide* (labeled "g") and *shuffle* (labeled "s") planes.

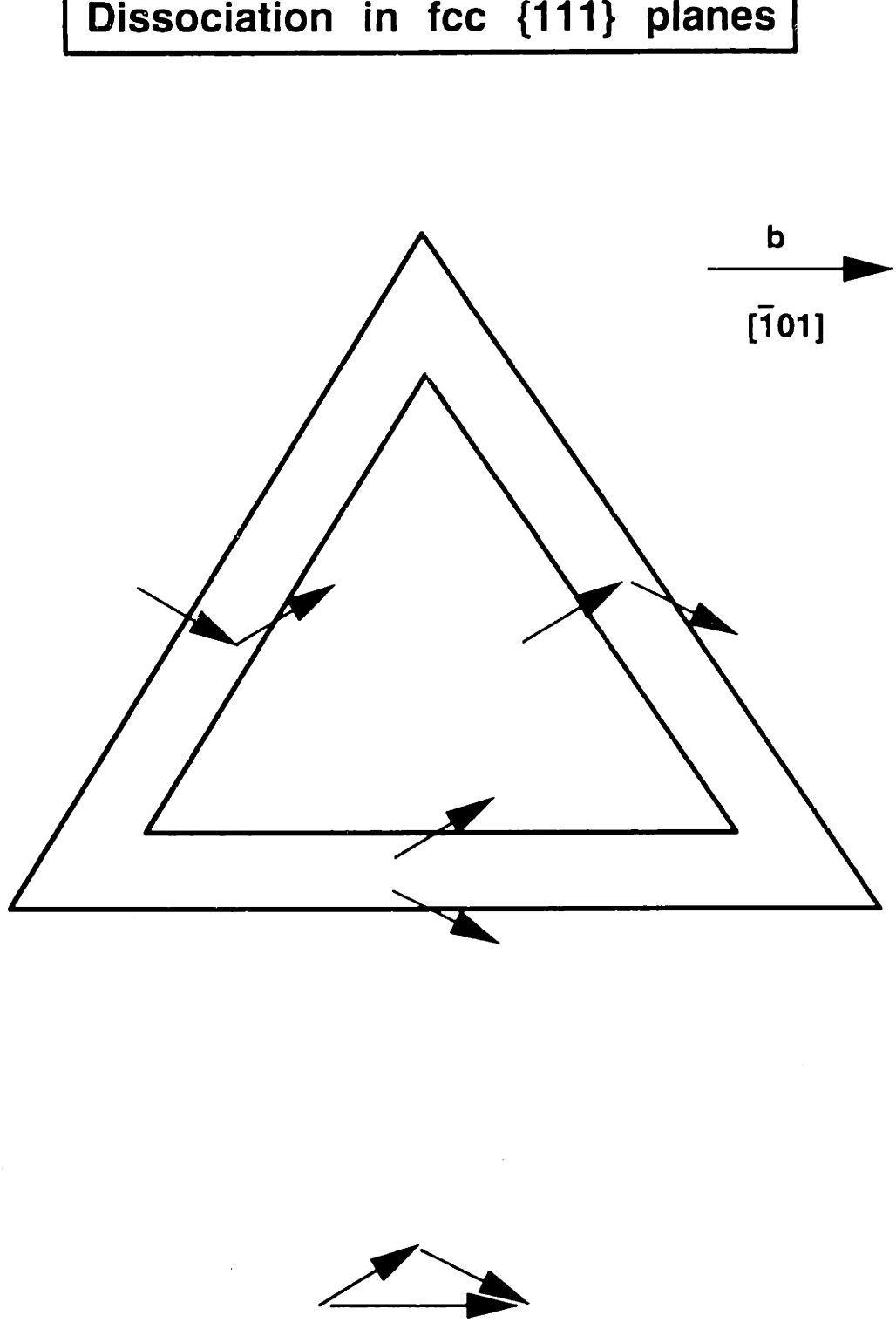

Figure 4-2: Dissociation of full dislocations into partial dislocations.

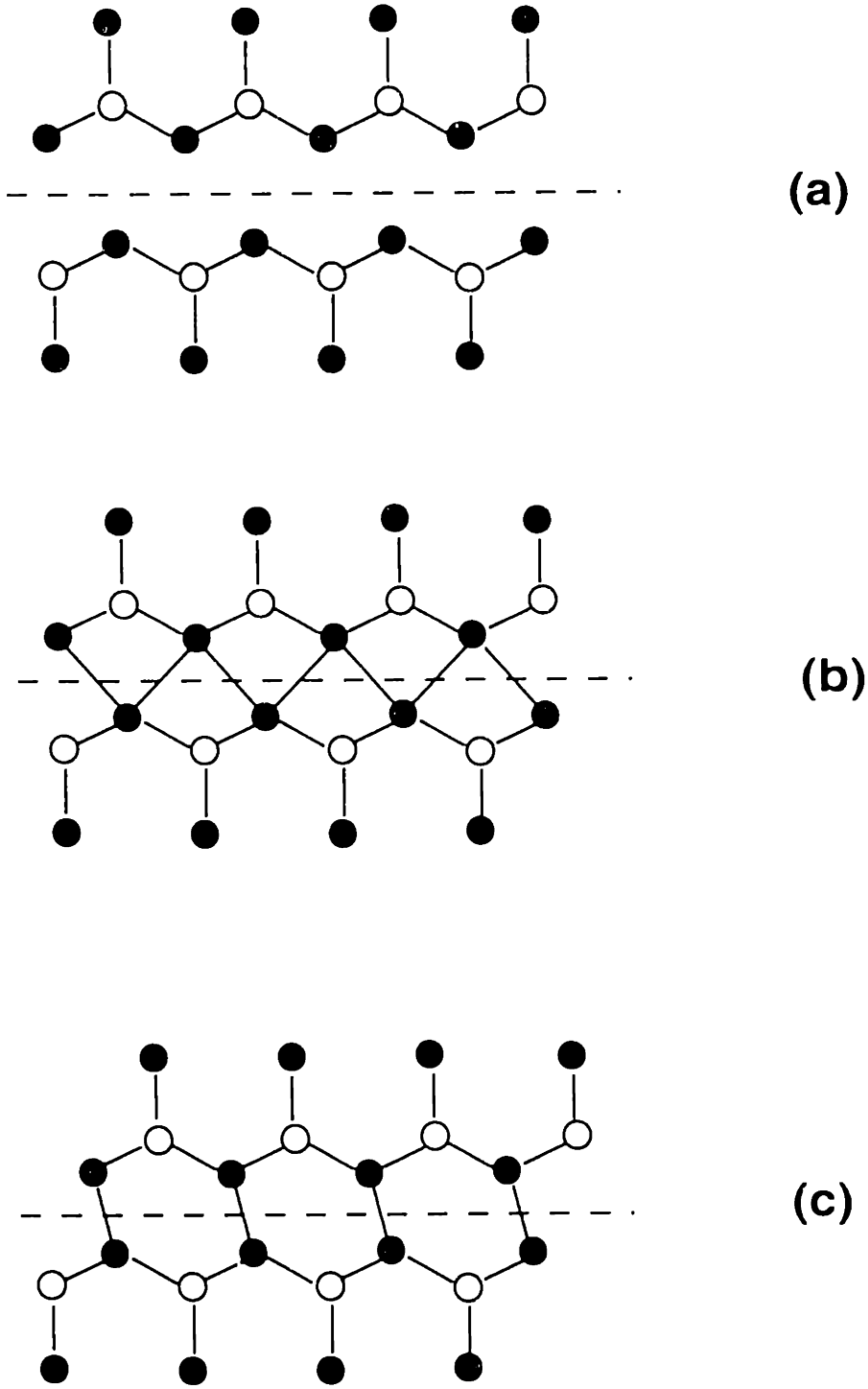

Figure 4-3: Reconstruction of 90° partial dislocation:
(a) unreconstructed high energy core structure,
(b) the symmetric reconstruction, and
(c) the asymmetric reconstruction obtained in our calculations.

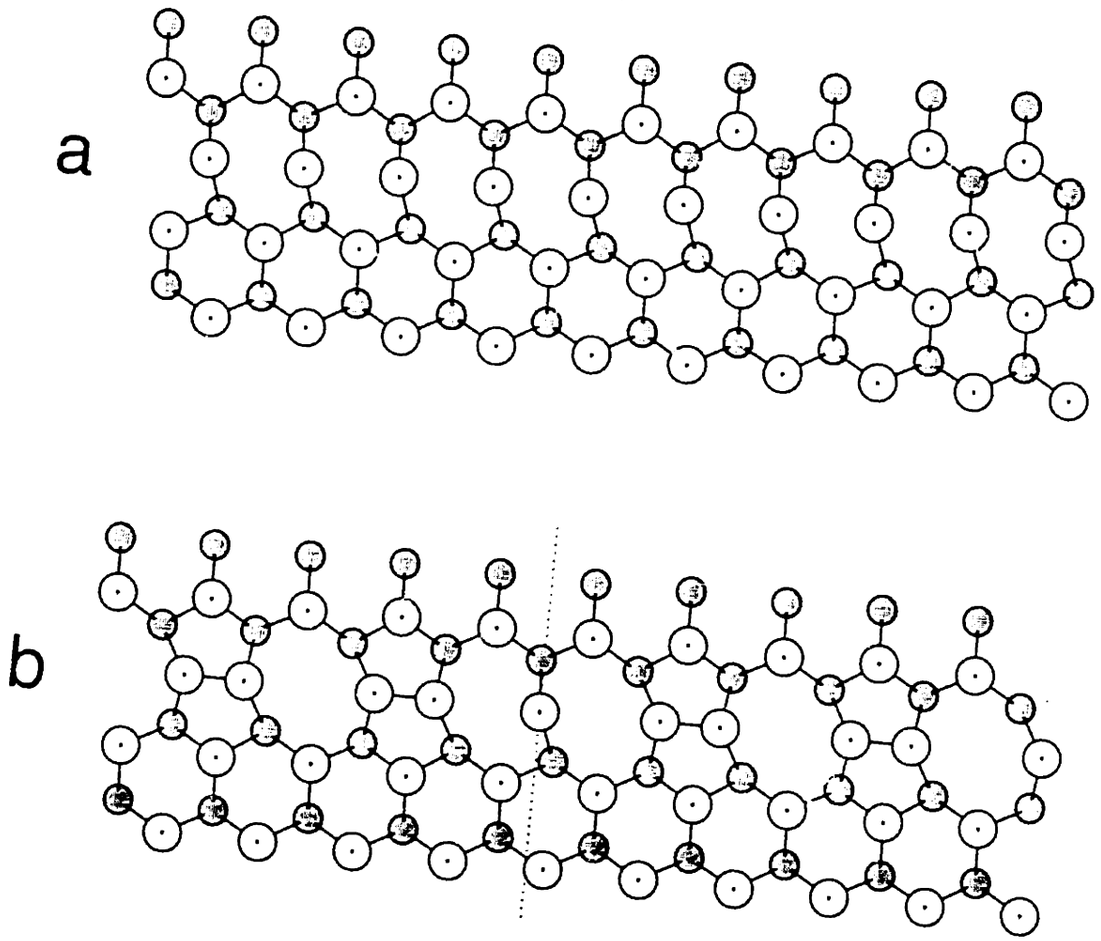

Figure 4-4: Reconstruction of 30° partial dislocation and the APD defect:
(a) unreconstructed high energy core structure,
(b) reconstructed core with an APD defect.

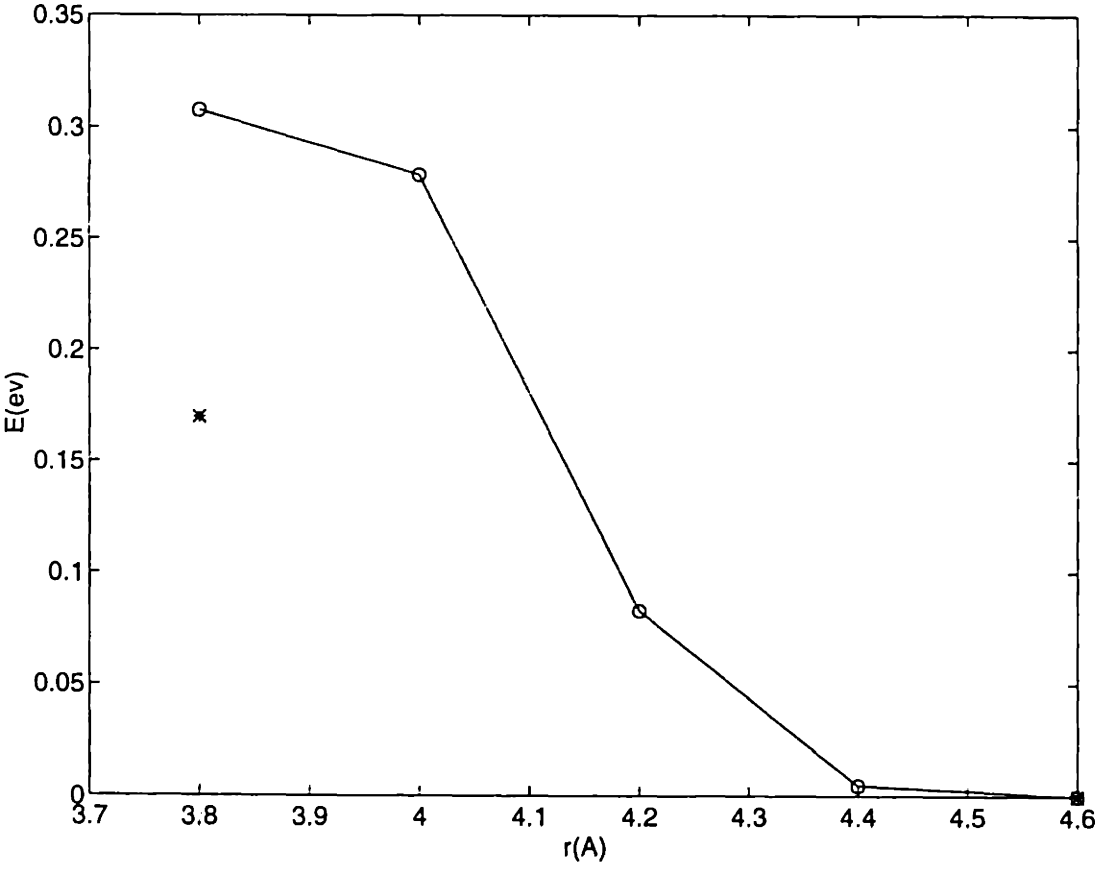

Figure 4-5: Energy barrier to APD movement. Circles show the results obtained using the TB method; crosses show the results obtained using the SW potential.

Chapter 5

Application of the TB Method to Silicon Carbide

5.1 Model Formulation

In this section, we will apply the orthogonal TB method to SiC for molecular dynamics simulation. The crystal structure of SiC is zincblende with two atoms in the primitive cell as shown in Figure 5-1. The zincblende structure can be tought as two interpenetrating fcc lattices one of which is moved 1/4 of the body diagonal along the body diagonal. Because SiC is composed of two different kinds of atoms, silicon and carbon, there are C-C, Si-Si and Si-C interactions. To develop an accurate TB method for the MD simulation of SiC, We need to determine what sorts of interactions there are between Si-Si, C-C and Si-C. The most important interaction is Si-C interaction because the nearest neighbors of each atom are the other kind of atoms and the nearest-neighbor interactions are the most important interactions. First of all, we need to determine hopping parameters for the band-structure energy and those parameters can be taken as averages of the parameters for silicon and carbon for which there is extensive literature[82, 83]. It is a good approximation to take averages of the hopping parameters of silicon and carbon for silicon carbide because Harrison showed that[36] it is possible to use only one set of hopping parameters for all nonmetals with reasonable accuracy, so we expect that our results are not very

sensitive to the hopping parameters.

The band-structure energy is the attractive interaction which is obtained by diagonalizing the Hamiltonian matrix and summing the occupied eigenvalues and then multiplying by 2 due to the fact that there are two electrons per orbital[15, 16]. The repulsive part of the total energy can be represented by a short-range potential as shown by Foulkes et al. [27]. The repulsive part of the total energy corresponds to the ion-ion interactions minus electron-electron interactions which is double counted in the band-structure energy. We know that ion-ion interaction can be represented as a pair potential due to the Coulombic nature of the interaction. The double counting part of the repulsive potential is shown to be pairwise too by Foulkes et al. [27]. One way of determination of the pair potential is by subtracting the band-structure energy calculated by diagonalization of the Hamiltonian matrix from the total energy for the system represented as a function of nearest neighbor distance and calculated by ab-initio methods. The total energy as a function of the nearest neighbor distance can be written as a very general function of only three parameters. This functional form which is called the universal binding curve, is shown to be valid for hundreds of materials. The universal binding curve is given as [84]

$$E(r) = E(r_0)(1 + (r - r_0)/A)exp(-(r - r_0)/A) \tag{5.1}$$

where $E(r_0)$ is the cohesive energy, r_0 is the bond length and A is a parameter which is calculated by using the bulk modulus

$$B = -VE(r_0)(\frac{\partial r}{\partial V})^2/A^2. \tag{5.2}$$

Even though this method was used by Wang et al. in many of their papers on silicon to calculate the pairwise pair potential, there are some disadvantages to it. For example, the equilibrium volume of fcc silicon is predicted to be more than twice as large as its ab-initio value. In general, Wang et al. 's method is not suitable for close-packed systems like fcc lattice, even though it is fine for open structures like tetrahedral silicon. To be able to work on liquid and amorphous SiC and clusters we

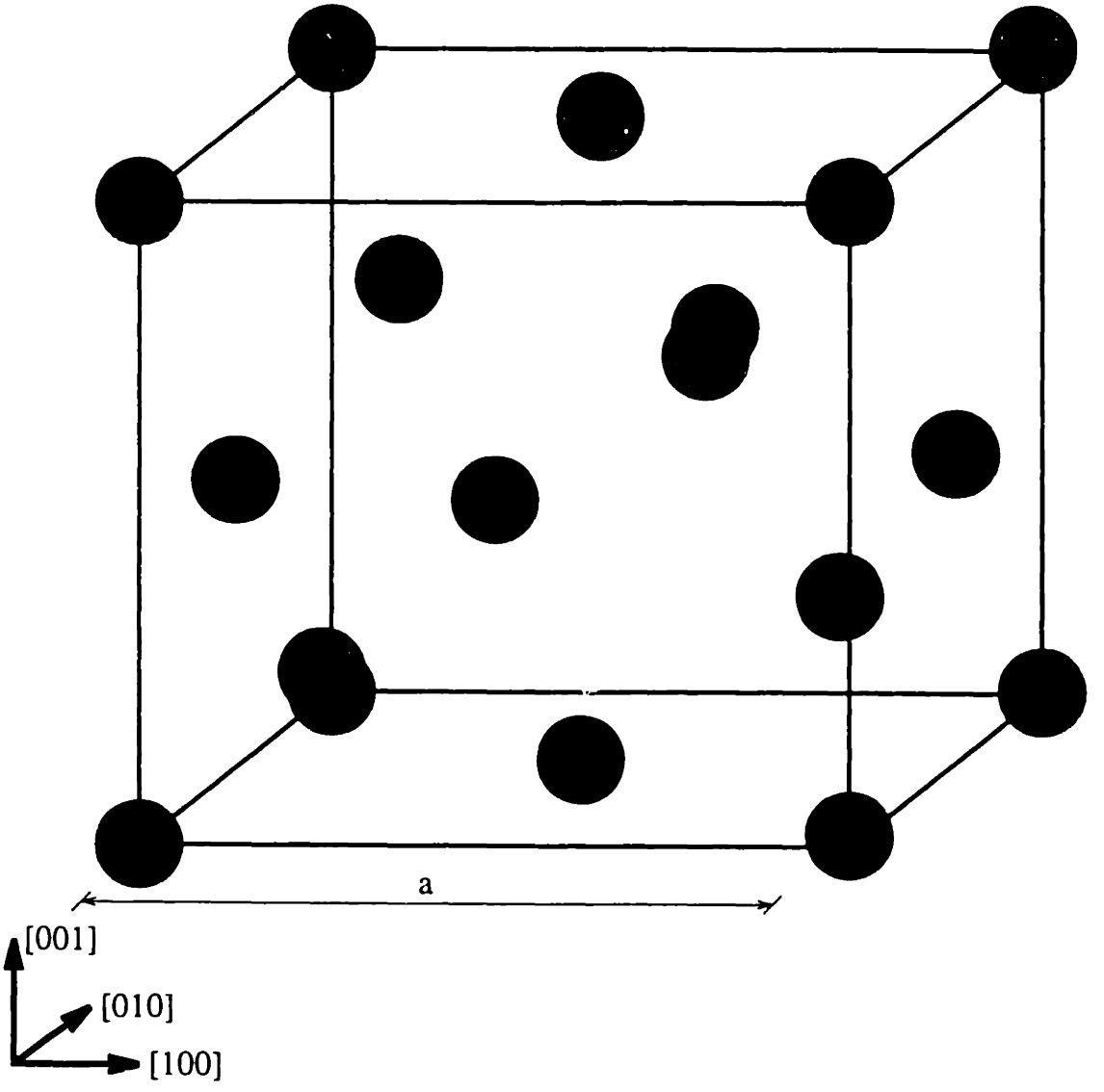

Figure 5-1: A unit cube of zincblende structure.

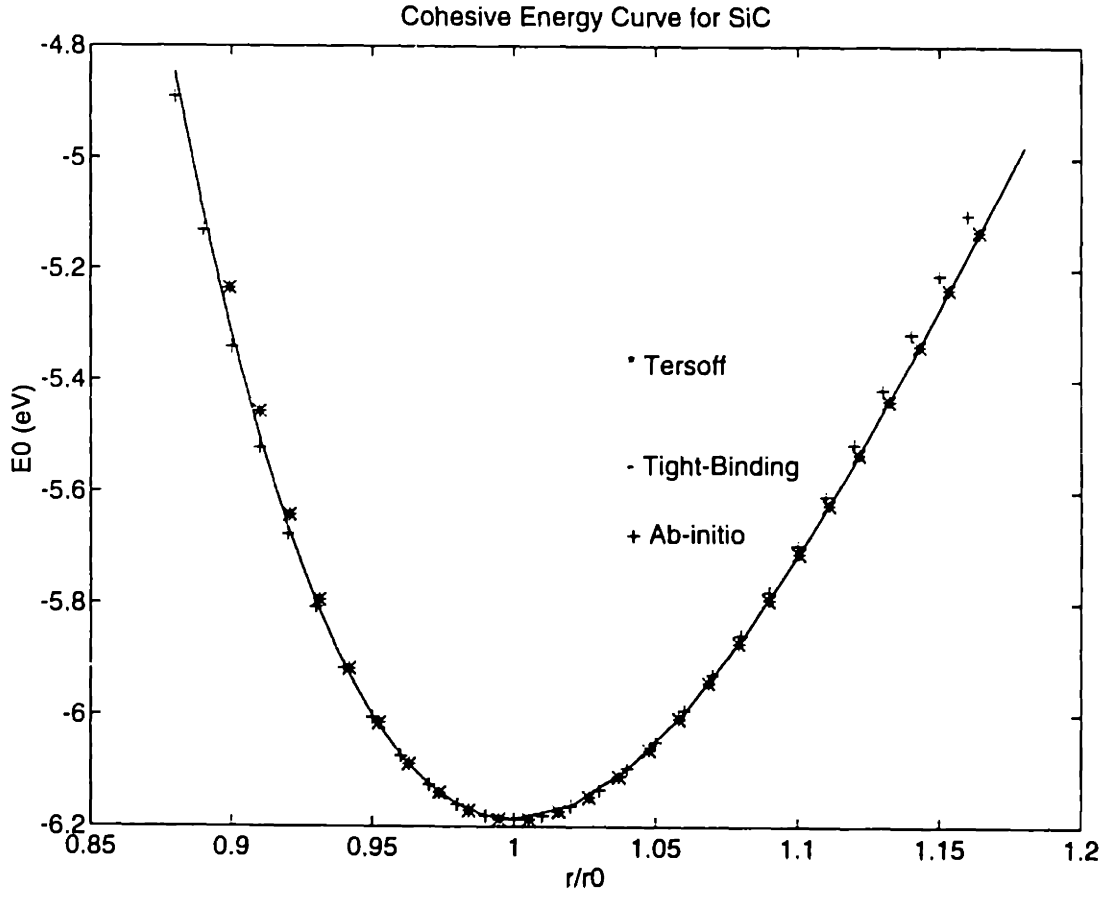

Figure 5-2: The cohesive energy versus lattice constant curves of β-SiC for various models.

need a more sophisticated model. A solution to the shortcomings of the method developed by Wang et al. was offered by Goodwin et al. [41] by rescaling the interatomic dependence of the Hamiltonian matrix elements and the pair potential. Goodwin et al. multiplied the hopping parameters and the pair potential by an exponential which is a function of bond length in order to reduce the range of interactions in silicon and thus reduce the volume of the close-packed systems such as fcc silicon. Goodwin et al. took hopping parameters from Harrison's work and introduced a rescaling function for both band-structure energy and the pair potential. Their method which we used in our calculations of dislocations in silicon decribed in detail in Chapter 2. Here we will describe the TB model we developed for the molecular dynamics simulation of SiC.

Wang et al. developed a TB model to carry out MD simulation of solid and liquid carbon and to investigate properties of carbon clusters [17]. In developing their method, unlike Goodwin et al. who used a simple pair potential for repulsive interaction, they used a many-body repulsive interaction similar to the embedded atom model. Their aim was to reproduce the cohesive energy curves of the most stable carbon polytypes which are diamond, graphite and the linear chain. Their method describes other polytypes of carbon less accurately, like fcc, sc and bcc carbon. The cohesive energy curves of the polytypes of carbon are calculated by using ab-initio local density functional approximation [85]. In those calculations, graphite was regarded as a two-dimensional substance due to the large distance between graphite layers compared to intralayer bond length. The total energy of carbon is expressed as a sum of the band-structure energy and a repulsive potential

$$E_{tot} = E_{bs} + E_{rep} \tag{5.3}$$

where E_{bs} is the sum of the occupied eigenvalues which are calculated by diagonalizing the Hamiltonian matrix and E_{rep} is a short range repulsive potential. The off-diagonal elements of the Hamiltonian are calculated by multiplying the hopping parameters with a scaling function s and the diagonal elements are the atomic orbital energies of

corresponding orbitals. The repulsive energy is calculated as

$$E_{rep} = \sum_i f(\sum_j \phi(r_{ij})) \tag{5.4}$$

where $\phi(r_{ij})$ is a pairwise potential between atoms i and j and f is a functional expressed as a fourth order polynomial with argument $\sum_j \phi(r_{ij})$. The $s(r)$ and $\phi(r)$ have the same forms given by Goodwin et al. [41]:

$$s(r) = (r_0/r)^n exp\{n[-(r/r_c)^{n_c} + (r_0/r_c)^{n_c}]\} \tag{5.5}$$

$$\phi(r) = \phi_0(d_0/r)^m exp\{m[-(r/d_c)^{m_c} + (d_0/d_c)^{m_c}]\} \tag{5.6}$$

where r_0 denotes the nearest-neighbor distance in diamond and $n, n_c, r_c, \phi_0, m, d_c$ and m_c are parameters which need to be determined. Unlike Goodwin et al. 's model (GSP model), the parameters r_c and n_c are not the same at the corresponding d_c and m_c for $\phi(r)$ in Wang et al. 's model. In order to be able to simulate liquid and amorphous carbon, Wang et al. replaced the tails of $s(r)$ and ϕ_r with a third order polynomial which smoothly goes to zero at some designated cut-off distance. The coefficients of these two polynomials are determined by requiring that at the match point $s(r)$ and $t_s(r - r_1)$ are smooth up to the first derivative, and $t_s(r - r_1)$ and its first derivative are zero at r_m. The same procedure is used to determine $t_\phi(r - d_1)$ which replaces the tail of $\phi(r)$. Wang et al. also checked to ensure that the model gives reasonable results for the electronic band-structure, elastic moduli and phonon frequncies in the diamond and graphite structures. The resulting sp^3 parameters are: $E_s = -2.99eV$, $E_p = 3.71eV$, $V_{ss\sigma} = -5.0eV$, $V_{sp\sigma} = 4.7eV$, $V_{pp\sigma} = 5.5eV$ and $V_{pp\pi} = -1.55eV$. The parameters for $s(r)$ and $\phi(r)$, the coefficients of the tail functions $t_s(r - r_1)$ and $t_\phi(r - d_1)$ and the coefficients for the polynomial function $f(x) = \sum_{n=0}^{4} c_n x^n$, with $x = \sum_j \phi(r_{ij})$ are given in Table 5.1 and Table 5.2 respectively. Wang et al. calculated vibrational and elastic properties of diamond and compared the results with experimental data[17]. They obtained good agreement with the experiment for

phonon frequencies (errors all within 10%). Calculated elastic constants are too soft in comparision with experimental data. Wang et al. also calculated vibrational and elastic properties of graphite. Again they obtained good agreement in comparision with the experimental data.

We decided to use the method developed by Wang et al. for the interactions between carbon atoms because of the good agreement of the results of this method with experimental data. Because we are using a nearest-neighbor model for SiC, the important interaction is Si-C interaction. Especially at temperatures below melting point at which only nearest neighbors are counted, we expect that C-C interaction has no importance for the simulation purposes. C-C interaction becomes important if we are investigating liquid SiC or SiC alloys for which the coordination number is different from 4.

We used GSP method for the development of SiC TB model. We employed the same scaling function for both the off-diagonal elements of the Hamiltonian matrix and the pair potential. The total energy of the lattice is taken as

$$E_t[\frac{r_0}{r}] = E_{bs}[\frac{f(\frac{r_0}{r})}{f(1)}] + E_{rep}[\frac{f(\frac{r_0}{r})}{f(1)}]. \tag{5.7}$$

This rescaling affects both the off-diagonal elements of the Hamiltonian matrix and the repulsive potential. For the off-diagonal elements of the Hamiltonian we have

$$h_\alpha(\frac{r_0}{r}) = h_\alpha(1)(\frac{f(\frac{r_0}{r})}{f(1)})^n \tag{5.8}$$

and

$$\phi_{ij}(\frac{r_0}{r}) = \phi(1)(\frac{f(\frac{r_0}{r})}{f(1)})^m. \tag{5.9}$$

GSP have chosen the function f as a smoothed step function, with the step positioned midway between first and second nearest neighbors in the diamond lattice. The effect of this function is to reduce the range of the atomic interactions and thereby reduce the bond lengths, and the equilibrium volumes, for the close packed lattices. The

function is given as

$$f(\frac{r_0}{r}) = \frac{r_0}{r} exp(-(\frac{r}{r_c})^{n_c}). \tag{5.10}$$

The position of the step, and its sharpness, are set by r_c and n_c. If n_c tends to infinity, we have infinitely sharp cutoff and we obtain the nearest neighbor model. The new hopping parameters and the pairwise potential are given in the following equations:

$$h_\alpha(\frac{r_0}{r}) = h_\alpha(1)(\frac{r_0}{r})^n exp[n(-(\frac{r}{r_c})^{n_c} + (\frac{r_0}{r_c})^{n_c})], \tag{5.11}$$

$$\phi_{ij}(\frac{r_0}{r}) = \phi(1)(\frac{r_0}{r})^m exp[m(-(\frac{r}{r_c})^{n_c} + (\frac{r_0}{r_c})^{n_c})]. \tag{5.12}$$

We determined $\phi(1), r_c, n_c$ and m by fitting to the lattice parameters and the bulk moduli of diamond-cubic and rocksalt SiC. The band-structure energy can be calculated as a function of $g = f(r_{dc}/r)/f(1)$ for various values of g. We changed g from 0.5 to 1.5 and obtained Hamiltonian matrix elements, and then diagonalized the Hamiltonian matrix. By summing eigenvalues over the occupied states we found the band-structure energy. Then we fitted a third order polynomial to the band-structure energy for both the diamond-cubic and the rocksalt structures. The diamond-cubic structure has 4 and the rocksalt structure has 6 neighbors. The equilibrium bond-length can be found by determining the bond length at which the derivative of the total energy with respect to bond length is zero. We know the ab-initio results for the bond-lengths of diamond cubic and the rocksalt silicon carbide. This gives us two equations. We can also calculate bulk moduli of the diamond-cubic and the rocksalt silicon carbide if we know the second derivative of the total energy with respect to the bond length at the equilibrium bond length. We found the following band-structure energies for the diamond-cubic and the rocksalt silicon carbide:

$$E_{bs}^{dc}(g(r)) = 4.5222g^3 - 46.4920g^2 + 24.2701g - 8.4896 \tag{5.13}$$

$$E_{bs}^{rs}(g(r)) = 10.1235g^3 - 69.0672g^2 + 47.2682 * g - 17.4455 \tag{5.14}$$

where *dc* stands for the diamond cubic structure and *rc* stands for the rocksalt structure. We do not have to know how g changes as a function of r in order to find the band structure energy. The equilibrium bond length can be calculated by finding the root of the following equation:

$$\frac{\partial E_{tot}(g(r))}{\partial r}|_{r=r_e} = \frac{\partial E_{tot}(g(r))}{\partial g(r)}\frac{\partial g(r)}{\partial r} = 0. \tag{5.15}$$

It is clear that either $\frac{\partial E_{tot}(g(r))}{\partial g(r)}$ or $\frac{\partial g(r)}{\partial r}$ is zero. It is unlikely that $\frac{\partial g(r)}{\partial r}$ is zero, so that $\frac{\partial E_{tot}(g(r))}{\partial g(r)}$ must be zero. From this observation we obtain the following equations:

$$\frac{\partial E_{tot}^{dc}(g(r))}{\partial g(r)}|_{r=r_{dc}} = \frac{\partial E_{bs}^{dc}(g(r))}{\partial g(r)} + 2 * m * g(r)^{(m-1)} = 0 \tag{5.16}$$

and

$$\frac{\partial E_{tot}^{rs}(g(r))}{\partial g(r)}|_{r=r_{rs}} = \frac{\partial E_{bs}^{dc}(g(r))}{\partial g(r)} + 3 * m * g(r)^{(m-1)} = 0. \tag{5.17}$$

We must multiply the pair potential with 2 in the case of diamond because there are two bonds per atom in diamond cubic structure. We need to multiply the pair potential with 3 in the case of the rocksalt structure because there are three bonds per atom in the rocksalt structure. We notice that $g(r_{dc}) = 1$ which fixes the bond length for the diamond cubic structure.

We need to find the bulk moduli for the diamond cubic and the rocksalt structures for SiC as a function of the second derivative of the total energy at the equilibrium bond length. The bulk modulus for the diamond cubic structure is

$$B_{dc} = \frac{1}{8\sqrt{3}r_{dc}}\frac{\partial^2 E_{tot}^{dc}(r)}{\partial r^2}|_{r=r_{dc}}, \tag{5.18}$$

and the bulk modulus for the rocksalt structure is

$$B_{rs} = \frac{1}{9r_{rs}} \frac{\partial^2 E_{tot}^{rs}(r)}{\partial r^2}|_{r=r_{rs}}. \tag{5.19}$$

We know the second derivative of the total energy in terms of the four parameters we are trying to determine. The other two equations for the fit are then

$$\frac{1}{8\sqrt{3}r_{dc}} \frac{\partial^2 E_{tot}^{dc}(r)}{\partial r^2}|_{r=r_{dc}} - B_{dc}^{ex} = 0 \tag{5.20}$$

and

$$\frac{1}{9r_{rs}} \frac{\partial^2 E_{tot}^{rs}(r)}{\partial r^2}|_{r=r_{rs}} - B_{rs}^{ex} = 0 \tag{5.21}$$

where ex stands for the experimental value. So we have a total of four unknowns and four equations 5.16, 5.17, 5.20 and, 5.21. Those four equations are trancendental. We cannot find the roots of these four equations exactly. Instead we can minimize the sum of the squares of these four equations with respect to these four parameters. We have chosen the Monte Carlo simulated annealing method to minimize these four equations. It can be noticed that the sum of the squares of the four funtions can be minimum zero at which the four parameters give the perfect fit. We have chosen an exponential cooling schedule for the simulated annealing method and approximately 0.5 acceptance ratio. We obtained the four parameters at the end of simulation. Our result for these four parameters are

$$n_c = 0.20727 \tag{5.22}$$

$$p = 2.22987 \tag{5.23}$$

$$m = 10.34121 \tag{5.24}$$

$$\phi = 2.66603 \tag{5.25}$$

where $p = (r_{dc}/r_c)^{n_c}$. By using those parameters, we calculated the lattice parameters and the bulk moduli of the diamond cubic and rocksalt structures of silicon carbide

by fitting a third order polynomial to the total energy curves of the two structures. The result is given below in Table 5.3. As can be seen from Table 5.3, the result of the fit is very good and all the discrepancies are below five percent. In the rest of our calculations, we used this fit.

We used our TB model for silicon carbide to calculate bulk properties of silicon carbide. In order to simulate liquid silicon carbide, we need to smooth the cutoff. We used a third order polynomial to smooth the cutoff. A third order polynomial has four parameters. We require that $g(r)$ and its first derivative are smooth at the matching point, and we also require that $g(r)$ and its first derivative are zero at the cutoff. Those conditions give us four equations which are solved to find the parameters of the polynomial. It should be noted that even though the first derivative of the $g(r)$ is smooth, the second derivative is not smooth and this fact is observed as an abrupt change of the slope of the pressure-volume curve.

The band-structure curve for SiC is shown in Figure 5-3.

In our calculations, we are neglecting charge transfer and non-orthogonality effects. Charge transfer is a result of the strong potential of the carbon atom. Carbon does not have p-type core orbitals, so that the charge of carbon nucleus is shielded weakly. As a result, the Coulomb potential of carbon is strong and charge is transferred from silicon to carbon. But SiC is strongly covalent, as a result the charge transfer is not very big. In calculation of bulk properties, we can obtain reasonable results by ignoring the charge transfer. In the case of the surfaces and interfaces, the charge transfer effects cannot be ignored.

One of the approximations which is employed to deal with the charge-transfer effects is the local charge neutrality approximation[41]. The basis of this approximation is to prevent the charge transfer completely. An iterative process is necessary to eliminate charge transfer. First the Hamiltonian matrix is diagonalized. The amount of charge transferred is calculated by using the eigenvectors of the Hamiltonian. Then the diagonal elements of the Hamiltonian are modified and the Hamiltonian is diagonalized again. The amount of the charge transfer is calculated and the diagonal elements of the Hamiltonian are modified. This procedure is repeated until there is

zero charge transfer. Usually between 2 to 10 iterations are enough [42]. The reason for eliminating the charge transfer is that the TB method produces unphysically large charge transfers between atoms.

SiC is a slightly ionic compound. Under compression, it becomes more ionic[88], so there are long range Coulomb interactions in this compound. Charge transfer effects can be taken into account by carrying out a self-consistent TB calculation as Kohyama et al. did [34, 43]. But to be able to simulate large systems, we neglected the self-consistency.

The orthogonality of the atomic orbitals used in the TB method is another issue. In general the atomic orbitals are non-orthogonal, so in the calculation of the band-structure energy and the Hellmann-Feynman forces[37] the overlap matrix should be used[46]. This matrix is unitary in the case of orthogonal TB method[15]. The overlap matrix elements are calculated by using the extended Huckel approximation[89]. According to this approximation, the overlap matrix elements are proportional to the Hamiltonian matrix elements. The proportionality constant is found by fitting to the lattice parameter in the crystal. Menon et al. [46] claim that to simulate carbon reasonably, we have to take into account non-orthogonalities. But Wang et al. succesfully simulated amorphous carbon [90] and Zhang et al. [91] the buckyball collisions by using orthogonal TB method.The explanation for the success of the orthogonal TB method even for carbon is that because we are using experimental values for the TB parameters, the nonorthogonality is already taken into account.

5.2 Pressure

Pressure is the negative derivative of the Helmholtz free energy with respect to volume at constant temperature[92]:

$$P = -(\frac{\partial F}{\partial V})_T \tag{5.26}$$

where

$$dF = -SdT - PdV \tag{5.27}$$

or

$$P = -(\frac{\partial U}{\partial V})_S \tag{5.28}$$

where U is the internal energy.

Stress can be calculated by using the virial theorem [93]. A good derivation of stress from individual interatomic forces is given in one of the appendices of [94]. For a pairwise interatomic potential stress can be calculated by the following formula

$$\sigma_{ij} = V^{-1}(\sum_a p_{ai}p_{aj}/m_a + \sum_{a,b} r_{abi}F_{abj}) \tag{5.29}$$

where p_{ai} is the i component of the momentum of particle a. The first term represents the momentum transfer as a result of crossing of a particle through a given surface. The second term represents momentum transfer across surfaces via interatomic forces. The TB method gives us the interatomic force $\vec{F}_{ij}$, and those forces are in general non-central. The pressure is the average of the diagonal elements of the stress tensor. The pressure for SiC calculated from the virial is given in Figure 5-5.

5.3 Elastic Constants

Elastic constants of SiC have been calculated using the stress-strain curves as described in Chapter 3. Our results for elastic constants are given in Table 5.4. The stress-strain curves are shown in Figure 5-6.

5.4 Phonon Dispersion Curves of SiC

Phonon dispersion relations for SiC are shown in Figure 5-7. The acoustic modes are in agreement with experimental data, but the optical modes are incorrect due to our neglect of long range Coulomb forces.

5.5 Elastic Instability in SiC

Materials undergo phase transitions, develop cracks or are disordered under sufficiently high stresses. We investigated at which stress covalent materials become unstable. As is mentioned in Chapter 3, some phonon modes become imaginary at the point of instability. It is known that there are relations between elastic constants and phonon dispersion curves[106]. Elastic instabilities can be determined from the behavior of elastic constants.

For a crystal to be stable, the determinant of the elastic constants matrix should be greater than zero. For cubic systems, we have three distinct elastic constants, c_{11}, c_{12} and, c_{44}. The determinant of the elastic constant matrix gives us the three conditions of elastic stability:[107]

$$(c_{11} + 2c_{12})/3 > 0 \tag{5.30}$$

$$(c_{11} - c_{12})/2 > 0 \tag{5.31}$$

$$c_{44} > 0 \tag{5.32}$$

Actually, elastic stiffness constants, rather than elastic constants are more important in determining elastic instabilities[108]. Elastic stiffness constants can be calculated by stress-strain experiments or from fluctuation formulas. The two sets of numbers are different for finite stresses. In the static calculation, one has to allow for

strain relaxation within the unit cell when dealing with the elastic constants because diamond cubic structure has two atoms per unit cell [107, 109]. The left hand sides of (5.30), (5.31), and (5.32) are bulk modulus, the modulus against tetragonal shear G', and the modulus against rhombohedral shear G respectively. Then we can write that

$$K(P) > 0, \quad G'(P) > 0, \quad G(P) > 0 \tag{5.33}$$

where P is the hydrostatic pressure. Recently, it has been shown that (5.30), (5.31), and (5.32) do not predict correctly lattice instability induced in an fcc metallic lattice by hydrostatic tension [108, 110]. It has been also shown that by replacing the elastic constants by the stiffness coefficients, the resulting stability criteria will have the following forms:

$$K = (c_{11} + 2c_{12})/3 + P/3 > 0 \tag{5.34}$$

$$G' = (c_{11} - c_{12})/2 - P > 0 \tag{5.35}$$

$$G = c_{44} - P > 0. \tag{5.36}$$

If we carry out stress-strain experiments, the numbers we will find will not be elastic constants, but elastic stiffness constants, so that we can directly use those numbers in (5.30), (5.31), and (5.32) to determine elastic instability stress and strain. To determine elastic instability stress and strain, we apply a strain to the system and determine elastic stiffness constants at this strain and repeat this procedure for various strain values until one of the elastic stability criteria is violated. Our results for elastic moduli at various strain values are shown in Figure 5-8.

The bulk modulus goes to zero at 17% strain for the TB model and sipinodal instability sets in. We calculated the stress at the instability point and found that it is $0.38 Mbar$. Tersoff potential predicts spinodal instability too, but strain at the elastic instability point is 15% and the stress is $0.36 Mbar$. There are no ab inito or experimental data for instability for hydrostatic tension. But we believe that our

results are more reliable due to the fact that we include electronic effects as well.

n	n_c	$r_c(A)$	$r_0(A)$	$r_1(A)$	$\phi_0(eV)$
2.0	6.5	2.18	1.1.5363	2.45	8.185
m	m_c	$d_c(A)$	d_0	$d_1(A)$	
3.303	8.665	2.1052	1.64	2.57	

Table 5.1: Parameters for functions s(r) and $\phi(r)$

	$t_s(r-r_1)$	$t_\phi(r-d_1)$	f(x)
c_0	$6.739x10^{-3}$	$2.250x10^{-8}$	-2.590
c_1	$-8.188x10^{-2}$	$-1.440x10^{-6}$	0.572115
c_2	0.193236	$2.10433x10^{-5}$	$-1.789x10^{-3}$
c_3	0.354287	$6.602439x10^{-5}$	$2.3539x10^{-5}$
c_4			$-1.242x10^{-7}$

Table 5.2: Coefficient of the polynomial functions $t_s(r-r_1), t_\phi(r-d_1)$, and $f(x)$.

	$r_{dc}(A)$	$r_{rs}(A)$	$B_{dc}(eV/A^3)$	$B_{rs}(eV/A^3)$
exp't	1.89	2.015	1.3233	1.93884
fit	1.89	2.027	1.3875	1.95658

Table 5.3: The results of the fit to diamond cubic and rocksalt silicon carbide.

	C_{11}	C_{12}	C^0_{44}
Tersoff	4.36	1.20	3.11
TB	3.72	1.57	2.56
Exp't.	3.9	1.42	2.56

Table 5.4: Elastic constants of SiC obtained using Tersoff potential and the TB method compared with experiment (in MBar).

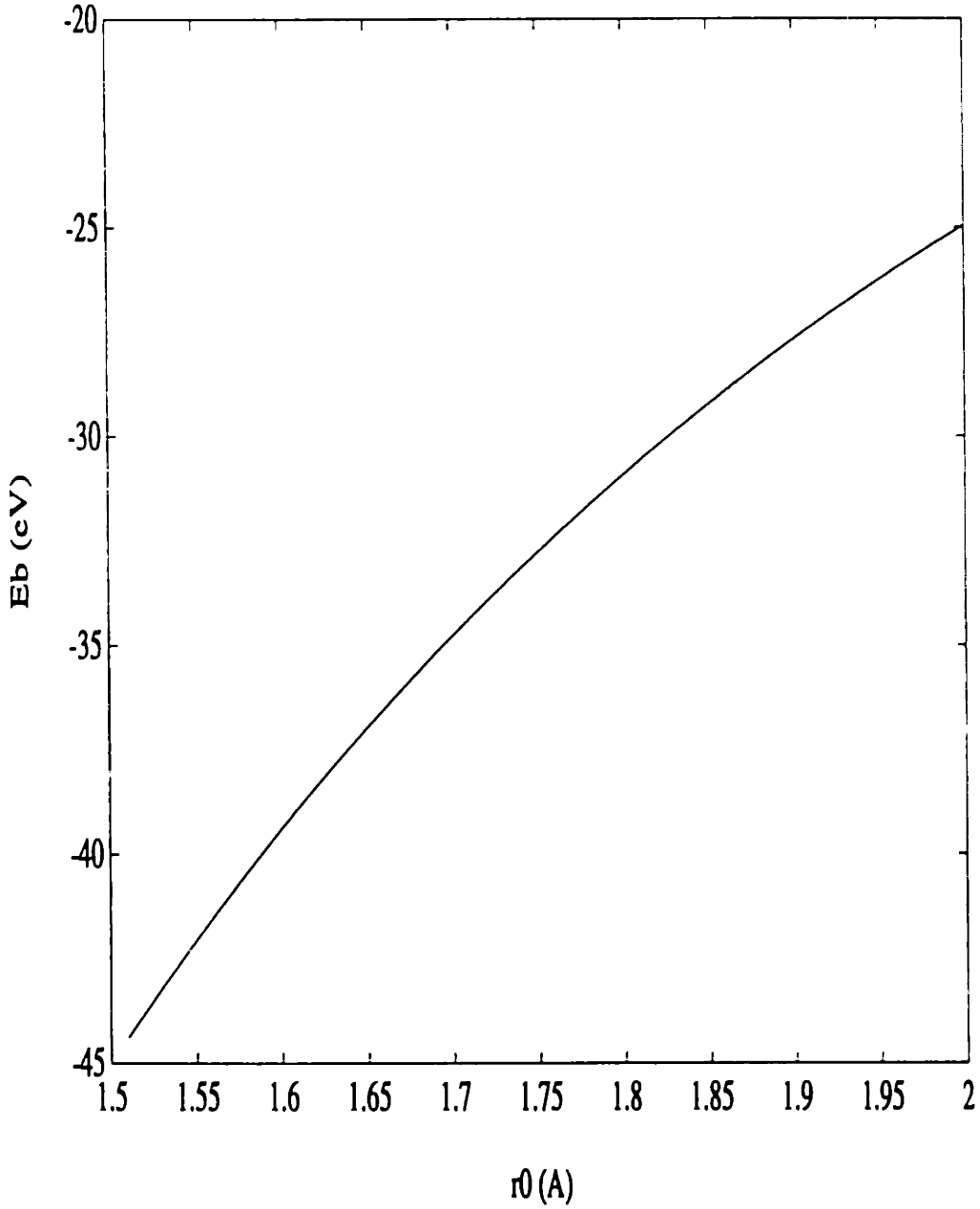

Figure 5-3: The band-structure energy for SiC.

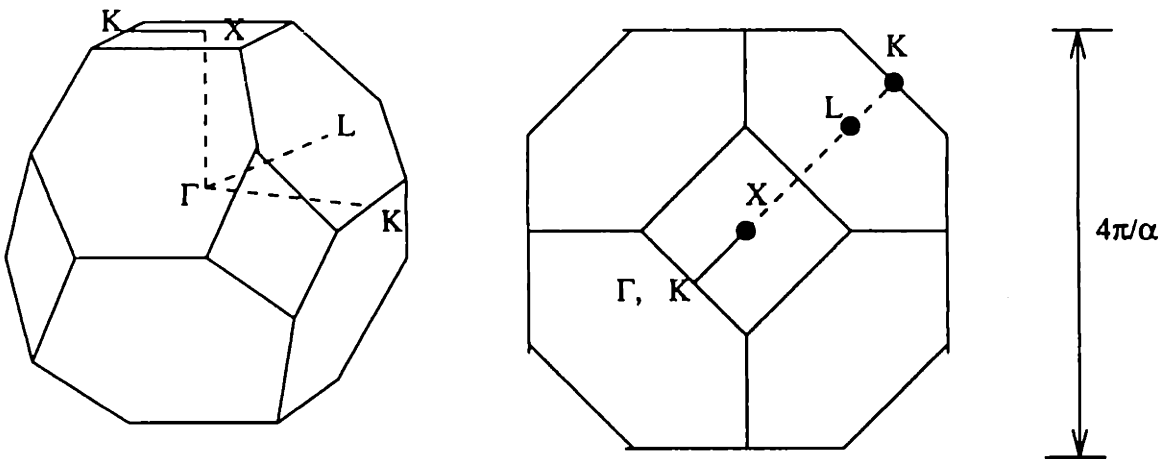

Figure 5-4: The Brillouin Zone and symmetry points for the zincblende lattice.

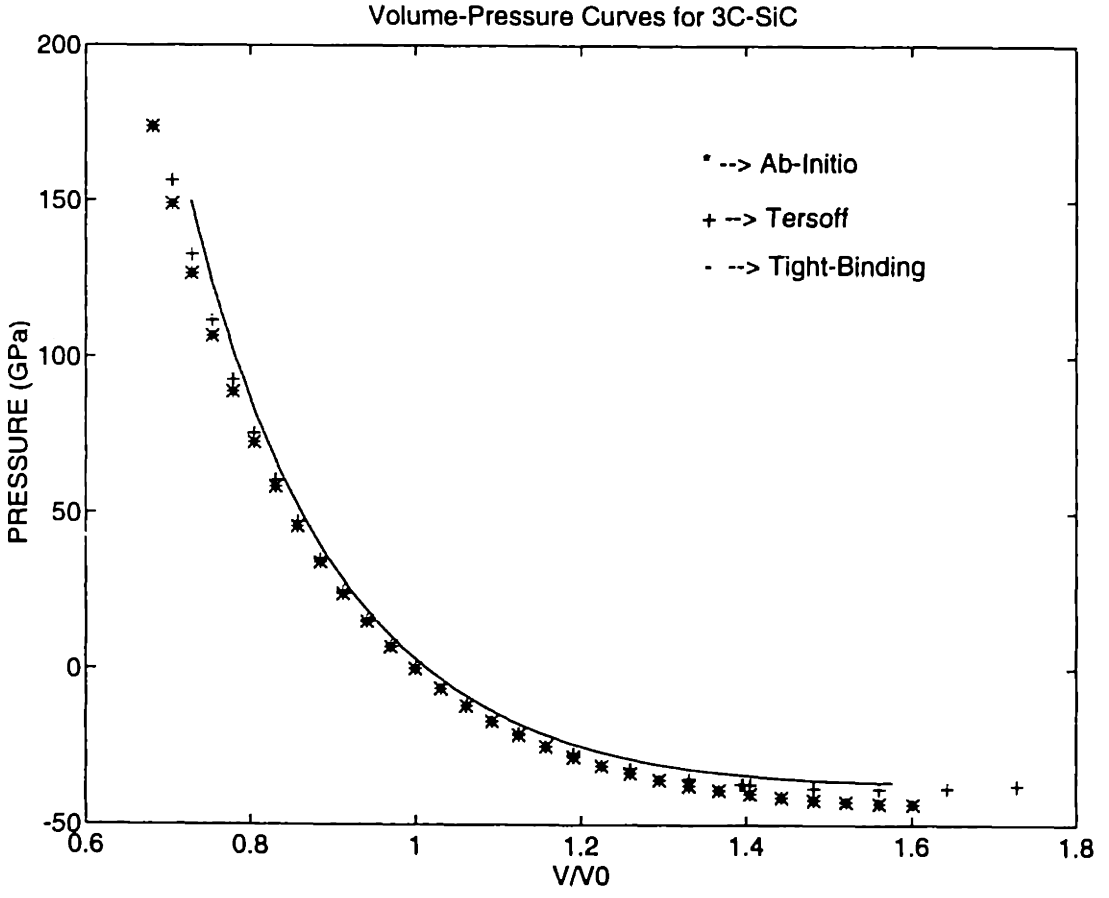

Figure 5-5: Pressure vs. volume curves of β SiC for various models.

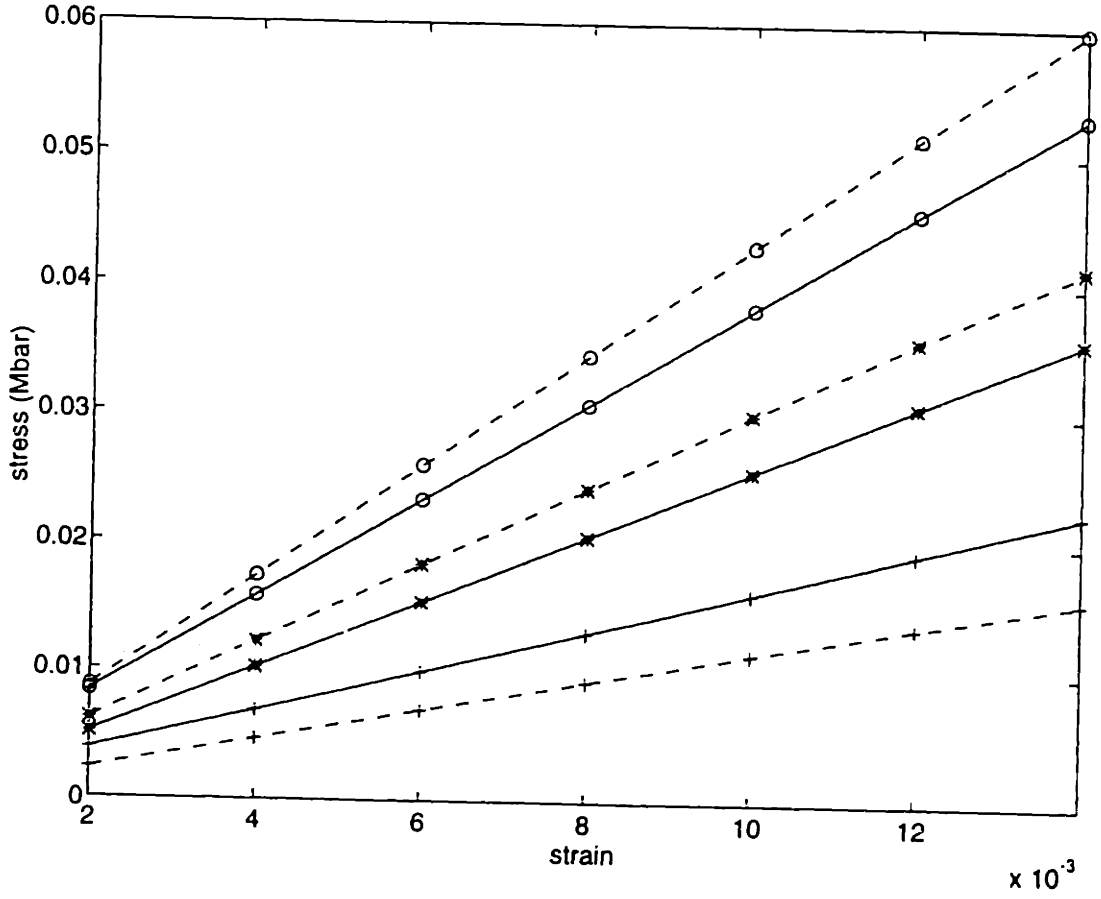

Figure 5-6: The stress-strain curves for SiC.

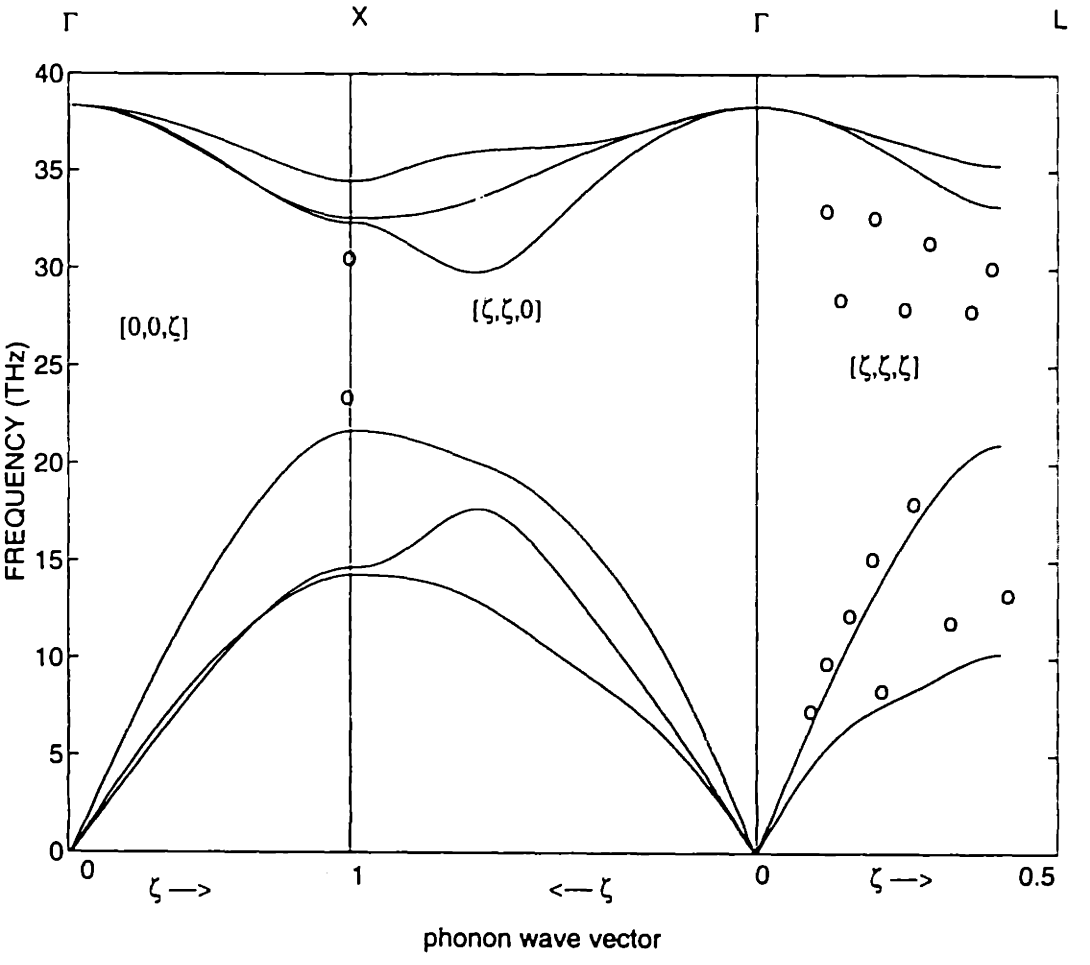

Figure 5-7: Phonon dispersion curves for SiC. Lines show the TB calculation results. The experimental data (open circles) are from [15].

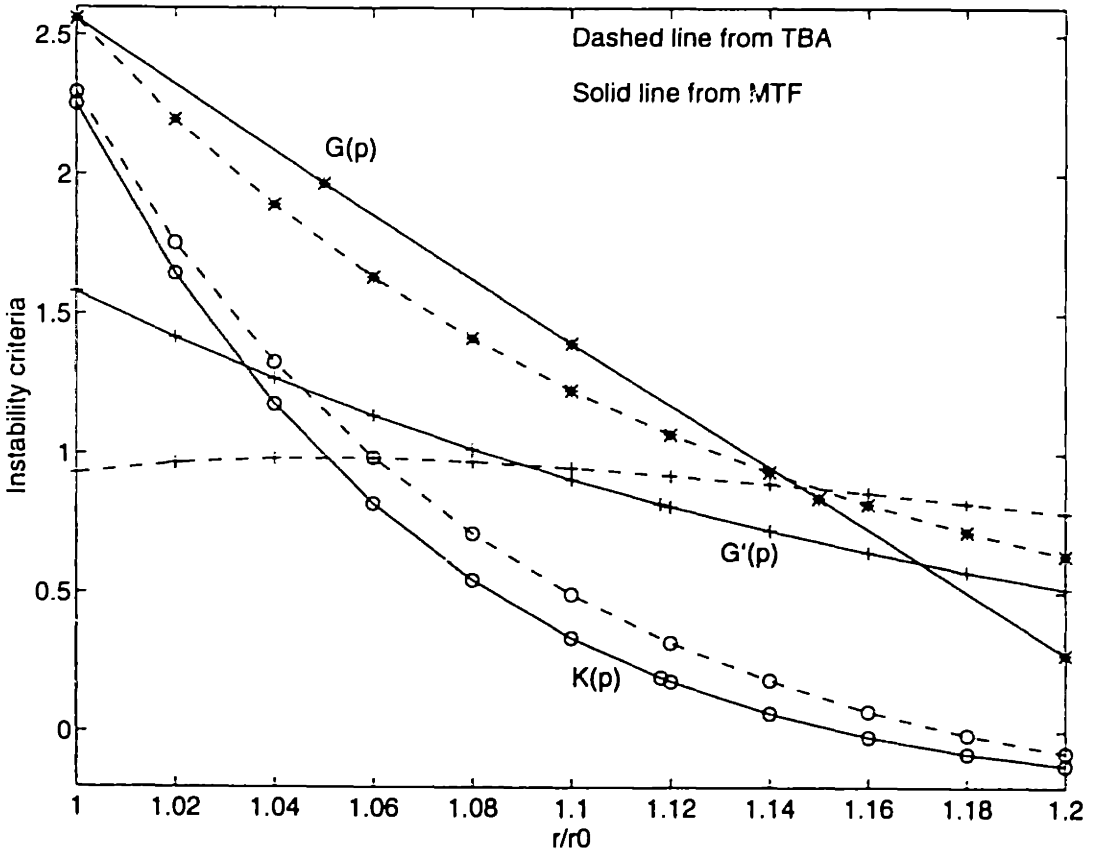

Figure 5-8: K, G' ,and G with respect to r/r0, showing that K becames zero, thus triggering spinodal instability.

Chapter 6

Conclusions and Future Work

We have shown in this dissertation that the TB approach provides an efficient and transferable method for calculating properties of covalent materials. We have established that the TB method is transferable in the sense that it is equally applicable to clusters, liquids, crystals, and crystal defects.

We calculated various properties of Si, C, and SiC by using the TB method. We found that C clusters form chain and ring structures for $N < 10$. We calculated elastic constants for Si, C, and SiC and found them in good agreement with the experiment. These calculations proved that the TB method describes angle dependent forces adequately.

For the first time we investigated partial dislocations in Si by the TB method and obtained results in agreement with the experimental data. We have proved that APD defects are important agents in dislocation movement.

We developed a new TB method for SiC and investigated elastic stability of SiC and determined critical stress, strain and the mode of elastic instability. We have found that under uniform dilatation the spinodal or decohesion instability sets in first. Phonon dispersion curves and elastic constants are in reasonable agreement with experimental results. The results on elastic constants, particularly the shear elastic constant c_{44} for all three systems investigated give a measure of the robustness of the TB approach to atomic cohesion. The results on clusters, properties of which we are not using in determining the TB parameters, serve to emphasize the transferability

of this approach. Taking all of the results together, we can conclude that the TB method is in general more reliable than empirical potential functions.

In the case of SW and Tersoff empirical potentials, we have shown that they can be used to give satisfactory results in most but not all situations. Since empirical potentials are simpler to use than any TB method, it would be useful to develop a hybrid method where both can be applied in a single simulation, the TB method being used only in the most critical region where the description of local bonding is important.

Several further improvements are possible to make the TB method a quantitative tool for investigating atomistic phenomena. Charge transfer effects can be included in the calculations. Application of the recursion method to calculate electronic structure effects may allow larger number of particles to be treated by the TB method.

Appendix A

The MD Program

The flowchart of the tight-binding MD program is shown in Figure A-1[15]. The computationally most intensive part of the program is the calculation of the tight binding eigenvalues and eigenvectors. A very large matrix should be diagonalized in order to calculate the interatomic forces. The Jacobi method[111] is used to diagonalize the Hamiltonian matrix. The derivatives of the Hamiltonian matrix elements are calculated analytically. The program is suitably coded to make vectorization possible. The periodic boundary conditions are applied in all three directions. If an atom leaves the central unit cell in one direction, another atom enters the central unit cell in the opposite direction. The periodic boundary conditions in two dimensions are shown in Figure A-2.

The MD program consists of two parts: one part calculates the Hellmann-Feynman forces and the other part calculates the pair potential forces. The program combines the two forces to obtain the total force. The pair potential forces are calculated very quickly compared to the Hellmann-Feynman forces. One of the reasons for that is the simple form of the pair potential chosen. The total energy is conserved to the fifth digit.

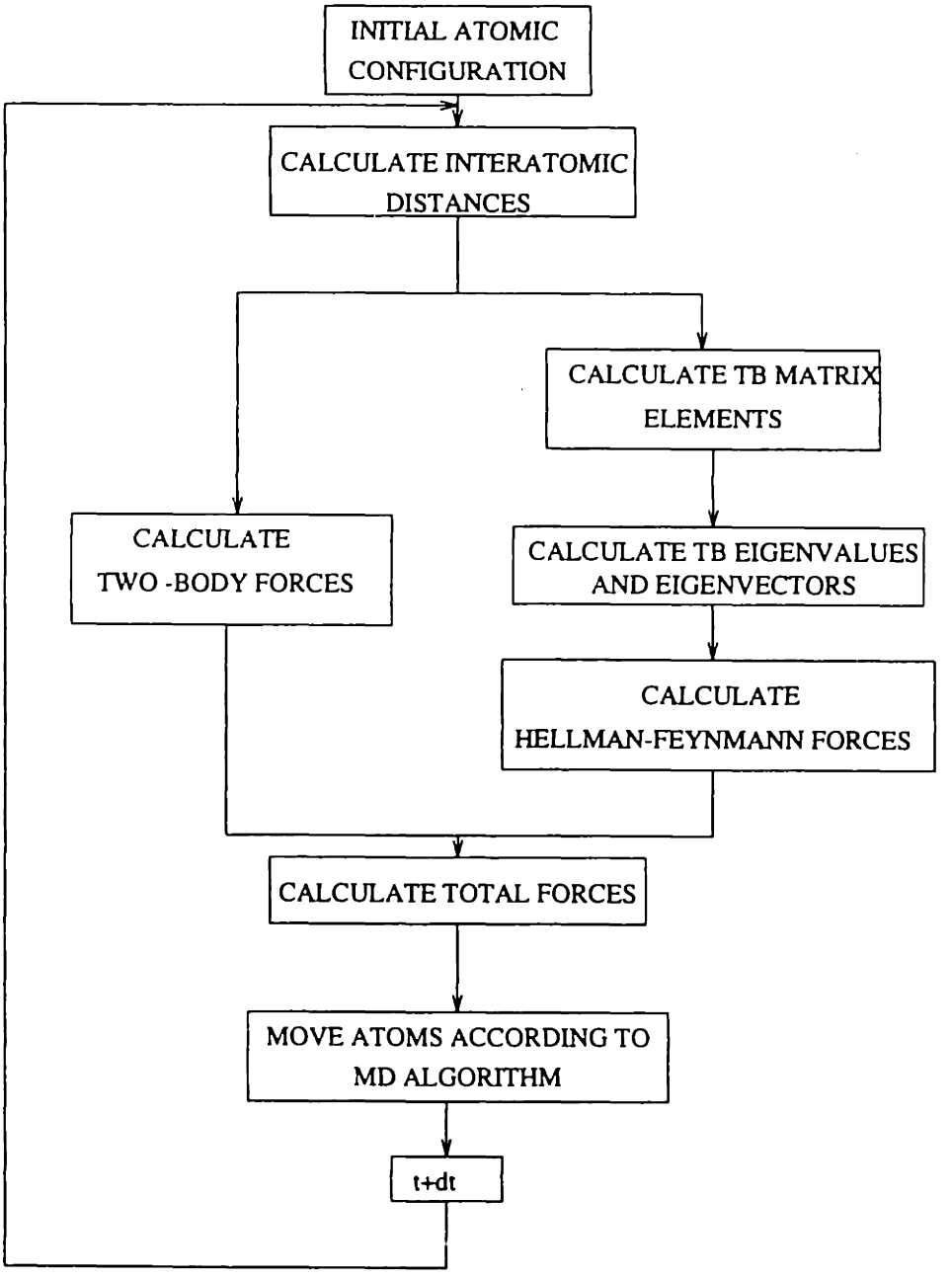

Figure A-1: The flowchart of the tight binding MD simulation program for SiC.

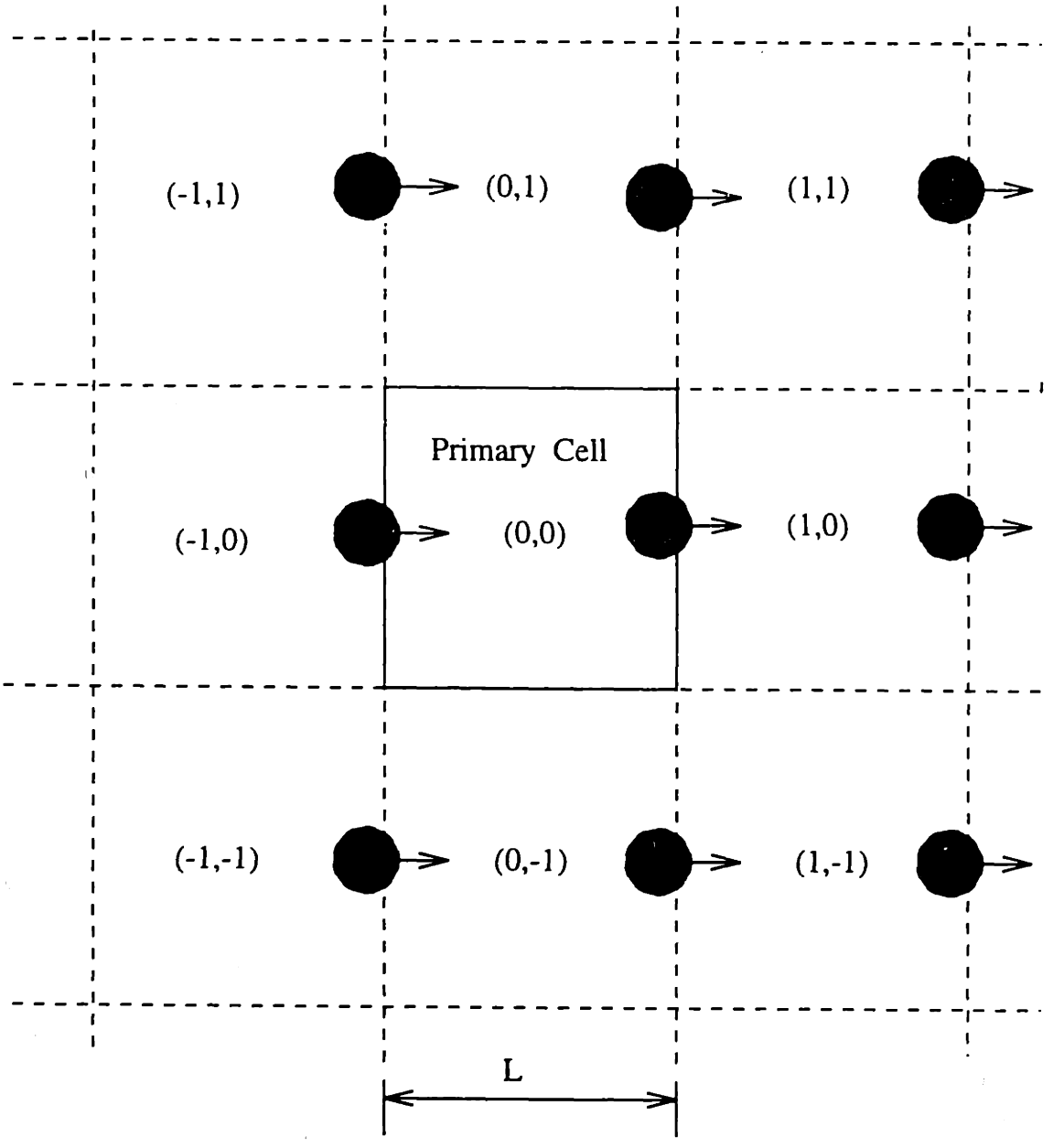

Figure A-2: Application of the periodic boundary conditions in two dimensions.

Bibliography

[1] A.E. Carlsson. *Solid State Phys.*, 43:1, 1985.

[2] F.H. Stillinger and T.A. Weber. *Phys. Rev.B*, 31:5262, 1985.

[3] J. Tersoff. *Phys. Rev.B*, 39:5566, 1989.

[4] H. Balamane, T. Halicioglu, and W.A. Tiller. *Phys. Rev. B*, 46:2250, 1992.

[5] P. Hohenberg and W. Kohn. *Phys. Rev.*, 136:864B, 1964.

[6] W. Kohn and L.J. Sham. *Phys. Rev.A*, 140:1133, 1965.

[7] R.O. Jones and O. Gunnarson. *Rev. Mod. Phys.*, 61:689, 1989.

[8] M.C. Payne, M.P. Teter, D.C. Allan, T.A. Arias, and J.D. Joannopoulos. *Rev. Mod. Phys.*, 64:1045, 1992.

[9] R. Car and M. Parrinello. *Phys. Rev.B*, 55:2471, 1985.

[10] J.C. Slater and G.F. Koster. *Phys. Rev.*, 94:1498, 1954.

[11] L. Pauling and E.B. Wilson. *Introduction to Quantum Mechanics.* Dover, New York, 1985.

[12] I.N. Levine. *Quantum Chemistry.* Prentice Hall, New Jersey, 1991.

[13] D.J. Chadi. *Phys. Rev. Lett.*, 41:1062, 1978.

[14] D.J. Chadi. *Phys. Rev. B*, 29:785, 1984.

[15] C.Z. Wang, C.T. Chan, and K.M. Ho. *Phys. Rev. B*, 39:8592, 1989.

[16] C.Z. Wang, C.T. Chan, and K.M. Ho. *Phys. Rev. B*, 40:3390, 1989.

[17] C.H. Xu, C.Z. Wang, C.T. Chan, and K.M. Ho. *Phys. Rev.B*, 43:5024, 1991.

[18] C.Z. Wang, C.T. Chan, and K.M. Ho. *Phys. Rev.B*, 45:12227, 1992.

[19] R. Virku inen, K. Laasonen, and R.M. Nieminen. *J. Phys.:Condens. Matter*, 3:7455, 1991.

[20] K. Laasonen and R.M. Nieminen. *J. Phys.:Condns Matter*, 2:1509, 1989.

[21] J.M. Ziman. *Principles of the Theory of Solids.* Cambridge University Press, New York, 1989.

[22] O. Madelung. *Introduction to Solid State Theory.* Springer-Verlag, 1981.

[23] A. Haugh. *Theoretical Solid State Physics.* Pergamon Press, New York, 1972.

[24] I.N. Levine. *Properties of Homogeneous Electron Gas.* Prentice Hall, New Jersey, 1991.

[25] D.M. Ceperley and B.J. Alder. *Phys. Rev. Lett.*, 45:566, 1980.

[26] I. Stich, R. Car, and M. Parrinello. *Phys. Rev. Lett.*, 63:2240, 1989.

[27] W. Foulkes and R. Haydock. *Phys. Rev. B*, 39:12520, 1989.

[28] U. von Barth and C.D. Gelatt. *Phys. Rev. B*, 21:2222, 1980.

[29] G.B. Bachelet, D.R. Hamann, and M. Schluter. *Phys. Rev. B*, 26:4199, 1980.

[30] R. C. Chaney, T. K. Tung, C. C. Lin, and E. E. Lafon. *J. of Chem. Phys.*, 52:361, 1970.

[31] E. E. Lafon and C. C. Lin. *Phys. Rev*, 152:579, 1966.

[32] J.A. Majewski and P. Vogl. *Phys. Rev. B*, 35:9666, 1987.

[33] F. Ducastelle. *Order and Phase Stability in Alloys.* Elsevier Science Publishers B.V., 1991.

[34] M. Kohyama, S.Kose, M. Kinoshita, and R. Yamamoto. *J. Phys.*, 2:7791, 1990.

[35] D.J. Chadi. *At. Data Nucl. Data Tables*, 14:177, 1974.

[36] W.A. Harrison. *Electronic Structure and the Properties of Solids.* Freeman, San Fransisko, 1980.

[37] B. M. Deb. *The Force Concept in Chemistry.* Van Nostrand Reinhold Company, New York, 1981.

[38] R.P. Feynman. *Phys. Rev*, 56:340, 1939.

[39] R. Hoffman. *J. Chem. Phys.*, 39:1397, 1963.

[40] M. Schilfgaarde and W.A. Harrison. *Phys. Rev. B*, 33:2653, 1986.

[41] L. Goodwin, A.J. Skinner, and D.G. Pettifor. *Europhys. Lett.*, 9:701, 1989.

[42] M.W. Finnis, A.T. Paxton, D.C. Pettifor, A.P. sutton, and Y. Ohta. *Phil. Mag.*, 58:143, 1988.

[43] M. Kohyama, R. Yamamoto, Y. Ebata, and M. Kinoshita. *Phys. Stat. Sol.*, 152:533, 1989.

[44] A. L. Companion and F. O. Ellison. *J. Chem. Phys.*, 32:1132, 1960.

[45] M. T. Yin and M. L. Cohen. *Phys. Rev. B*, 26:3259, 1982.

[46] K.R. Subbaswami M. Menon. *Phys. Rev. B*, 67:3487, 1991.

[47] A. K. Mahan. *Phys. Rev. B*, 30:5835, 1984.

[48] B. Holland, H. S. Greenside, and M. Schluter. *Phys. Stat. Sol. (b)*, 126:511, 1984.

[49] K. J. Cheng and M. L. Cohen. *Phys. Rev. B*, 31:7819, 1985.

[50] N. W. Ashcroft and N. D. Mermin. *Solid State Physics.* Saunders College Publishing, 1976.

[51] M. T. Yin and M. L. Cohen. *Phys. Rev. Lett.*, 50:2006, 1983.

[52] S.F. Ahmad, H. Kiefte, M.J Clouter, and M.D. Whitmore. *Phys. Rev. B*, 26:4239, 1982.

[53] P. Korpium and E. Lusher. Rare gas solids. volume II, chapter 12. Academic,London, 1977.

[54] M. Powell and G. Dolling. Rare gas solids. volume II, chapter 15. Academic,London, 1977.

[55] P. Stoicheff. Rare gas solids. volume II, chapter 16. Academic,London, 1977.

[56] D.R. Squire, A.C. Holt, and W.G. Hoover. *Physicc*, 42:338, 1969.

[57] J.R. Ray, M.C. Moody, and A. Rahman. *Phys. Rev. B*, 32:733, 1985.

[58] E. B. Barojas and D. Levesque. *Phys. Rev. B*, 34:3910, 1986.

[59] K. Raghavachari. *J. Chem. Phys.*, 83:3520, 1985.

[60] K. Raghavachari. *J. Chem. Phys.*, 84:5672, 1986.

[61] K. Raghavachari. *J. Chem. Phys.*, 89:2219, 1988.

[62] D. Tomanek and M. A. Schluter. *Phys. Rev.B*, 36:1208, 1987.

[63] F. S. Khan and J. Q. Broughton. *Phys. Rev. B*, 39:3688, 1989.

[64] J. R. Chelikowisky and J. C. Phillips. *Phys. Rev.B*, 44:1538, 1991.

[65] s. Kirkpatrick, C. Gellat, and M. Vecchi. *Science*, 220:671, 1983.

[66] C. H. Xu, C.Z. Wang, C.T. Chan, and K.M. Ho. *J. Phys.: Condens. Matter*, 4:6047, 1992.

[67] A. Taylor and R. M. Jones. *Phys. Rev.B*, 39:5120, 1989.

[68] P. B. Hirsch. *J. Microsc.*, 118:3, 1980.

[69] A. George and G. Champier. *Phys. Stat. Solidi*, A53:529, 1979.

[70] J.R.K Bigger, D.A. McInnes, and A.P. Sutton. *Phys. Rev. Lett*, 69:2224, 1992.

[71] S. Marklund. *Phys. Status Solidi B*, 92:83, 1979.

[72] M. S. Duesbery and G. Y. Richardson. *CRC Crit. Rev. Solid State Mater. Sci.*, 17:1, 1991.

[73] C.S. John. *Phil. Mag.*, 32:1193, 1975.

[74] G. Michot and A. George. *Scripta Metall.*, 16:519, 1986.

[75] B. Y. Farber, Y.L. Lunin, and V.I. Nikitenko. *Phys. Stat. Solidi A*, 97:469, 1986.

[76] V.V. Bulatov, S. Yip, and A.S. Argon. to be published.

[77] I.L.F. Ray and D.J.H. Cockayne. *J. Micros.*, 98:173, 1973.

[78] K.W. Lodge, A. Lapicirella, and C. Battistoni. *Philos. Mag. A*, 60:643, 1989.

[79] M. S. Duesbery, B. Joos, and D.J. Michel. *Phys. Rev. B*, 43:5143, 1991.

[80] M.I. Heggie and R. Jones. *Philos. Mag.*, 48:365, 1983.

[81] J.M. Ziman. *Models of Disorder.* Cambridge University Press, Cambridge, 1979.

[82] Y. Li and P.J. Lin-Cheung. *Phys. Rev. B*, 36:1130, 1987.

[83] B. J. Min, Y. H. Lee, C. Z. Wang, C. T. Chan, and K. M. Ho. *Phys. Rev. B*, 46:9677, 1992.

[84] Rose J, H, J. R. Shmidt, F. Guinea, and J. Ferrante. *Phys. Rev. B*, 29:921, 1984.

[85] S. Fahy and S. G. Louie. *Phys. Rev. B*, 36:3373, 1987.

[86] D. H. Lee and J.D. Joannopoulos. *Phys. Rev. B*, 48:1846, 1982.

[87] G. Wiech. Soft x-ray band spectra and the electronic structures of metals and materials. Academic,New York, 1968.

[88] D. Olego, M. Cardona, and P. Vogl. *Phys. Rev. B*, 25:3878, 1982.

[89] M. Schilfgaarde and W.A. Harrison. *J. Phys. Chem. Solids*, 46:1093, 1985.

[90] C.Z. Wang, C.T. Chan, and K.M. Ho. *Phys. Rev.B*, 70:661, 1993.

[91] B. L. Zhang, C.Z. Wang, C.T. Chan, and K.M. Ho. *J. Phys. Chem*, 97:3134, 1993.

[92] F. W. Sears and G. H. Salinger. *Thermodynamics, Kinetic Theory, and Statistical Thermodynamics.* Addison-Wesley Publishing Company, 1975.

[93] J.R. Ray and A. Rahman. *J. Chem. Phys*, 80:4423, 1984.

[94] J.M. Haile. *Molecular Dynamics Simulation, Elementary Methods.* John Wiley and Sons, Inc, 1992.

[95] J. F. Nye. *Physical Properties of Crystals.* Oxford University Press, New York, 1990.

[96] W. G. Hoover, A. C. Holt, and D. R. Squire. *Physica*, 44:437, 1969.

[97] J.R. Ray and A. Rahman. *Phys. Rev. B*, 33:895, 1986.

[98] M Parrinello and A. Rahman. *J. Appl. Phys.*, 52:7182, 1981.

[99] L. D. Landau and E. M. Lifshitz. *Theory of Elasticity.* Pergamon, Oxford, 1959.

[100] X-Q Guo, R. Podloucky, and A. J. Freeman. *J. Mater. Res.*, 6:324, 1991.

[101] M. D. Kluge and J. R. Ray. *J. Chem. Phys.*, 85:4028, 1986.

[102] R. J. Wolf, K. A. Mansour, M. W. Lee, and J. R. Ray. *Phys. Rev.B*, 46:8027, 1992.

[103] J. Goodisman. The force concept in chemistry. volume I, chapter 5. Van Nostran Reinhold Company, 1981.

[104] J. Ashkenazi, M. Dacorogna, M. Peter, Y. Talmor, E. Walker, and S. Steinemann. *Phys. Rev. B*, 18:4120, 1978.

[105] D. H. Lee and J. D. Joannopoulos. *Phys. Rev. Lett.*, 48:1509, 1982.

[106] H.M.J. Smith. *Proc. Roy. Soc. A*, 241:105, 1947.

[107] M. Tang and S. Yip. unpublished.

[108] J. Wang, S. Yip, S.R. Phillpot, and D. Wolf. *Phys. Rev. Lett.*, 71:4182, 1993.

[109] E. Pearson, T. Takai, T. Halicioglu, and W.A. Tiller. *J. Cryst. Growth*, 70:33, 1984.

[110] J. Wang, S. Yip, S. R. Phillpot, and D. Wolf. to be published.

[111] W.H. Press, B.P. Flannery, S.A. Teukolsky, and W.T. Vetterling. *Numerical Recipes in Fortran.* Cambridge University Press, Cambridge, 1990.